Reservoir Characterization of the Cretaceous Cedar Mountain and Dakota Formations, Southern Uinta Basin, Utah: Year-Two Report

by Brian S. Currie, Mary L. McPherson, Joshua P. Dark, and Justin S. Pierson

Open-File Report 516
Utah Geological Survey
a division of
Utah Department of Natural Resources
2008

Reservoir Characterization of the Cretaceous Cedar Mountain and Dakota Formations, Southern Uinta Basin, Utah: Year-Two Report

Brian S. Currie
Department of Geology
114 Shideler Hall
Miami University
Oxford, OH 45056
513-529-7578
curriebs@muohio.edu

Mary L. McPherson
McPherson Geologic Consulting
86 South 3500 West
Vernal, UT 84078
435-781-8025
mcph2@sbtnet.com

Joshua P. Dark
Department of Geology
114 Shideler Hall
Miami University
Oxford, OH 45056
513-529-3216
darkjp@muohio.edu

Justin S. Pierson
Department of Geology
114 Shideler Hall
Miami University
Oxford, OH 45056
513-529-3216
piersojs@muohio.edu

UTAH DNR GEOLOGICAL SURVEY

Open-File Report 516
Utah Geological Survey
a division of
Utah Department of Natural Resources
2008

TABLE OF CONTENTS

INTRODUCTION **1**
STRATIGRAPHY AND SEDIMENTOLOGY **3**
Lower Cretaceous Cedar Mountain Formation 4
Buckhorn Conglomerate Member 4
Yellow Cat Member 5
Poison Strip Sandstone Member 6
Ruby Ranch Member 6
Lower-Upper Cretaceous Dakota Formation 7
PALYNOLOGY **9**
Outcrop Data 9
Westwater Section (Sec. 33, T. 19S, R. 25E) 9
Agate Wash Section (Sec. 26, T. 20S, R. 24E) 13
Yellow Cat Section (Sec. 28, T. 22S, R. 21E) 16
Core Data 18
Trapp Spring 13-25 (API 43-047-30978), Sec. 25, T. 14S, R. 23E 18
Drilling Samples 21
Stratigraphic Implications 21
CORRELATION MODEL **22**
Dakota Silt 24
Dakota Formation 24
Cedar Mountain Formation 26
"Upper Shale" 26
Buckhorn Conglomerate 29
Basal contact with the Morrison Formation 30
WELL CORRELATION **34**
POTENTIAL RESERVOIR ARCHITECTURE **35**
Lateral Channel Dimensions 35
Architectural Profiles 36
Westwater West Point (NW 1/4, Sec. 10, T. 20S, R. 25E) 37
South Agate (NE 1/4, Sec. 34, T. 20S, R. 24E) 37
Paleocurrent Orientations 39
POROSITY AND PERMEABILITY **40**
RESERVOIR CONTROLS **46**
Depth 47
Reservoir Architecture 47
Stratigraphic Position 49
Cedar Mountain Formation 49
Dakota Formation 53
Structural Influence 53
CONCLUSIONS **61**
ACKNOWLEDGMENTS **62**
BIBLIOGRAPHY **63**

LIST OF FIGURES

Figure 1. Study area location maps. 1
Figure 2. Time-stratigraphic diagram of the Cedar Mountain and Dakota Formations in eastern Utah 3
Figure 3. Westwater outcrop measured section and gamma ray log, sample horizons, and interpreted palynological ages. 10
Figure 4. Thermal alteration index, kerogen content, and taxa distribution for Westwater palynology samples. 12
Figure 5. Agate Wash measured section, sample horizons, and interpreted palynological ages. 15
Figure 6. Thermal alteration index (T.A.I.), kerogen content, and taxa distribution for samples from the Agate Wash section. 15
Figure 7. Yellow Cat measured section, sample horizons, and interpreted palynological ages. 16
Figure 8. Thermal alteration index, kerogen content, and taxa distribution for samples from the Yellow Cat section. 18
Figure 9. Thermal alteration index, kerogen content, and taxa distribution for samples from the Trapp Spring core. 20
Figure 10. Map of study area subsurface/surface correlation lines. 22
Figure 11. Westwater outcrop measured section and gamma ray log 23
Figure 12. Log showing criteria for picking Dakota Silt datum and top of the Dakota Formation 24
Figure 13. Gamma ray and resistivity logs of the Dakota interval 26
Figure 14. Geologic map of the Westwater area with measured sections/outcrop gamma ray log locations. 27
Figure 15. Cross section of outcrop gamma ray logs in the southeastern part of the study area. 28
Figure 16. Aerial photograph of an exhumed Cedar Mountain Formation channel. 30
Figure 17. Measured section and outcrop gamma ray log of the Buckhorn Conglomerate, eastern flank of the San Rafael Swell. 31
Figure 18. Log showing signature gamma ray and resistivity curves of the Buckhorn Conglomerate 32
Figure 19. Cross section showing correlation of subsurface and outcrop gamma ray logs across the top of the Morrison Formation. 33
Figure 20. Map of South Agate outcrop area showing interpreted dimensions and paleocurrent orientations of basal upper Dakota Formation fluvial channels. 36
Figure 21. Paleocurrent orientations measured from Dakota Formation fluvial channel sandstones. 39
Figure 22. Map showing the locations of wells and outcrops with core data. 40
Figure 23. Plot of volume percent porosity versus well depth. 43
Figure 24. Plot of permeability versus well depth. 43
Figure 25. Plot of volume percent porosity versus permeability for grainsize. 44
Figure 26. Plot of mean porosity versus mean permeability for grainsize. 45
Figure 27. Map showing the locations of oil and gas fields in the study area. 46

Figure 28. Map showing study area cumulative gas production for the CMD interval and top Dakota Formation 7000 foot measured depth contour. 48
Figure 29. Structural cross section of the Flat Rock field showing Buckhorn Conglomerate completions. 50
Figure 30. Cross section across the Segundo Canyon and Moon Ridge fields showing Cedar Mountain Formation reservoir intervals. 51
Figure 31. Cross section over Seep Ridge field showing possible Poison Strip Sandstone Member production. 52
Figure 32. Stratigraphic cross section across Fence Canyon field showing well-developed amalgamated sandstones of the basal Dakota Formation. 54
Figure 33. Stratigraphic cross section over Main Canyon field showing the well-developed upper sandstone of the upper Dakota Formation. 55
Figure 34. Stratigraphic cross section over Pine Springs field showing well-developed upper and basal Dakota Formation sandstones. 56
Figure 35. Structure contour map on top of the Dakota Silt 57
Figure 36. Structure contour map on the Dakota Silt showing locations of CMD production. 58

LIST OF TABLES

Table 1. Palynomorph assemblage from the Westwater section. 11
Table 2. Palynomorph assemblage from the Agate Wash section. 14
Table 3. Palynomorph assemblage from the Yellow Cat section. 17
Table 4. Palynomorph assemblage from the Trapp Spring core. 19
Table 5. Lithofacies documented at Westwater West Point and South Agate outcrop localities. 38
Table 6. Well information and production data for cores used to construct the porosity and permeability database. 41
Table 7. Width and thickness data for CMD sandstone bodies. 47

LIST OF APPENDICES

Appendix 1: Cross Sections
Appendix 2: Isopach Maps
Appendix 3: Stratigraphic Tops
Appendix 4: Porosity and Permeability Data

LIST OF PLATES

Plate 1: Westwater West Point Mosaic
Plate 2: Westwater West Point Measured Sections
Plate 3: South Agate Mosaic
Plate 4: South Agate Measured Sections

INTRODUCTION

Fluvial-channel sandstones in the Lower/Upper Cretaceous Cedar Mountain and Dakota Formations (CMD) are economic natural gas reservoirs in the southern Uinta Basin of eastern Utah (figure 1). Although most gas production to date has been from structural traps, off-structure discoveries in several locations have illustrated the potential for more extensive play development. It has been estimated that the Cedar Mountain/Dakota stratigraphic interval in the Uinta Basin contains about 70 TCF gas (Rose et al., 2004). To date, however, only about 250 BCF has been produced from these targets. The risk for successful hydrocarbon exploitation is extremely high because of complex stratigraphic relationships within the CMD as well as local variability in reservoir-sandstone thickness, distribution, and quality.

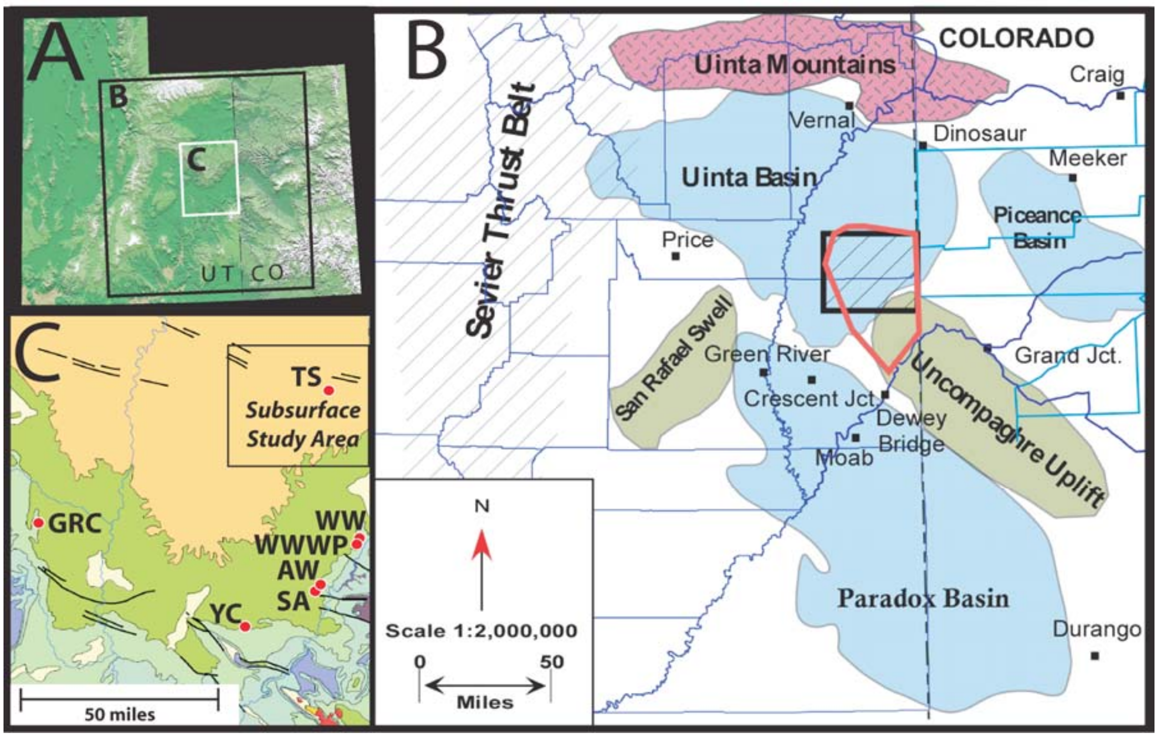

Figure 1. Study area location maps. A) Study area in eastern Utah with outlined locations of insets B and C. B) Regional map showing the location of geologic features and towns referred to in this report. The red polygon is the area in which wells and outcrops were correlated; black rectangle with hash marks indicates the subsurface study area. C) Selected outcrops/core locations referred to in text. AW: Agate Wash; GRC: Green River Cutoff; SA: South Agate; TS: Trapp Spring Core Locality; WW: Westwater; WWWP: Westwater West Point; YC Yellow Cat. Geologic map of eastern Utah modified from Willis (2005).

In order to determine the primary controls on the distribution of economically-viable CMD gas reservoirs, we have conducted an evaluation of well and outcrop data derived from the southern Uinta Basin. Our subsurface work has focused on a approximately 1000 mi^2 area in northern Grand and southern Uinta counties (figure 1). Additionally, CMD outcrops, situated about 25 miles south of the southern boundary of the subsurface data, were used as surface control (figure 1).

Work conducted during this two-year project has focused on evaluating regional well data. Wells that penetrated the CMD Formations were identified and well completion reports and borehole logs were compared to determine the stratigraphic position of producing intervals. Outcrop gamma ray logs were acquired across the CMD interval to provide a subsurface correlation model. Well logs from across the southern Uinta Basin were correlated within the context of CMD lithologic and palynological data derived from core and nearby outcrops. Isopach maps of CMD stratigraphic units and intervals were constructed. Detailed reservoir architecture descriptions of the CMD were generated at several outcrops. Porosity and permeability relationships were analyzed and the risk of finding economic gas resources within the CMD was assessed. These new data are evaluated in conjunction with a regional well completion and well database for CMD penetrations in the southern Uinta Basin that were presented in the year-one report associated with this project (McPherson et al., 2006).

The results of each of the project components, as well as our conclusions as to the controls on economic gas production from the CMD interval, are described below in more detail. Throughout this report, text that is underlined and colored indicates a hyperlink. “Control-clicking” on the hyperlink text will automatically open the link.

STRATIGRAPHY AND SEDIMENTOLOGY

The CMD interval is of Early to Late Cretaceous age. The Upper Jurassic Morrison Formation lies below the CMD and the Upper Cretaceous Mancos Shale lies above. Figure 2 shows a time-stratigraphic diagram for the area. The CMD interval crops out in many places around the Uinta Basin and has been studied by many geologists. Significant contributors to the understanding of the CMD interval are Stokes (1952), Simmons (1957), Quigley (1959), Young (1960), Ryer et al. (1987), Molenaar and Cobban (1991), Currie (1997), Kirkland et al. (1997), Aubrey (1998), Currie (2002), Demko et al. (2004), Stikes (2007), Roca and Nadon (2007), and Kirkland and Madsen (2007). The following descriptions and interpretations represent a compilation of these authors' observations as well as our own.

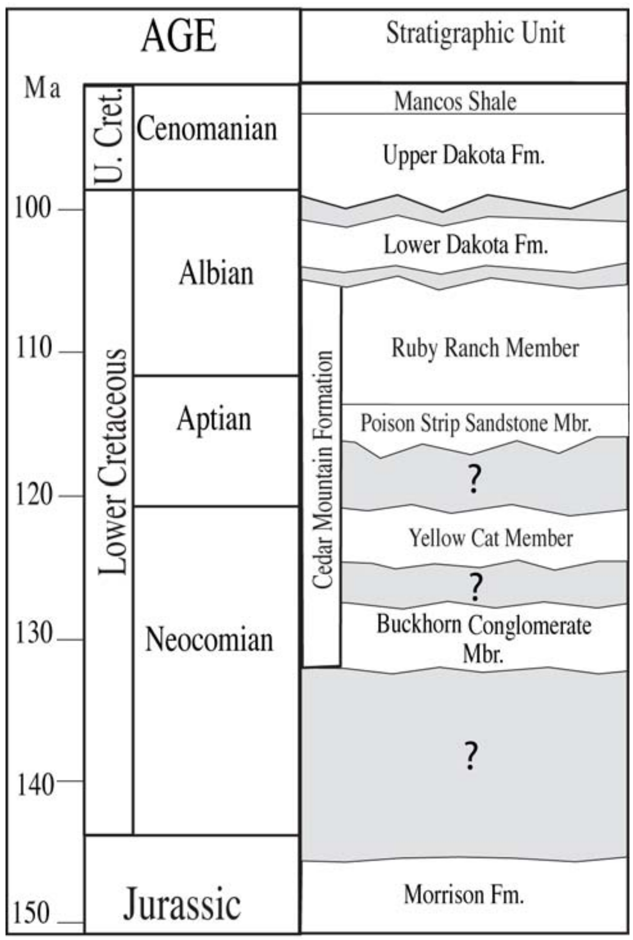

Figure 2. Time-stratigraphic diagram of the Cedar Mountain and Dakota Formations in eastern Utah. Ages are based on CMD palynomorphs, marine fossils in the overlying Mancos Shale, and regional stratigraphic relationships. Compiled from Stokes (1952), Molenaar and Cobban (1991), Currie, (2002), Stikes (2007), Kirkland and Madsen (2007), and this report.

Lower Cretaceous Cedar Mountain Formation

In the study area, the Cedar Mountain Formation is comprised of the Buckhorn Conglomerate, Yellow Cat, Poison Strip Sandstone, and Ruby Ranch Members (Stikes, 2007; Kirkland and Madsen, 2007). The Cedar Mountain Formation contains fluvial channel conglomerates, sandstones, and associated overbank lithologies. Detailed descriptions of each unit are listed below.

Buckhorn Conglomerate Member

The Buckhorn Conglomerate is best exposed along the northern and eastern flanks of the San Rafael Swell near its type section in central Utah (Stokes, 1944; Stokes, 1952) (figure 1). We also identified the Buckhorn Conglomerate in northwest corner of our subsurface study area (figure 1). In addition, the Buckhorn Conglomerate is exposed at the northeastern edge of the Uinta Basin along a 20 mile wide outcrop belt centered near Dinosaur, Colorado (figure 1) (Currie, 1997; Currie, 1998). Where exposed, the Buckhorn Conglomerate consists of up to 100 feet of upward fining conglomerate, sandstone, and minor volumes of mudstone. The unit overlies bentonitic mudstones of the Brushy Basin Member of the Upper Jurassic Morrison Formation and is capped by the Ruby Ranch Member of the Cedar Mountain Formation (see below).

The Buckhorn Conglomerate consists of laterally and vertically amalgamated channel-form lenses of conglomerate and sandstone that give the unit an overall sheet-like geometry. Calculated width-to-thickness ratios of Buckhorn channel complexes range from 1000 to 3000 (Currie, 1998; Roca and Nadon, 2007). Conglomerates are clast supported and dominated by pebble-sized clasts of gray, black, and white chert with lesser amounts of sandstone, quartzite, quartz, and rare silicified wood and bone fragments. Buckhorn Conglomerate Member sandstones consist of approximately equal proportions of chert and quartz grains with less than 6% feldspar grains (Currie, 1998; Roca and Nadon, 2007). Sandstones and conglomerates are cemented primarily by calcite, although silica cement is also common. Fine-grained lithologies in the member consist of 3 to 15 foot thick beds of gray, green, and red bentonitic mudstone. Buckhorn mudstones contain common root and burrow traces and pedogenic carbonate horizons. Mudstone in the unit is interpreted as overbank deposits preserved between individual channel complexes.

The Buckhorn Conglomerate Member was deposited by a gravelly-sandy braided-fluvial system that was incised into the underlying Morrison Formation (Currie, 1997, 1998). The Buckhorn fluvial system was oriented southwest-northeast with a major east-flowing tributary feeding into the overall drainage system in the northern part of the San Rafael Swell (Conley, 1986; Yingling, 1987; Currie, 1998). Lateral to this incised drainage, a well-developed argillic paleosol marks the contact between Morrison and Cedar Mountain Formations (Demko et al., 2004).

Although the Buckhorn Conglomerate contains no age-diagnostic fossils or volcanic ash horizons, it has historically been placed at the base of the Lower Cretaceous stratigraphic interval in eastern Utah (Stokes, 1952). However, recent workers have interpreted the Buckhorn Conglomerate as the uppermost member of the Upper Jurassic Morrison Formation (Aubrey, 1998; Roca and Nadon, 2007). These interpretations may need to be reevaluated given observed stratigraphic relationships in the northern part of the San Rafael Swell. Near the Cleveland-Lloyd dinosaur quarry in Carbon County, the paleosol interpreted as forming at the Jurassic-Cretaceous unconformity is erosionally truncated by the Buckhorn Conglomerate (Demko et al., 2004). This superposition of the Buckhorn Conglomerate above the Jurassic-Cretaceous unconformity suggests an Early Cretaceous age of deposition of the unit. In addition, the recent discovery of a possible Early Cretaceous ankylosaur from the Buckhorn Conglomerate near its type section at Buckhorn Reservoir (Kirkland, 2005) supports the original Lower Cretaceous stratigraphic interpretation of Stokes (1952).

Yellow Cat Member

The Yellow Cat Member is restricted to the southern part of the study area west of Dewey Bridge in Grand County (Kirkland and Madsen, 2007). In this area, the Buckhorn Conglomerate is absent and the Yellow Cat Member lies unconformably on the Brushy Basin Member of the Upper Jurassic Morrison Formation. In most places, the Yellow Cat Member rests above the thick argillic paleosol at the top of the Brushy Basin Member (Demko et al., 2004). Where the paleosol is absent, the contact between the Morrison and Cedar Mountain Formations is represented by a thin concentration of chert pebbles at the base of the Yellow Cat Member (Kirkland and Madsen, 2007).

In the study area, the Yellow Cat Member consists of up to 45 feet of green and red pebbly mudstone with abundant nodular carbonate horizons and calcrete beds (Stikes, 2007). The unit also contains thin sandstone beds (< 6 feet thick) displaying symmetrical ripples and bivalve escape structures. Some beds are poorly-sorted mixtures of mud, sand, and gravel containing granule- to cobble-sized clasts of chert and nodular carbonate. Yellow Cat Member lithologies are interpreted as pedogenically-modified fluvial overbank and shallow lacustrine deposits (Stikes, 2007). Poorly sorted, gravelly beds are interpreted as marginal lacustrine debris flow deposits (Eberth et al., 1997).

Dinosaur fossils, charophytes, and pollen collected from the Yellow Cat Member indicate the unit is late Neocomian (Berremian) in age (Kirkland and Madsen, 2007). This age interpretation is supported by detrital zircons sampled from Yellow Cat Member mudstones, which indicate a 126 ± 2.5 Ma maximum age of deposition (Greenhalgh et al., 2006).

Poison Strip Sandstone Member

The Poison Strip Sandstone Member consists of 6 to 45 feet of fluvial conglomerate and sandstone (Stikes, 2007). The unit forms a laterally continuous sheet-sandstone body from Green River to Dewey Bridge (figure 1) (Kirkland et al., 1997). In the study area west of Dewey Bridge, the Poison Strip Sandstone Member unconformably overlies the Yellow Cat Member. East of Dewey Bridge, rare lenticular sandstones appear correlative with the Poison Strip Sandstone and rest unconformably on the Upper Jurassic Morrison Formation (Kirkland and Madsen, 2007).

The Poison Strip Sandstone Member is composed primarily of upward-fining conglomerate, and very-coarse to very-fine sandstone (Stikes, 2007). Sedimentary structures include trough and planar-cross stratification, horizontal stratification, and ripple-cross lamination. Paleocurrent orientations indicate an overall northeast flow direction (050°) of Poison Strip Sandstone fluvial systems (Stikes, 2007). The framework mineralogy of Poison Strip sandstones is dominated by quartz (89%), with subsidiary chert (9%) and feldspar (2%) grains (Stikes, 2007). Sandstones are cemented primarily by calcite, although patchy silica cement is commonly observed in outcrop as well. Clast-supported conglomerates make up the basal portion of channel-form bodies and consist primarily of granule- to pebble-sized clasts of chert and quartzite. Pebble- to boulder-sized intraclasts of mudstone and carbonate are also abundant in conglomeratic beds.

The Poison Strip Sandstone Member is interpreted as the deposits of northeast flowing, sand-dominated, low-sinuosity/braided fluvial systems. It consists of multi-storey, multi-lateral lenticular sand bodies 6 to 45 feet thick. Width to thickness ratios of individual channel bodies range between 20 and 100 (Stikes, 2007). Internally, individual channel bodies display scour-bounded, upward-fining packages of cross- and horizontally stratified sandstone and conglomerate up to 25 feet thick deposited by migrating dunes and downstream/laterally migrating bar forms (Stikes, 2007).

Based on the similarity of dinosaur fossils discovered in both the Poison Strip and overlying Ruby Ranch Members (see below), the Poison Strip Sandstone Member is interpreted as late Aptian-early Albian in age (Kirkland et al., 1997).

Ruby Ranch Member

In the study area, the Ruby Ranch Member conformably overlies the Poison Strip Sandstone. Where the Poison Strip Sandstone is absent, the Ruby Ranch Member rests directly above the unconformity paleosol at the top of the Morrison Formation. The Ruby Ranch Member consists of 50 to 80 feet of green, red, and gray mudstone. Mudstones contain abundant calcic and vertic paleosols and associated pedogenic-carbonate nodules and groundwater-calcrete beds in all but the upper parts of the member. Near the top of the Ruby Ranch Member, mudstones become bentonitic and contain rare altered ash beds. The Ruby

Ranch Member also contains rare lenticular fluvial channel deposits up to 30 feet thick. Width/thickness ratios of these sandstones range from 10 to 25. Sedimentary structures in Ruby Ranch sandstones include trough- and planar-cross stratification, horizontal stratification, and ripple-cross lamination. Paleocurrent orientations indicate an overall east-northeast direction of paleo-flow (Harris, 1980; Currie, 2002). The mineralogical composition and cements of these sandstones are similar to those in the Poison Strip Sandstone Member (Currie, 1998).

The Ruby Ranch Member is interpreted as overbank and channel deposits of low sinuosity, east/northeast-flowing, fluvial systems (Currie, 2002). Dinosaur fossils and U-Pb ages of detrital zircons sampled from the member indicate a late Aptian-Albian (115-105 Ma) age of deposition (Kirkland and Madsen, 2007).

Lower-Upper Cretaceous Dakota Formation

The Dakota Formation is a complex mix of alluvial, paludal, and marginal-marine deposits. Based on the architectural arrangement of fluvial sandstones, overbank mudstones and associated marginal/shallow marine deposits in northeastern Utah and northwestern Colorado, the Dakota Formation can be subdivided into upper and lower stratigraphic units that are separated by a sequence-bounding unconformity (Ryer et al., 1987; Currie, 2002). In the southern Uinta Basin, each sequence consists of basal fluvial-channel sandstones that are overlain by gray smectitic/carbonaceous overbank deposits, and isolated channel sandstones. In outcrops along the southern part of the study area, the lower Dakota Formation is up to 65 feet thick. In the same area, the upper Dakota is up to 165 feet thick. Both the lower and upper units were deposited in paleovalleys incised into underlying units. In study area outcrops, the lower Dakota Formation is incised as much as 30 feet into the underlying Cedar Mountain Formation, whereas upper Dakota fluvial channels are incised as much as 50 feet into the lower Dakota.

Dakota Formation channel sandstones are commonly conglomeratic near their bases. Clasts are composed primarily of chert, sandstone, and quartzite pebbles/cobbles as well as pebble- to boulder-sized rip-up clasts of underlying lithologies. Dakota Formation sandstones have framework compositions similar to those in the Poison Strip and Ruby Ranch Members of the Cedar Mountain Formation. The basal sandstones and conglomerates of the lower Dakota sequence are coarser than those in the upper sequence.

Dakota Formation sandstones are commonly cemented by silica, kaolinite, smectite, hematite, and rarely by calcite. In some localities, Dakota sandstones are pervasively cemented by kaolinite and smectite clay. In outcrop, these sandstones are white and appear to have been bleached. Most of the clay-cemented sandstones observed are in the lower Dakota Formation. The abundant clay cement in some lower Dakota sandstones results in poor outcrop exposures, especially where overlying upper Dakota Formation sandstones are absent.

The fluvial channel deposits in both the lower and upper Dakota Formation have similar architectural geometries. The channels in both units are interpreted as the deposits of northeast-flowing, sand-dominated, low-sinuosity, single-channel fluvial systems (cf. Bridge et al., 1986; Miall, 1996). Internally, individual channel bodies display scour-bounded, upward-fining packages of cross- and horizontally stratified sandstone and conglomerate up to 20 feet thick deposited by migrating dunes and downstream/laterally migrating bar forms. The measured flow-perpendicular widths of both lower and upper Dakota Formation fluvial channel bodies are between 600 and 3000 feet. Width to thickness ratios of these channel sands range from 24 to 35. However, the majority of lower Dakota channel sands that have been observed in outcrop are truncated by upper Dakota channel sands. In some locations, stacked channel complexes of both lower and upper Dakota channels result in overall sandstone thickness of 75 to 100 feet. Lateral amalgamation of channel sands also results in sheet-sand bodies that are up to 5000 feet wide and have width-to-thickness ratios between 100 and 125.

Lithologies overlying or lateral to the basal sandstones of each Dakota sequence consist primarily of gray-black smectitic and carbonaceous mudstones/siltstone, fine-grained sandstones, altered-ash horizons, and thin coals. Pyrite and siderite nodules are common in the mudstones. Fine-grained lithologies are interpreted as swamp and paludal deposits whereas sandstones are interpreted as crevasse or channel deposits.

In the study area, the lower Dakota sequence is entirely nonmarine. The upper Dakota, however, contains tidally-influenced channel deposits and mudstones. The marine influence on the upper Dakota increases east-northeast of the study area. The top of the Dakota Formation is commonly marked by a sandy/silty conglomeratic lag that was deposited during Cenomanian encroachment of the Western Interior Seaway.

Channel sandstones, carbonaceous shales, and coal deposits in the upper part of the Dakota Formation of east-central Utah have been interpreted as middle Cenomanian in age (Molenaar and Cobban, 1991; Carroll, 1992; Cushman, 1994). Although unsupported by biostratigraphic evidence, the lower Dakota Formation in the study area was thought to be Late Albian-Early Cenomanian in age (Currie, 2002). New palynology data presented below indicates that the lower Dakota Formation is Late Albian in age while the upper Dakota Formation is Late Albian-Early Cenomanian. Middle-Late Cenomanian palynomorphs and marine mollusks sampled from the lower Mancos Shale immediately overlying the Dakota Formation in the study area support this interpretation.

PALYNOLOGY

As part of this study, 77 samples were processed and analyzed for fossil palynomorphs. Samples were collected from carbonaceous mudstones of the Dakota Formation, and gray mudstones of the Cedar Mountain Formation. Sample locations are shown in figure 1. Outcrop samples were taken from 1 to 3 inch thick beds of unweathered mudstone that were devoid of modern plant material. Approximately 100 to 200 grams of mudstone were collected at each outcrop sample horizon, but only 3 to 5 grams were processed for palynomorphs. Core samples were 1 to 3 grams in volume. Of these samples, 58 yielded identifiable fossil pollen, spores, and dinoflagellate cysts. The palynological content, stratigraphic age, estimated visual thermal alteration index (T.A.I.) values, kerogen content, taxa distribution, and paleoenvironmental interpretations for the samples were used as stratigraphic guides in the correlation of cross sections constructed for this project. All analyses were conducted by Gerald Waanders, consulting palynologist and are summarized below by locality.

Outcrop Data

Westwater Section (Sec. 33, T. 19S, R. 25E)

Twelve samples from the Dakota Formation and the lower parts of the Mancos Shale were taken at the Westwater Section in Grand County, Utah (figure 1; measured section shown in figure 3). The basal Mancos Shale samples yielded Middle Cenomanian-Upper Cenomanian/Turonian palynomorphs while those from the Dakota Formation yielded Early Cenomanian and Late Albian taxa (table 1). The organic recoveries were good to excellent and consisted mostly of mixed woody and cuticular kerogens (figure 4). The palynomorph recoveries from the Mancos Shale samples consisted of both marine microplankton and land-derived spores and pollen suggesting a nearshore marine paleoenvironment. The palynomorph recoveries from the Dakota Formation were all land-derived indicating deltaic or swamp paleoenvironments. Good to excellent organic recoveries of woody and cuticular kerogens from all samples suggest source rock potential for gas. The visual T.A.I. values for this interval are 0.3-0.4% estimated vitrinite reflectance (figure 4). Further information on the stratigraphic-age determinations on each sample is listed in more detail below.

Samples WW7.22.06.1-4 (Turonian-Upper Cenomanian)

These samples were taken from marine siltstones and shales in the lower part of the of the Mancos Shale, 30 to 50 feet above the top of the Dakota Formation (figure 3). The sample interval was 10 to 30 feet below the top of the Coon Springs Sandstone (Molenaar and Cobban, 1991), which is commonly referred to in the southern Uinta Basin as the Dakota Silt (Munger, 1965). The presence of *Isabelidinium acuminatum* (*Alterbia* sp. A) indicates Turonian-Upper Cenomanian

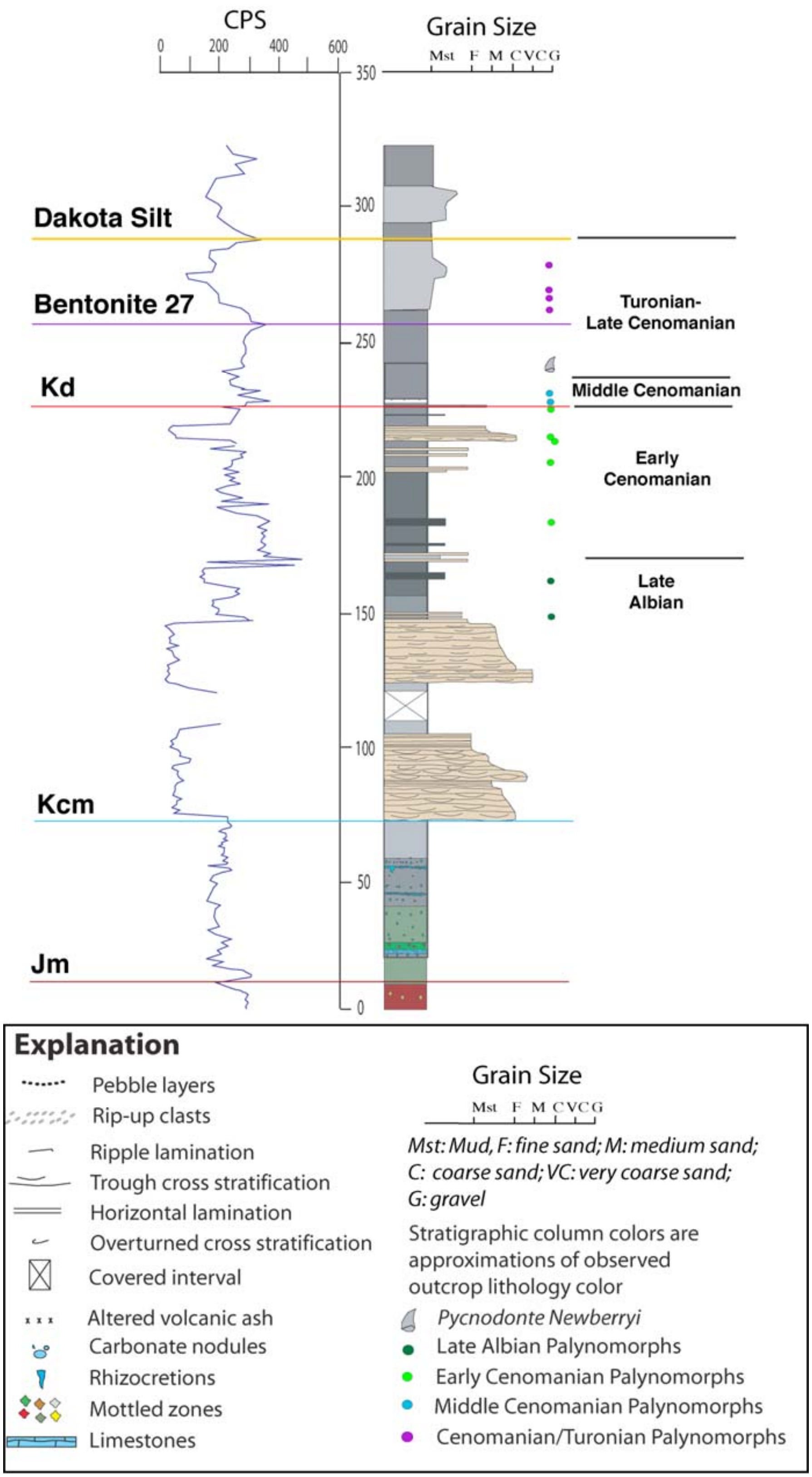

Figure 3. Westwater outcrop measured section and gamma ray log showing palynology sample horizons and age determinations. Thickness in feet.

Table 1. Palynomorph assemblage from the Westwater section. A: Abundant > 30 specimens/slide, C: Common, 30-16 specimens/slide, F: Frequent, 15-6 specimens/slide, R: Rare, < 6 specimens/slide.

SPORES AND POLLEN

Age	Sample	*Araucariacites australis*	*Camarozonosporites insignis*	*Camarozonosporites* sp.	*Cicatricosisporites australiensis*	*Cicatricosisporites brevilaesuratus*	*Cicatricosisporites crassiterminatus*	*Cicatricosisporites hallei*	*Cicatricosisporites venustus*	*Classopollis classoides*	*Costatoperforosporites foveolatus*	*Deltoidospora* spp.	*Densosporites* sp. (Pz reworked)	*Exesipollenites tumulus*	*Foraminisporis dailyi*	*Foraminisporis wonthaggiensis*	*Foveotriletes* sp.	*Gleicheniidites senonicus*	*Laevigatosporites* spp.	*Rouseisporites radiatus*	*Rugubivesiculites reductus*	*Rugubivesiculites rugosus*	*Trizonites subrugulatus*	*Cingulatisporites distaverrucosus*	*Taurocusporites spackmani*	Taxodiaceae
Upper Cenomanian-Turonian	WW7.22.06.1	R	R							R								R								F
	WW7.22.06.2	R	R		R	R				R		R						R								R
	WW7.22.06.3	F	R							F			R	R				R			R		R			R
	WW7.22.06.4		R							R														R		R
Middle Cenomanian	WW4 33.5													R												
	WW4 32.5	F	R	R	R	R	R	F	R	F	R	R			R	R	R	A	R	R		R			R	R
Early Cenomanian	WW4 31.4	R														R		R		R						
	WW4 27.6	R										R				F				R						
	WW4 27.4																									
	WW4 25.1	F										R				R				R						R
	WW4 19	R	F									R		R				F								
Late Albian	WW4 12		R		R	R			R	R		F		R	R	R		F	R							R
	WW4 8.5	R	R		C	R						A				A		A	R							

SPORES AND POLLEN (continued)

Age	Sample	Undifferentiated Bisaccates	*Retitriletes cenomanianus*	*Lycopodiumsporites* sp.	*Schizosporis reticulatus*	*Schizosporis parvus*	*Appendicisporites potomacensis*	*Cicatricosisporites imbricatus*	*Cicatricosisporites pseudotripartitus*	*Klukisporites areolatus*	*Klukisporites pseudoreticulatus*	*Osmundacidites wellmanii*	*Rouseisporites reticulatus*	*Sphagnumsporites regium*	*Apiculatisporites* sp. A	*Appendicisporites bifurcatus*	*Appendicisporites jansonii*	*Callialasporites dampieri*	*Concavissimisporites punctatus*	*Lycopodiumsporites austroclavatidites*	*Neoraistrickia robusta*	*Pilosisporites trichopapillosus*	*Rouseisporites triangularis*	*Trilobosporites apiverrucatus*	*Trilobosporites crassus*	*Trilobosporites trioreticulosus*
Upper Cenomanian-Turonian	WW7.22.06.1	R																								
	WW7.22.06.2	F																								
	WW7.22.06.3	R																								
	WW7.22.06.4	R																								
Middle Cenomanian	WW4 33.5		R	R																						
	WW4 32.5	R																								
Early Cenomanian	WW4 31.4				R																					
	WW4 27.6					C																				
	WW4 27.4																									
	WW4 25.1					F																				
	WW4 19						R																			
Late Albian	WW4 12				R		R	R	R	R	R	R	R	R												
	WW4 8.5	R					A			R			R		A	F	R	R	R	R	R	F	A	R	R	R

MICROPLANKTON

Age	Sample	*Circulodinium distinctum*	*Cribroperidinium edwardsi*	*Hystrichodinium pulchrum*	*Isabelidinium acuminatum* (*Alterbia* A)	*Florentinia stellata*	Microforaminifera linings	*Micrhystridium* sp.	*Trichodinium castanea*	*Hystrichosphaeridium recurvatum*	*Florentinia ferox*	*Odontochitina operculata*	*Palaeohystrichophora infusorioides*	*Spiniferites ramosus*	*Alterbidium acutula*	*Cleistosphaeridium* spp.	*Coronifera oceanica*	*Dinopterygium cladoides*	*Odontochitina costata*	*Oligosphaeridium complex*	*Operculodinium* spp.	*Spiniferites cingulatus*	*Surculosphaeridium longifurcatum*	*Impletosphaeridium whitei*	*Crassosphaera ornata*	*Pterospermella* spp.	*Schizosporites reticulatus*	*Schizosporis reticulatus*	*Canninginopsis colliveri*	*Subtilisphaera terrula*	*Downiesphaeridium multispinosum*
Upper Cenomanian-Turonian	WW7.22.06.1	R	R	R	A	R	F	R	F																						
	WW7.22.06.2						R			R	R	R	R	R																	
	WW7.22.06.3	R	F	R	A					R		R	R	A	R	R	R	R	R	R	F	R	R								
	WW7.22.06.4	R					F		F	R		R	F	A			F		R	F	R			F							
Middle Cenomanian	WW4 33.5																								R	R	R	R			
	WW4 32.5	R	R									C														R			F	C	R
Early Cenomanian	WW4 31.4																														
	WW4 27.6																														
	WW4 27.4																														
	WW4 25.1																														
	WW4 19																														
Late Albian	WW4 12																														
	WW4 8.5																														

Age	Sample Number	T.A.I.	Amorphous	Cuticular	Woody	Organic Recovery	Pollen/Spores	Microplankton
Upper Cenomanian/ Turonian	WW7.22.06.1	0.3-0.4	30%	20%	50%	Excellent	6	8
	WW7.22.06.2	0.3-0.4	40%	30%	40%	Excellent	8	6
	WW7.22.06.3	0.3-0.4	10%	10%	80%	Good	11	17
	WW7.22.06.4	0.3-0.4	90%	5%	5%	Very Good	5	12
Middle Cenomanian	WW4 33.5	0.3-0.4	0%	10%	90%	Fair	3	3
	WW4 32.5	0.3-0.4	30%	30%	40%	Excellent	21	7
Early Cenomanian	WW4 31.4	0.3-0.4	10%	30%	60%	Excellent	5	
	WW4 27.6	0.3-0.4	25%	40%	35%	Excellent	5	
	WW4 25.1	0.3-0.4	25%	45%	30%	Excellent	6	
	WW4 19.0	0.3-0.4	0%	10%	90%	Very Good	6	
Late Albian	WW4 12.0	0.3-0.4	10%	60%	30%	Excellent	21	
	WW4 8.5	0.3-0.4	15%	15%	70%	Good	24	

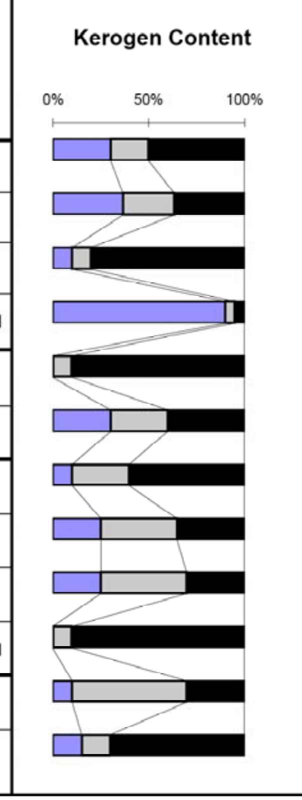

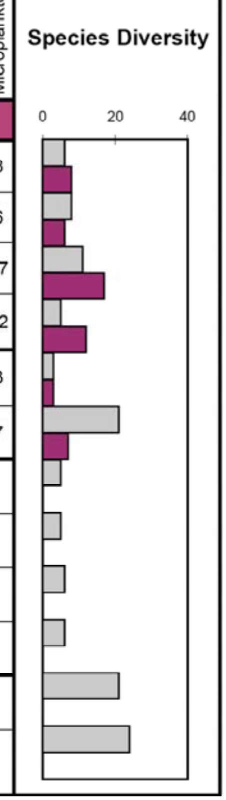

Figure 4. Thermal alteration index (T.A.I.), kerogen content, and taxa distribution for samples from the Westwater section.

age of deposition (Nichols and Jacobson, 1982). This interpretation is supported by Middle Turonian fossils sampled from the Dakota Silt interval on the east flank of the San Rafael Swell (Molenaar and Cobban, 1991). In addition, upper Cenomanian mollusk fossils (*Pycnodonte Newberryi*) have been identified at the Westwater section about 25 feet below the sample interval (Cross Section D).

Samples WW4 33.5 and WW4 32.5 (Middle Cenomanian)

These samples were taken from the lower-most part of the Mancos Shale within 4 feet above the contact with the Dakota Formation and approximately 10 to 13 feet below an interval of silty shale containing abundant *Pycnodonte Newberryi* fossils (figure 3). A Middle Cenomanian age from the lower-most Mancos Shale is indicated for this sample by occurrences of *Cicatricosisporites crassiterminatus* and by the dinoflagellate species *Cribroperidinium edwardsi, Palaeohystrichophora infusorioides,* and *Subtilisphaera terrula*.

Samples WW4 31.4-WW4 19 (Early Cenomanian (?))

The palynomorphs recovered from these samples are all long ranging throughout the Cretaceous. A Cenomanian age for this interval is suggested by a decrease in overall taxa diversity compared to the definitive Albian-aged assemblage recovered lower in the section.

Samples WW4 12-WW4 8.5 (Late Albian)

The Late Albian portion of this section is indicated by the first occurrences of *Klukisporites pseudoreticulatus, K. areolatus, Rouseisporites spp. and Neoraistrickia robusta, Pilosisporites trichopapillosus, Trilobosporites apiverrucatus, T. crassus and T. trioreticulosus*.

Agate Wash Section (Sec. 26, T. 20S, R. 24E)

Eight samples from the Dakota Formation were collected from the Agate Wash section in Grand County, Utah (SA in figure 1; measured section shown in figure 5). All samples yielded identifiable palynomorphs. Two samples from the upper part of the Dakota Formation yielded possible Early Cenomanian palynomorphs, while six samples from the lower Dakota Formation yielded Late Albian palynomorphs (table 2). The organic recoveries were good to very good and consisted mostly of mixed woody and cuticular kerogens (figure 6). The palynomorph recoveries were all land-derived indicating deltaic or swamp paleoenvironments. Good to very good organic recoveries of woody and cuticular kerogens suggest source rock potential for gas.

The visual T.A.I. values for this interval are 0.3-0.4% estimated vitrinite reflectance indicating thermal maturities associated with early gas generation. Further information on the stratigraphic-age determinations on each sample is listed in more detail below.

Samples AW44.5, AW41.5, AW25.5 (Early Cenomanian)

The palynomorphs recovered from these samples are all long ranging throughout the Cretaceous. An Early Cenomanian age for this interval is suggested by a decrease in overall taxa diversity as compared to the definitive Albian-aged assemblage recovered lower in the section.

Samples AW2-AW17 (Late Albian)

A Late Albian age is defined here by the first occurrences of several pteridophyte spore taxa. Those that best define this age are *Trilobosporites marylandensis*, *T. apiverrucatus, T. crassus, Neoraistrickia robusta* and *Pilosisporites trichopapillosus*. An age no older than late Albian is suggested by the angiosperm taxa *Liliacidites peroreticulatus*, *Liliacidites inaequalis* and *Fraxinoipollenites inaequalis*. However, these species were only found as low as sample AW 21 and not in the lowest samples of the interval.

Table 2. Palynomorph assemblage from the Agate Wash section. A: Abundant > 30 specimens/slide, C: Common, 30-16 specimens/slide, F: Frequent, 15-6 specimens/slide, R: Rare, < 6 specimens/slide.

SPORES AND POLLEN

Age	Sample	*Apiculatisporis* sp.	*Deltoidospora* sp.	*Exesipollenites tumulus*	*Foraminisporis dailyi*	*Lusatisporis circumundulatus*	*Retitriletes cenomanianus*	Taxodiaceae	*Laevigatosporites ovatus*	*Araucariacites australis*	*Concavissimisporites punctatus*	*Foraminisporis wonthaggiensis*	*Gleicheniidites senonicus*	*Balmeisporites* sp.	*Callialasporites* sp.	*Trilobosporites marylandensis*	Undifferentiated Bisaccates	*Appendicisporites bifurcatus*	*Appendicisporites potomacensis*	*Cicatricosisporites australiensis*
Early Cenomanian	AW 44.5	R	R	R	R	R	R	R												
	AW 41.5								R											
	AW 25.5		F	R	R					C	R	R	R							
Late Albian	AW 24				R		R		R	A	R	R	C	R	R	R	F			
	AW 22		C						R	C	R		F				A	R	R	R
	AW 21		C	R					R	A		R	C	R			A		R	R
	AW20.3		R	R	R					C	R		C			R	A	R	R	F
	AW 17.5		R		R				R	R	R	R				R	A			
	AW 17		F		R			R	R	R	C					R	C			

Age	Sample	*Cicatricosisporites hallei*	*Cicatricosisporites mahroides*	*Liliacidites peroreticulatus*	*Lycopodiumsporites marginatus*	*Ornamentifera echinata*	*Rouseisporites reticulatus*	*Trilobosporites apiverrucatus*	*Appendicisporites jansonii*	*Appendicisporites problematicus*	*Cicatricosisporites imbricatus*	*Cingulatisporites distaverrucosus*	*Foveotriletes* sp.	*Fraxinoipollenites venustus*	*Liliacidites inaequalis*	*Matonisporites excavatus*	*Microreticulatisporites* sp.	*Taurocusporites spackmani*	*Trilobosporites crassus*	*Aequitriradites ornatus*
Early Cenomanian	AW 44.5																			
	AW 41.5																			
	AW 25.5																			
Late Albian	AW 24																			
	AW 22	R	R	R	R	R	R	R												
	AW 21	R				R			R	R	R	R	R	R	R	R	R	R	R	
	AW20.3	R				R	R			R		R						R		R
	AW 17.5						R					R								
	AW 17				R		R					R				R				

Age	Sample	*Camarozonosporites insignis*	*Cicatricosisporites brevilaesuratus*	*Cicatricosisporites potomacensis*	*Lycopodiumsporites* sp. A	*Matonisporites equiexinus*	*Platysaccus* sp.	*Rouseisporites radiatus*	*Trilobosporites minor*	*Apiculatisporis babsae*	*Apiculatisporis* sp. A	*Arcelites disciformis*	*Callistosporites graniferus*	*Neoraistrickia robusta*	*Perotrilites pannuceus*	*Pilosisporites trichopapillosus*	Tasmanaceae	*Taurocusporites segmentatus*	*Trilobosporites humilis*
Early Cenomanian	AW 44.5																		
	AW 41.5																		
	AW 25.5																		
Late Albian	AW 24																		
	AW 22																		
	AW 21																		
	AW20.3	R	R	R	R	R	R	R	R										
	AW 17.5		R	R		R		F		R	R	R	R	C	R	R	R	R	R
	AW 17		R			F		R		R	R			F	R	F	R	R	R

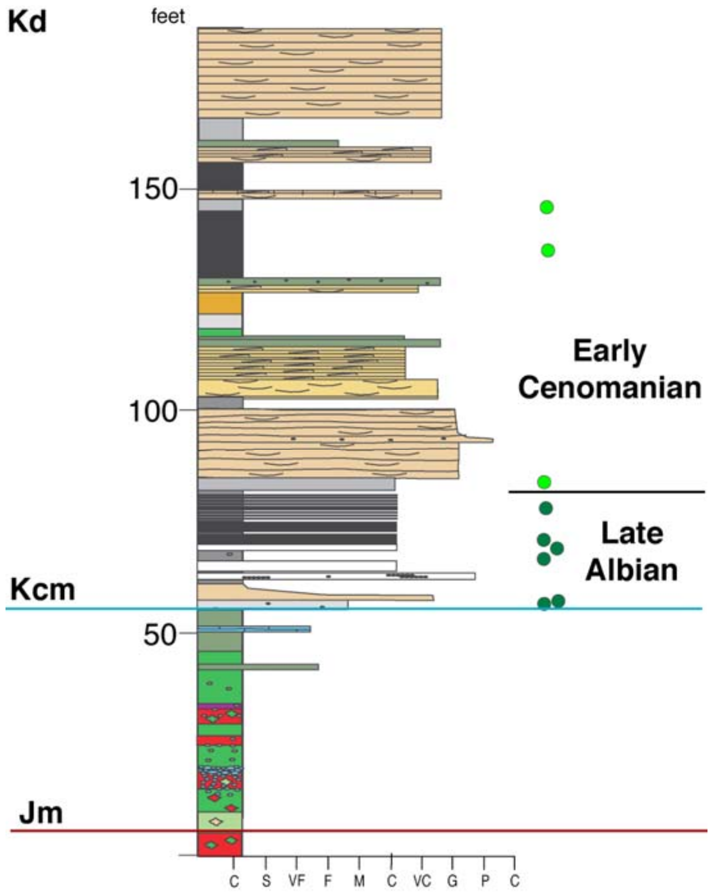

Figure 5. Agate Wash measured section, sample horizons, and interpreted palynological ages. Thickness in feet. See figure 3 for lithological symbols.

Age	Sample Number	T.A.I.	Kerogen Distribution: Amorphous	Cuticular	Woody	Organic Recovery	Taxa Distribution: Pollen/Spores	Microplankton	Paleoenvironment
Early Cenomanian	AW 44.5	0.3-0.4	10%	50%	40%	Very Good	7		Swamp/Deltaic
	AW 41.5	0.3-0.4	0%	25%	50%	Very Good	1		
	AW 25.5	0.3-0.4	0%	15%	85%	Good	7		
Late Albian	AW 24	0.3-0.4	0%	60%	40%	Very Good	11		
	AW 22	0.3-0.4	0%	15%	85%	Very Good	23		
	AW 21	0.3-0.4	0%	25%	75%	Very Good	23		
	AW 20.3	0.3-0.4	0%	25%	75%	Very Good	26		
	AW 17.5	0.3-0.4	5%	10%	85%	Good	24		
	AW 17	0.3-0.4	0%	5%	90%	Good	23		

Figure 6. Thermal alteration index (T.A.I.), kerogen content, and taxa distribution for samples from the Agate Wash section.

Yellow Cat Section (Sec. 28, T. 22S, R. 21E)

Three samples from the lower part of the Dakota Formation were collected from the Yellow Cat Section in Grand County, Utah (McPherson et al., 2006). The location of the section is denoted in figure 1 as YC and the measured section is shown in figure 7. All samples yielded identifiable Late Albian palynomorphs (table 3). The organic recoveries were very good and consisted of mostly woody kerogens (figure 8). The palynomorph recoveries were all land-derived indicating deltaic or swamp depositional environments. Very good organic recoveries of woody kerogens suggest source rock potential for gas. The visual T.A.I. values for this interval are 0.3-0.4% estimated vitrinite reflectance. Further information on the stratigraphic-age determinations of each sample is listed in more detail below.

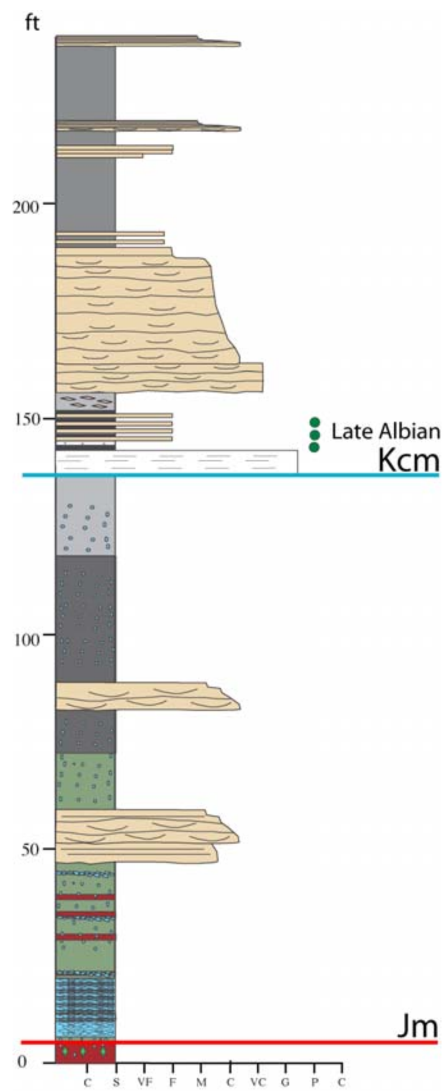

Figure 7. Yellow Cat outcrop measured section, sample horizons, and interpreted palynological ages. Thickness in feet. See figure 3 for lithological symbols.

Table 3. Palynomorph assemblage from the Yellow Cat section. A: Abundant > 30 specimens/slide, C: Common, 30-16 specimens/slide, F: Frequent, 15-6 specimens/slide, R: Rare, < 6 specimens/slide.

Age	Sample	Spores and Pollen																																				
		Alisporites microsaccus	*Annulispora* sp.	*Araucariacites australis*	*Concavissimisporites punctatus*	*Deltoidospora* spp.	*Gleicheniidites senonicus*	*Lycopodiumsporites austroclavatidites*	Undifferentiated Bisaccates	*Bennittiteaepollenites lucifer*	*Appendicisporites potomacensis*	*Callialasporites* sp.	Cicatricosisporites australiensis	*Foraminisporis Wonthaggiensis*	*Ischyosporites punctatus*	*Laevigatosporites* spp.	*Laricoides gigantea*	*Monosulcites scabratus*	*Osmundacidites wellmanii*	*Perinopollenites* sp.	*Perotrilites* sp.	*Pilosisporites trichopapillosus*	*Punctatosporites scabratus*	*Rouseisporites reticulatus*	*Schizosporis parvus*	*Trilobosporites trioreticulosus*	*Appendicisporites tricomitatus*	*Cingutriletes clavus*	*Foraminisporis dailyi*	*Foveotriletes subtriangularis*	*Klukisporites pseudoreticulatus*	*Camarozo nosporites insignis*	*Cicatricosisporites hallei*	*Ischyosporites disjunctus*	*Matonisporites excavatus*	*Parvisaccites radiatus*	*Rugubivesiculites rugosus*	*Undulatisporites undulosus*
Late Albian	YC-45.5		R	**C**	R	R	R	R	R	R	R	R	R	R	R	R	R	R	R	R	R	R	R	R	R	R												
	YC- 44.5	R	R	**F**	R	**F**					R			R			R	R									R	R	R	R	R							
	YC-43.5		R	**F**	R		R		**C**			R				R		R				R		R			R					R	R	R	R	R	R	R

Samples YC 43.5, YC 44.5, YC 45.5 (Late Albian)

An age no younger than Late Albian is indicated for this interval by occurrences of *Concavissimisporites punctatus*, *Ischyosporites disjunctus*, *I. punctatus*, *Klukisporites pseudoreticulatus*, *Pilosisporites trichopapillosus*, and *Trilobosporites trioreticulosus*. An age no older than Late Albian is suggested by *Rugubivesiculites rugosus*, which was found in the stratigraphically-lowest sample (YC 43.5).

Age	Sample Number	T.A.I.	Kerogen Distribution					Taxa Distribution			
			Amorphous	Cuticular	Woody	Organic Recovery	Kerogen Content (0% 50% 100%)	Pollen/Spores	Microplankton	Species Diversity (0 20 40)	Paleoenvironment
Late Albian	YC-45.5	0.3-0.4	5%	10%	85%	Very Good		24			Swamp/Deltaic
	YC- 44.5	0.3-0.4	0%	15%	85%	Very Good		13			
	YC-43.5	0.3-0.4	0%	20%	80%	Very Good		18			

Figure 8. Thermal alteration index (T.A.I.), kerogen content, and taxa distribution for samples from the Yellow Cat section.

Core Data

Trapp Spring 13-25 (API 43-047-30978), Sec. 25, T. 14S, R. 23E

Twenty-three samples of core from the Trapp Spring well in southern Uintah County yielded identifiable palynomorphs (table 4). The core, which is archived at the Utah Core Research Center, was taken from the lower part of the Mancos Shale and the Dakota Formation. The three samples from the Mancos Shale and the upper part of the Dakota Formation yielded probable Early-Middle Cenomanian palynomorphs. The other samples from the Dakota Formation contained Albian palynomorphs. Organic recoveries from the samples were mostly very good and consisted of mixed kerogens suggesting source rock potential for gas and oil. Visual T.A.I. values for this interval are 0.5-0.7% estimated vitrinite reflectance (figure 9). Further information on the stratigraphic-age determinations on each sample is listed in more detail below.

Samples TS 8654-TS 8752 (Early-Middle Cenomanian)

Samples from the lower Mancos Shale (TS 8654-8739) and Dakota Formation (TS 8743-TS 8752) yielded palynomorph assemblages indicative of an Early–Middle Cenomanian age of deposition. As noted above for the Cenomanian-aged palynomorphs of the Agate Wash and Westwater sections, the palynomorphs recovered from these samples are all long ranging throughout the Cretaceous.

Table 4. Palynomorph assemblage from the Trapp Spring core. A: Abundant > 30 specimens/slide, C: Common, 30-16 specimens/slide, F: Frequent, 15-6 specimens/slide, R: Rare, < 6 specimens/slide.

Age	Sample	SPORES AND POLLEN																																																													
		Araucaricites australis	*Classopollis classoides*	*Deltoidospora* spp.	*Perotrilites* sp.	*Sphagnum* sp.	*Lycospora* sp. (reworked Pz)	*Trilobosporites minor*	*Densosporites* sp. (reworked Pz)	*Lycopodiumsporites austroclavatidites*	*Murospora* sp. (reworked Pz)	*Punctatisporites* sp. (reworked Pz)	*Cicatricosisporites australiensis*	*Cingulatisporites distaverrucosus*	*Exesipollenites tumulus*	*Convolutispora* sp. (reworked Pz)	*Camarozonosporites insignis*	*Cicatricosisporites crassiterminatus*	*Gleicheniidites senonicus*	Taxodiaceae	*Callialasporites dampieri*	*Costatoperforosporites foveolatus*	*Aequitriradites spinulosus*	*Tasmanites* sp. (reworked Pz)	*Cicatricosisporites hallei*	*Foveosporites canalis*	*Psilatricolpites parvulus*	*Antulisporites baculatus*	*Cicatricosisporites brevilaesuratus*	*Matonisporites excavatus*	*Peromolites allensis*	*Cicatricosisporites hughesii*	*Laevigatosporites* spp.	*Taurocusporites spackmani*	*Leptolepidites verrucatus*	*Neoraistrickia robusta*	*Nevesisporites semiscalaris*	*Osmundacidites wellmanii*	*Retetricolpites georgensis*	*Rouseisporites reticulatus*	*Rouseisporites triangularis*	*Tigrisporites scurrandus*	*Trilobosporites trioreticulosus*	*Apiculatisporites babsae*	*Cicatricosisporites potomacensis*	*Cicatricosisporites venustus*	*Concavissimisporites punctatus*	*Cyathidites australis*	*Foraminisporis wonthaggiensis*	*Ischyosporites disjunctus*	*Pilosisporites trichopapillosus*	Undifferentiated Bisaccates	*Klukisporites pseudoreticulatus*	*Retitricolpites vulgaris*	*Appendicisporites jansonii*	*Appendicisporites problematicus*	*Cicatricosisporites annulatus*	*Cicatricosisporites imbricatus*	*Lycopodiumsporites* sp. A	*Cicatricosisporites pseudotripartitus*	*Klukisporites variegatus*	*Appendicisporites potomacensis*	*Biretisporites potonei*	*Foraminisporis wonthaggiensis*	*Schizosporis parvus*
Early to Middle Cenomanian	TS8654	R	R	R																																																											
	TS8667	R	R	R	R	R																																																									
	TS8670	R					R	R																																																								
	TS8689	R	R	R			R		R	R	R	R																																																			
	TS8702						R																																																									
	TS8708		R									R	R	R	R																																																
	TS8715		R				R		R			R			R	R																																															
	TS8724	R	R						R			R			R		R	R	R	R																																											
	TS 8731	R	R														R				R	R																																									
	TS8735												R										R	R																																							
	TS8739		R			R											R								R	R	R																																				
	TS8743	R	R											R			R									R		R	R	R	R																																		
	TS 8752	R	R	F				R							R		R															R	R	R																															
Late Albian	TS8758	R	R	R		R							R		R		R		R						R				R				R		R	R	R	R	R	R	R	R	R																						
	TS8767	R		R						R			R	R	R		R		R				R		R				R							R				R				R	R	R	R	R	F	R	R	R													
	TS8775		R											R	R		R																														R						R												
	TS8785		R	R		R									R		A	R	A	R									C																	R				R			R	R											
	TS8798		R	R									R	R			R		R																																				R										
	TS8810	C	F	C													R		F						R					R										R	R												R		R	R	R	R	R						
	TS 8834		R	R				R											R											R			R													R											R			R					
	TS 8845			R															R							C			R																	R															C				
	TS 8856	R		A									R		R		R		R		R															R							R			R	R															A	R	R	R

Age	Sample Number	T.A.I.	Kerogen Distribution: Amorphous	Cuticular	Woody	Organic Recovery	Taxa Distribution: Pollen/Spores	Microplankton
Early to Middle Cenomanian	TS8654	0.6-0.7	40%	10%	50%	Very Good	3	0
	TS 8667	0.5-0.6	70%	10%	20%	Very Good	5	0
	TS8670	0.6-0.7	60%	10%	30%	Very Good	3	0
	TS8680	0.6-0.7	40%	20%	40%	Fair	0	0
	TS8689	0.6-0.7	70%	10%	20%	Good	8	0
	TS8702	0.6-0.7	60%	10%	30%	Fair	1	0
	TS8708	0.6-0.7	70%	10%	20%	Good	5	0
	TS8715	0.6-0.7	70%	10%	20%	Very Good	6	0
	TS8724	0.6-0.7	60%	10%	30%	Very Good	9	0
	TS 8731	0.5-0.6	70%	10%	20%	Very Good	5	0
	TS8735	0.6-0.7	50%	10%	40%	Very Good	3	0
	TS8739	0.6-0.7	30%	20%	50%	Very Good	6	0
	TS8743	0.6-0.7	60%	10%	30%	Very Good	9	0
	TS 8752	0.5-0.6	30%	40%	30%	Very Good	9	0
Late Albian	TS8758	0.6-0.7	25%	25%	50%	Very Good	20	0
	TS8767	0.6-0.7	25%	25%	50%	Very Good	22	0
	TS8775	0.6-0.7	20%	20%	60%	Very Good	6	0
	TS8785	0.6-0.7	60%	20%	20%	Very Good	13	0
	TS8798	0.6-0.7	40%	20%	40%	Very Good	7	0
	TS 8810	0.5-0.6	25%	25%	50%	Very Good	15	0
	TS 8834	0.5-0.6	30%	20%	50%	Very Good	9	0
	TS 8845	0.5-0.6	40%	20%	40%	Very Good	6	0
	TS 8856	0.5-0.6	30%	10%	60%	Fair	15	0

Kerogen Content

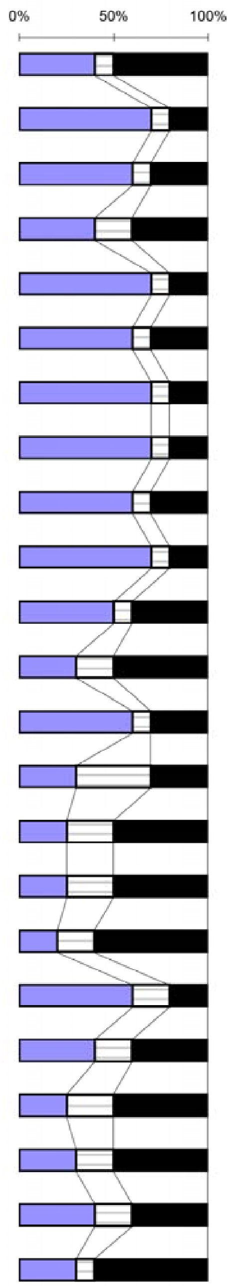

Species Diversity

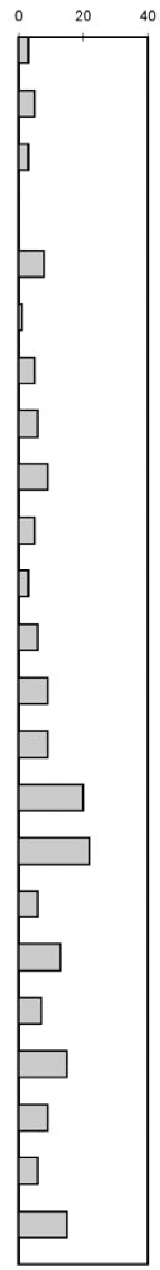

Figure 9. Thermal alteration index, kerogen and taxa distribution for samples from the Trapp Spring core.

However, the occurrences of *Cicatricosisporites crassiterminatus* and *Perotrilites allensis* indicate the possibility of an age at least as young as Middle Cenomanian.

Samples TS 8758-TS 8856 (Late Albian)

The Late Albian part of the sampled interval is indicated by the first occurrences of *Concavissimisporites punctatus*, *Klukisporites pseudoreticulatus*, *Neoraistrickia robusta*, *Pilosisporites trichopapillosus*, *Rouseisporites spp.*, and *Trilobosporites trioreticulosus*. *Retitricolpites georgensis* and *R. vulgaris* are angiosperms and confine the depositional age to the Late Albian.

Drilling Samples

Palynological sampling was attempted from cuttings of the WF 1P-1-15-19 well in 1-15S-19E. However, the material appeared to contain abundant up-hole cavings and was unsuitable for analysis.

Stratigraphic Implications

The palynology data have important implications to the regional stratigraphy of the Dakota Formation in the study area. Previously, the channel sandstones, carbonaceous shales, and coal deposits in the upper part of the Dakota Formation of east-central Utah have been interpreted as Middle Cenomanian in age (Molenaar and Cobban, 1991; Carroll, 1992; Cushman, 1994). Although unsupported by biostratigraphic evidence, the lower Dakota Formation in the study area was thought to be Late Albian-Early Cenomanian in age (Currie, 2002). Our data, however, indicate that the upper Dakota Formation is Late Albian-Early Cenomanian in age, while the lower Dakota Formation is Late Albian. This is significant as it indicates the lower/upper Dakota unconformity is confined to the Late Albian. It also indicates that the Dakota Formation in the study area is correlative to the Albian-aged Dakota Formation and Lower Cenomanian Mowry Shale in the northern part of the Uinta Basin (Currie, 2002).

CORRELATION MODEL

This study required the correlation (figure 10) of the following intervals from shallowest to deepest: Dakota Silt to Dakota Formation, Dakota Formation, Cedar Mountain Formation and Buckhorn Conglomerate Member where present. The correlation model was primarily developed from field work in this study but is also based on lithologic descriptions of other authors including Stokes (1952), Young (1960), Currie (1998, 2002), Kirkland et al. (1997), Anderson and Harris (2006), and Kirkland and Madsen (2007).

The correlation area was expanded from the original area of interest (Year One Report) to include the locations of outcrops where a scintillometer was used to acquire gamma ray data (figures 1 and 10). Outcrop gamma ray logs and their

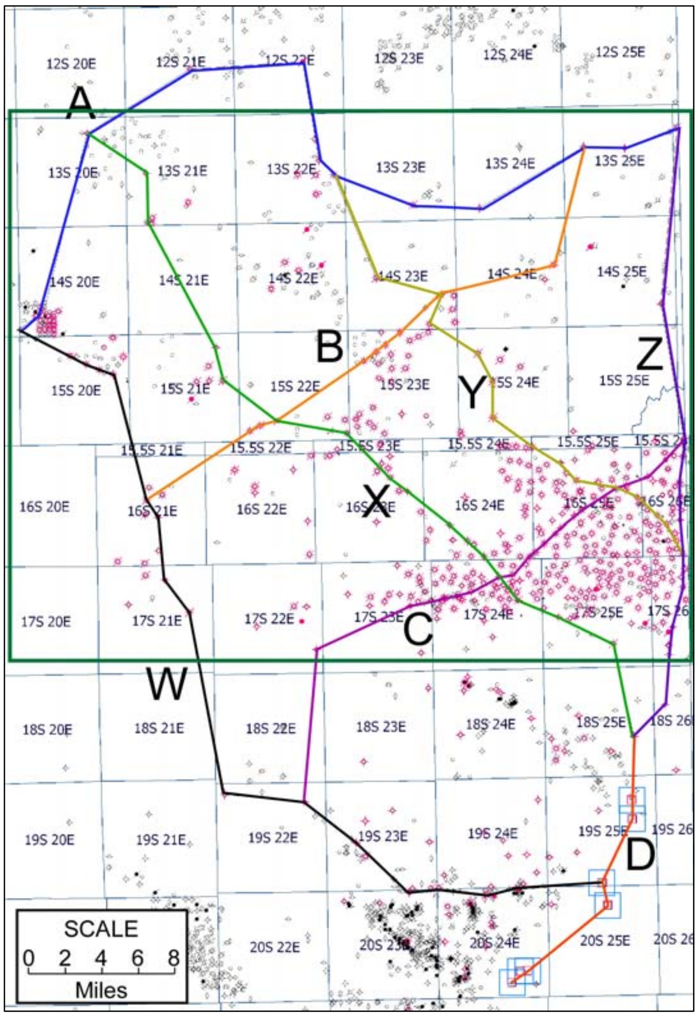

Figure 10. Map showing lines of stratigraphic correlation in the study area. The green box outlines the study area for the Year One Report. Blue squares represent outcrops. Red dots identify the wells that were correlated as part of this study. The colored lines show the correlation envelope that was used as the correlation basis. The cross sections are included in Appendix 1. Click on cross section letter to hyperlink to section.

corresponding section descriptions were used as the primary basis for the correlation model. An outcrop gamma ray log through the CMD interval was acquired at the Westwater locale immediately down section from the lower Mancos interval described and logged by Anderson and Harris (2006). The two were combined to provide complete outcrop gamma ray log coverage from the top of the Morrison Formation to the top of the Dakota Silt (figure 11).

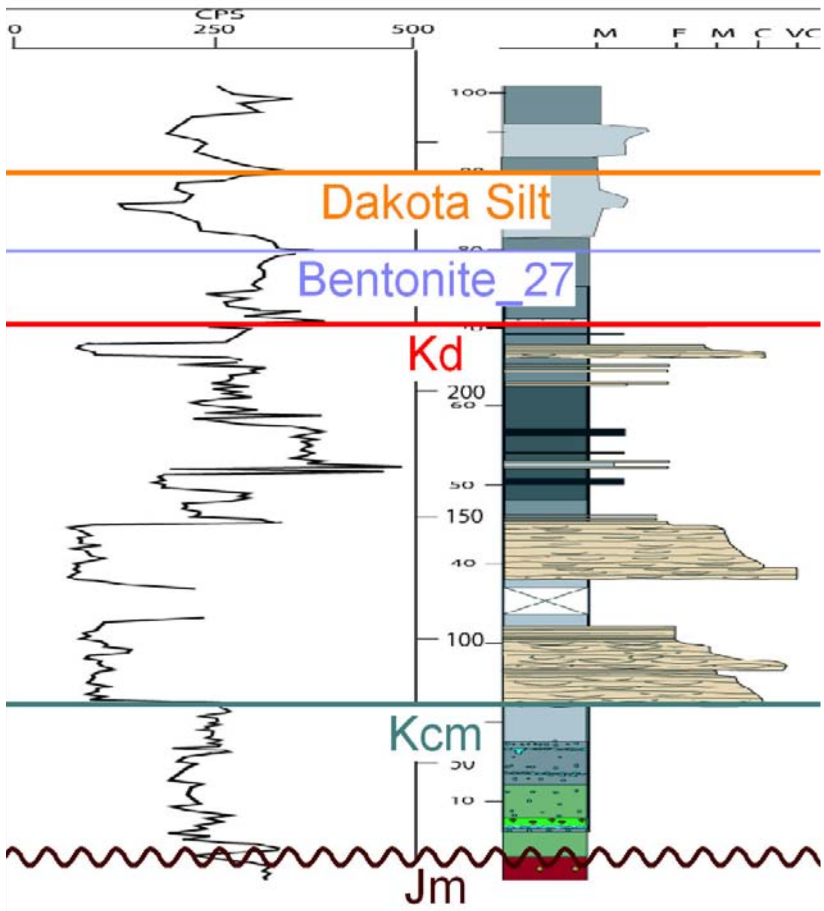

Figure 11. Westwater outcrop measured section and gamma ray log. Stratigraphic unit tops correlated in this study include the Dakota Silt, Dakota Formation (Kd), Cedar Mountain Formation (Kcm) and the Morrison Formation (Jm). The Buckhorn Conglomerate (Kbb) was correlated where it occurs in the northwest part of the subsurface study area. Bentonite_27 was identified and regionally correlated by Anderson and Harris (2006). See figure 3 for lithological symbols.

The Dakota Silt (Coon Springs Sandstone of the Tununk Member, Mancos Group) was used as the correlation datum for the subsurface. The top of the Cedar Mountain Formation was used as datum for Cross Section D as the Dakota Silt and lower Mancos were eroded or covered at some outcrops.

The thickness of the CMD interval is approximately 200 feet over most of the study area but thickens to approximately 350 feet in the extreme northwest of the study area where the Buckhorn Conglomerate is present. In the following discussion, the log character of the Dakota Silt will be described first as all wells were hung on this datum during correlation. The correlation model for the CMD interval will be described from the top down. This inverted description is used as it more closely coincides with how these rocks are correlated on well logs.

Dakota Silt

The datum for the cross sections used to correlate well logs is the Dakota Silt (Coon Springs Sandstone of the Tununk Member of the Mancos Shale), which has been historically used by the oil and gas industry as a reliable datum. In the study area, the Dakota Silt-Dakota Formation interval ranges in thickness from about 60 feet in the extreme southeast to a maximum thickness of about 110 feet in the west. The average thickness is 85 feet. We define the Dakota Silt datum as the gamma ray peak above a coarsening upward section near the base of the lower Mancos Shale. Figure 11 shows this pattern in the outcrop gamma and figure 12 is an example from the subsurface with open-hole logs.

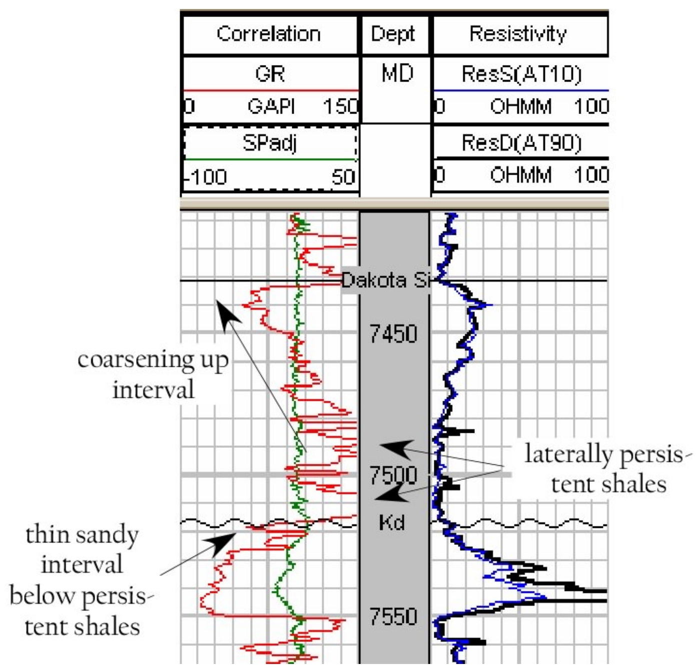

Figure 12. Log showing criteria for picking the Dakota Silt datum and the top of the Dakota Formation.

Dakota Formation

The Dakota Formation is not broken into any members in our study area but overall, we identify three systems that have differing log patterns. The top of the Dakota Formation frequently is marked by an upward-fining sandstone that can often be correlated to offset wells. Where this sandstone does not occur, the entire log character of the middle to upper parts of Dakota Formation is serrated in nature. This pattern results from the intercalated carbonaceous shales, coals, and crevasse splay/channel sandstones that make up the interval. Infrequently, thicker sandstone channels with a fining-upward profile may occur but are rarely correlatable between wells. The lowest part of the Dakota Formation is often defined by an overall blocky sandstone that fines-upward at the very top. It can commonly be correlated to offset wells.

The criteria for picking the top of the Dakota Formation remains essentially the same as was described in the Year One Report (McPherson et al., 2006):

"The criteria for picking the top of the Dakota Formation was made in collaboration with Dr. Donna Anderson and Nicholas Harris of the Colorado School of Mines who are conducting a UGS-funded project on the overlying Lower Mancos Shale. Anderson and Harris (2006) identified a bentonite bed (Bentonite_27) that is regionally persistent and occurs above the unconformity between the Mancos Group and the underlying Dakota Formation. The top of the Dakota Formation is defined at the coarsest part of the first silt or sandstone that is immediately below laterally persistent shales (figure 13). If the persistent shales lie immediately on top of a thick Dakota sandstone, the top of the Dakota Formation is placed at the top of the sand. In outcrops, there is commonly a thin lag deposit that marks the top of the Dakota Formation and our picks are designed to reflect that boundary. In the western part of the study area, the top of the Dakota Formation coincides with the basal Mancos (MTUNC) unconformity as defined by Anderson and Harris (2006)."

The gamma ray and/or high-resolution resistivity curves were used to correlate the top of the Dakota Formation. Figures 11 and 12-13 show the contact in outcrop and the subsurface, respectively. During the correlation exercise, it became apparent the interval from the Dakota Silt to Dakota Formation thinned to the southeast and that marginal-marine deposits occur in the central eastern part of the study area. Marine shales immediately overlying the Dakota Formation in the north area disappear to the south. This required a "jump" in our correlation of a high-frequency progradational cycle (10-15 feet) in the east-central part of the study area to maintain fluvial sandstones as part of the Dakota Formation. As we correlated westward, we tried to consistently keep track of an interpreted transgressive lag deposit that in places was at the same stratigraphic level as upper Dakota fluvial sandstones. However, there were spots were this thin bed becomes amalgamated with an overlying silty interval and the top of the Dakota Formation was placed at the top of this thicker, silty bed. These "jumps" in the west part of the study area did not change the thickness of the Dakota Silt to Dakota Formation by more than a few feet.

The middle of the Dakota Formation is often marked by a serrated log character, which is the result of thinly bedded coals, carbonaceous shales and thin crevasse splays (figure 13). Occasionally, channel sandstone may occur but is rarely correlatable between wells indicating a low width-to-thickness ratio.

The lowest pattern, which is not present everywhere, is a blocky gamma ray profile that fines upward (figures 12 and 13). Its profile is similar to that displayed by the Buckhorn Conglomerate (see below) but is thinner and can often be correlated between wells. In outcrop, these sandstone complexes evince scouring events and erode into the Cedar Mountain Formation. In the central part of the study area, the Cedar Mountain Formation appears to be completely eroded by one of these systems (figure 13).

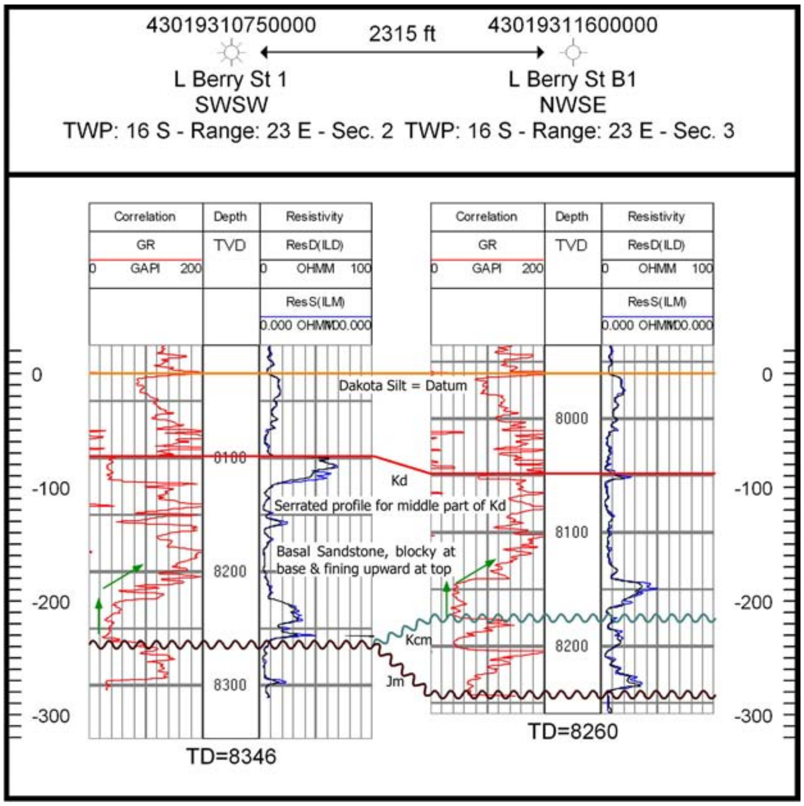

Figure 13. Gamma ray and resistivity logs of the Dakota Formation showing the serrated pattern of the middle Dakota interval and log signature of the basal Dakota sandstones.

Cedar Mountain Formation

"Upper Shale"

The Yellow Cat, Poison Strip Sandstone, and Ruby Ranch members of the Cedar Mountain Formation have been identified in outcrops along the southern part of the study area. However, lithological similarities between the Yellow Cat and Ruby Ranch members, as well as similar log signatures between the Poison Strip Sandstone and other Cedar Mountain Formation channel deposits, precludes differentiating individual members in the subsurface. For this reason, the upper members of the Cedar Mountain Formation are grouped as the "Upper Shale" in our sub-surface correlations.

Correlating the Upper Shale in the subsurface has always been a challenge and commonly requires access to quality sample descriptions. Six outcrop gamma logs were acquired across the Morrison Formation/Cedar Mountain Formation (LK-1 Unconformity) and the Cedar Mountain Formation/Dakota Formation (LK-2 Unconformity) contacts to evaluate the usefulness of the gamma ray for correlating these intervals. Figure 14 shows the locations of the outcrops and figure 15 is a cross section displaying the gamma ray profiles and the contacts observed in the field.

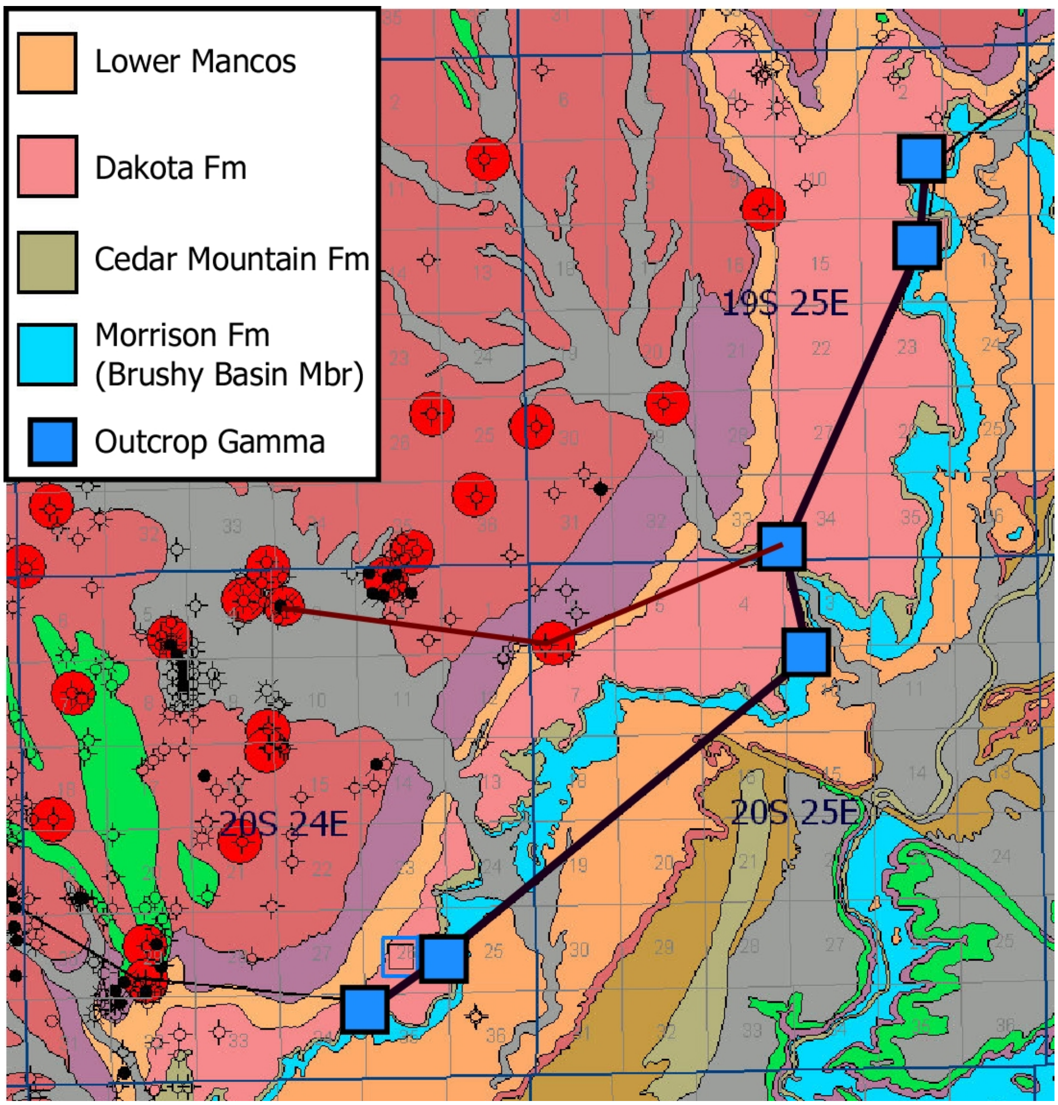

Figure 14. Geologic map of the Westwater area (Gualtieri, 1988) showing the location of the outcrop gamma ray logs (blue squares) constructed as part of this study. Black line marks the cross section displayed in figure 15; brown line is the cross section shown in figure 19.

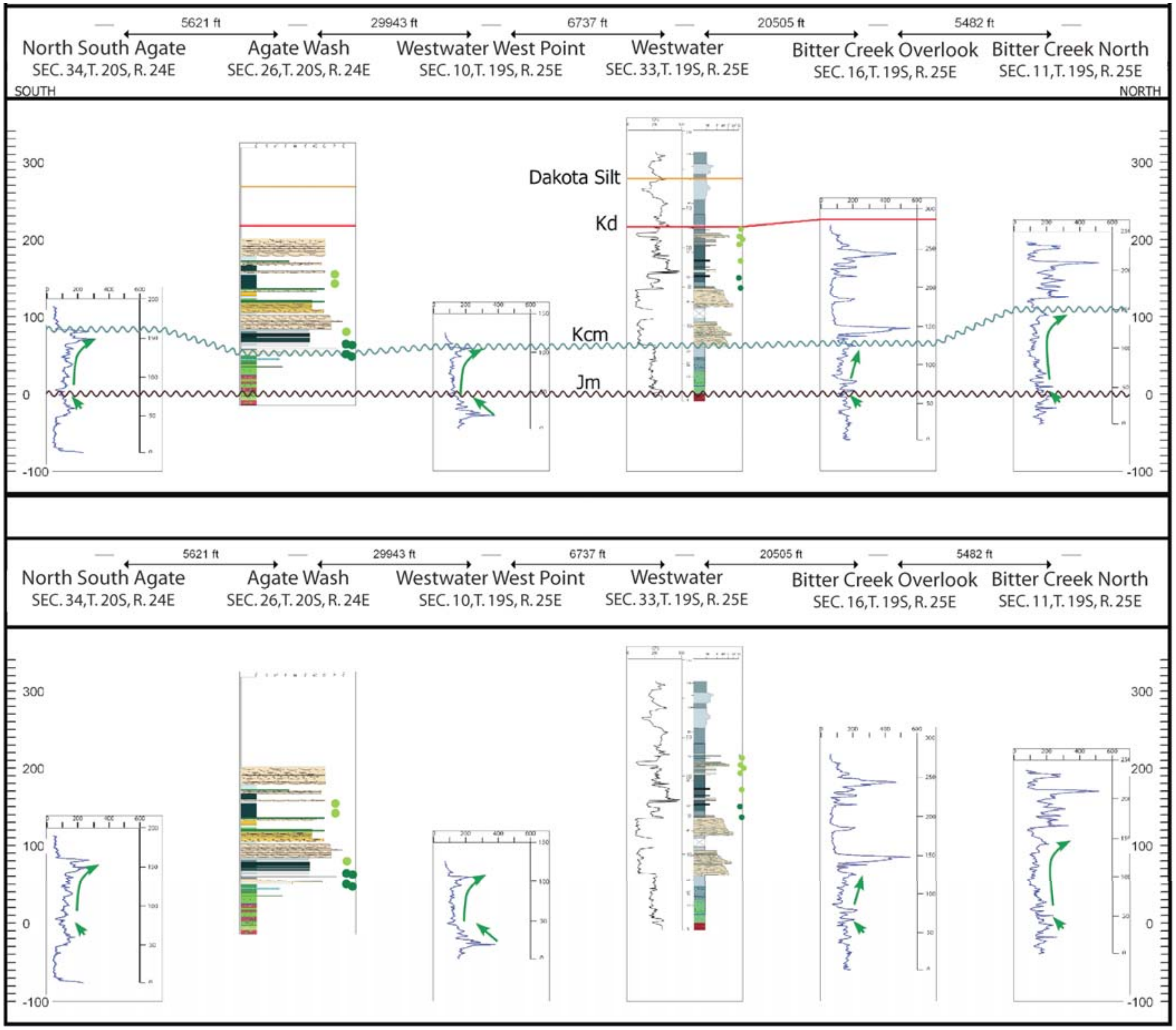

Figure 15. Cross section of outcrop gamma ray logs in the southeastern part of the study area. These sections show a consistent gamma ray signature for the Upper Shale and its contacts. The lower panel provides a clear view of the gamma signatures. The cross section location is shown in figure 14. See figure 3 for lithological symbols.

Overall, the Upper Shale exhibits a fining-upward log gamma ray signature. The base of the Upper Shale is placed at the top of the final apparent coarsening-upward gamma ray profile at the Morrison-Cedar Mountain contact (as documented in study area outcrops; figure 15), or at the top of the Buckhorn Conglomerate, where present.

The upper part of the Upper Shale is marked by increased smectite towards the Dakota Formation contact, which accounts for the apparent fining-upward signature. There is also diminished carbonate in the system that could be an indication of a wetter climate. However, there is evidence that carbonate nodules have been replaced by silica (Currie, 2002). Organic-rich fluids that were expelled from the carbonaceous-rich intervals of the Dakota Formation are probably responsible for the carbonate dissolution and the smectitic enrichment. The top of the Cedar Mountain Formation is put at the top of a high gamma ray peak.

Multiple discrete paleosols, accompanied by numerous calcrete nodules occur low in the interval and the occurrence of calcium carbonate diminishes up-section. In the middle of the Upper Shale, channel sandstones up to 60 feet thick may occur but are rarely correlatable with offset wells. The channels in the study area are likely similar to those exhumed south of Green River, Utah, on the eastern side of the San Rafael Swell (figure 16; see figure 1 for location). Harris (1980) mapped the exhumed channel systems that occur approximately 10 miles south of Green River, Utah. These channels are less than 700 feet across and exhibit a maximum width-to-thickness ratio of approximately 10 (Harris, 1980). Closer to the study area, Poison Strip Sandstone channels exhibit width-to-thickness ratios of 20 to 100 (Stikes, 2007) and Ruby Ranch Member sandstone channels exhibit width-to-thickness ratios of 10 to 25, more similar to those described by Harris (1980).

Buckhorn Conglomerate

The Buckhorn Conglomerate does not crop out along the southern part of the study area outcrop belt. Currie (1997) postulated that the Buckhorn Conglomerate was deposited in an approximately 20 mile wide paleovalley that can be traced across the Uinta Basin from the north flank of the San Rafael Swell to the southern Uinta Mountains region near Dinosaur, Colorado (figure 1). Figure 17 is an outcrop gamma ray log from the Buckhorn Conglomerate that was obtained on the northeastern part of the San Rafael Swell (Location GRC, figure 1). The log shows a blocky gamma ray signature with a thin mudstone interval in the middle and a fining-upward profile at the very top. This pattern appears to persist into the subsurface as is shown in figure 18.

Figure 16. Aerial photograph of an exhumed Cedar Mountain Formation channel approximately 10 miles south of Green River, Utah. This channel is ~700 feet wide at its widest point. The red arrow points to the channel. Photograph is from Ankyman (2007).

In our correlations, we identified the Buckhorn Conglomerate only in the northwest part of the subsurface portion of the study area. There are some basal Cedar Mountain channels in the eastern part of the study area but there are no well-defined channel complexes. These channels appear to be quite narrow and we are unsure as to how these sandstones correlate time-wise to the Buckhorn Conglomerate. However, the basal sandstones in the Cedar Mountain Formation in the eastern part of the study area may be age-correlative to the Poison Strip Sandstone as described in the Moab area by Kirkland et al. (1997) and Kirkland and Madsen (2007).

Basal contact with the Morrison Formation

Field observations assisted us in developing a correlation model for the top of the Morrison Formation. The outcrop gammas show a subtle, but consistent C-shape from the upper-most part of the Morrison to the Upper Shale contact with the Dakota Formation. As figure 15 illustrates, the overall pattern at the top of the Morrison Formation is "coarsening-upward" and the pattern of the Upper Shale is "fining-upward." The base of the Cedar Mountain Formation is put at the turnaround from the apparent coarsening-upward to the apparent fining-upward when the Buckhorn Conglomerate is not present. There appears to be a deviation from this pattern when thick basal Dakota Formation sandstone lies directly on the Morrison Formation. In this case, there may be a 2 to 10 feet thick interval of smectitic enrichment (identified by a gamma ray peak); similar to what is observed when Dakota Formation sandstone lies on top of the Cedar Mountain Formation.

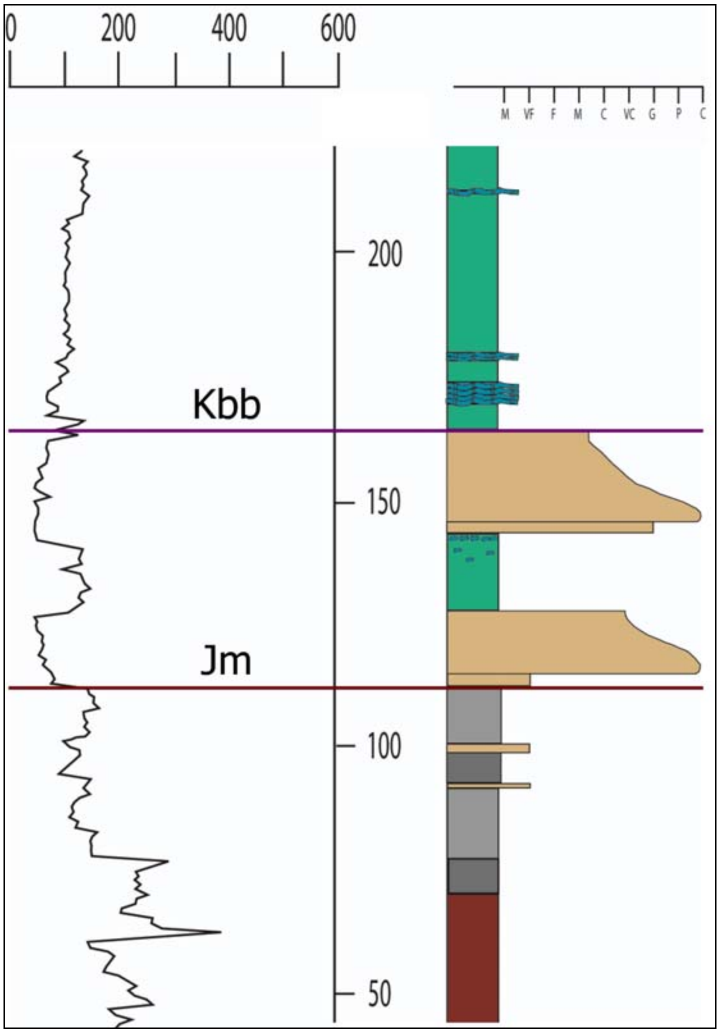

Figure 17. Outcrop gamma over the Buckhorn Conglomerate (Kbb). The outcrop is located on the northeastern edge of the San Rafael Swell and the location is shown in figure 1. See figure 3 for lithological symbols.

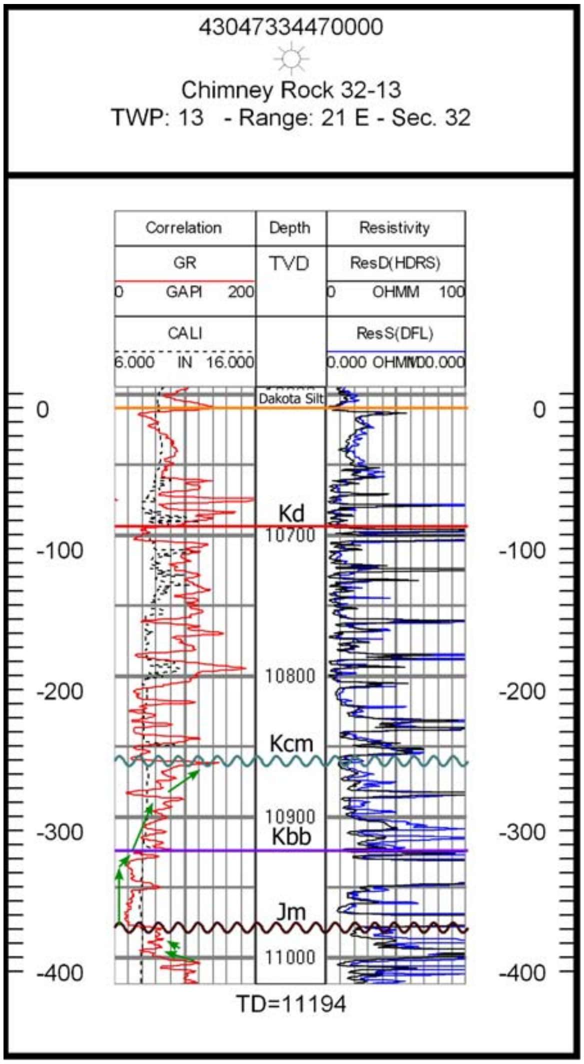

Figure 18. This well also shows the gamma ray pattern for the top of the Morrison (Jm) and the fining-upward pattern used to correlate the top of the Cedar Mountain Formation (Kcm) including the Buckhorn Conglomerate (Kbb). The Dakota Formation (Kd) has a basal sandstone package overlain by an interval with a serrated gamma ray pattern.

A regionally-extensive paleosol or weathered horizon occurs at the top of the Morrison Formation in outcrops across the Colorado Plateau (Currie, 1997; Demko et al., 2004). The very top of this paleosol is leached of clays and indurated with calcium carbonate, thereby causing an apparent coarsening-upward trend on the gamma ray. In the subsurface, this gamma ray profile is accompanied by a slight increase in resistivity on the high-resolution curve with no deflection of the SP (figure 19).

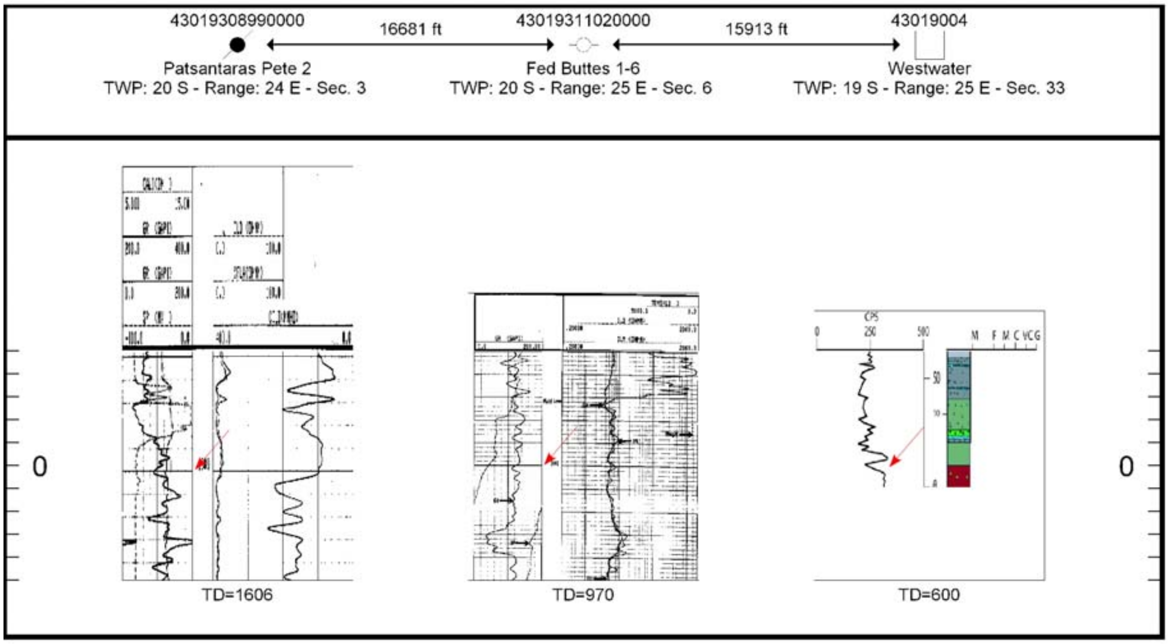

Figure 19. Cross section showing correlation of subsurface and outcrop gamma ray logs across the top of the Morrison Formation. The red arrow points to the top of the Morrison Formation. A subtle coarsening-upward trend is observed immediately below the top. The location of the cross section is shown in figure 14.

This paleoweathering effect is not as pronounced when a Morrison Formation channel lies directly below the Cedar Mountain Formation. Rarely, an Upper Shale channel (i.e. Poison Strip Sandstone) has eroded the paleosol. This has been identified in the field near Moab and between Green River and Crescent Junction, Utah (Kirkland and Madsen, 2007; see figure 1 for locations), and at one place in our study area near the section logged in Sec. 33,T.19S,R.25E. In the subsurface, it is problematic where to put the base of the Upper Shale when sandstone is present at or near the contact: Is it at the top of the channel or the base of the channel? In this study, adjacent logs were viewed to assist in where to place the contact.

WELL CORRELATION

The correlation model described above was used to correlate the wells in the study area. The vast majority of wells were correlated with raster logs provided by MJ Systems. Digital logs were supplied by operators Bill Barrett Corporation, Miller Dyer & Co., EOG Resources, Inc., Slate River Resources and some well digits were purchased from Centerline Data. Digits were also supplied by Dr. Donna Anderson for wells that were included in the UGS funded study of the Lower Mancos (Anderson and Harris, 2006).

A correlation envelope was developed by constructing eight cross sections, which are contained in Appendix 1. The cross section locations are shown in figure 10 and on the front piece of Appendix 1. Wells interior to the correlation envelope were then correlated. Wells that were faulted in the CMD interval, appeared to be deviated, or those with poor-quality logs, were not used in the correlation exercise.

Tops may be off in old wells with E-logs and old neutron logs. Bed resolution may be insufficient to define the subtle patterns that we looked for. These wells were compared with offset wells to minimize misinterpretation. An uncertainty is also introduced in many older wells where the logs are off depth from each other or the scanned image was extremely skewed. Usually, the gamma ray was used to pick tops. However, in few instances, the gamma ray quality was very poor and the resistivity log was used for the correlation.

Correlations of the five key intervals were quality checked by constructing isopach and structure contour maps of each horizon. These maps where constructed in Geographix Software and the following parameters: gridding algorithm = “Minimum curvature,” forced data honoring was implemented, “Max iterations” = 100, convergence = 0.01 and “simplified defaults” was selected for grid spacing. The maps were constructed for quality control purposes only and no bias was introduced. No hand editing of contours was performed. The following isopachs are included in Appendix 2: Dakota Silt, Dakota Formation, Cedar Mountain Formation, and Buckhorn Conglomerate. Isopachs of “top to top” intervals Dakota Formation plus Cedar Mountain Formation, Dakota Silt to Cedar Mountain Formation and Dakota Silt to Morrison Formation were also constructed. The measured depth tops for each correlated well are contained in Appendix 3.

POTENTIAL RESERVOIR ARCHITECTURE

Exposures of the Dakota Formation were mapped and measured between the Westwater and South Agate areas (figure 1) in order to define the internal structure and lithological variability of potential reservoir sandstones. In this part of the study area, the Dakota Formation overlies the Ruby Ranch Member of the Cedar Mountain Formation. The lower Dakota Formation is incised as much as 30 feet into the Ruby Ranch Member, whereas upper Dakota fluvial channels are incised as much as 50 feet into the lower Dakota. In some places, the upper Dakota completely erodes the lower Dakota sequence and rests directly on the Cedar Mountain Formation. In most parts of the mapped area, lower Dakota channel sands are erosionally truncated by upper Dakota channel sands, forming vertically amalgamated channel complexes up to 100 feet thick.

As part of this study, where possible, the lateral dimensions of individual Dakota channel complexes were mapped along the outcrop belt. In addition, photo mosaics of well-exposed, vertical outcrops of the basal Dakota interval were constructed and used to map lateral and vertical variations in lithofacies and the geometry of bounding surfaces separating individual lithofacies and lithofacies assemblages. Multiple stratigraphic sections for each outcrop-photo mosaic were measured to document the thickness and vertical grain-size variability of Dakota Formation channel complexes. Paleocurrent indicators were measured during both the outcrop and photo-mosaic mapping exercises to document Dakota fluvial system paleo-flow orientations.

Lateral Channel Dimensions

The lateral dimensions of channel deposits were mapped in detail near the South Agate outcrop locality (figure 1) along the Dakota Formation outcrop between Sec. 4, T. 21S, R. 24E and Sec. 26, T. 20S, R. 24E. In this locality, channel sandstones of the basal part of the upper Dakota Formation are well exposed and unconformably overlie channel and overbank deposits of the lower Dakota and Cedar Mountain Formations. Along the three-mile length of the Dakota Formation outcrop in the mapping area, four individual upper Dakota channel sandstones were identified (figure 20). Individual channel sands consist of single storey, upward-fining packages of beds of cross- and horizontally-stratified sandstone deposited by migrating dunes and downstream/laterally migrating bar forms. Conglomeratic beds are present along channel bases. Paleocurrent orientations from individual channel segments shows approximately 180° of variability between east and west, most likely reflecting the original sinuosity of the Dakota fluvial systems. Average paleocurrent orientations however are directed toward the N-NE.

The measured flow-perpendicular widths of observed upper Dakota Formation channel sandstones are between 600 and 3000 feet. The maximum thickness of the observed channels ranges from 25 to 45 feet. Width/thickness ratios of these channel sands range from 24 to 67. The dimensions of the upper Dakota channel forms near Agate are similar to those in both the lower and upper Dakota Formation throughout the study area. Near Westwater (figure 1), however, lateral amalgamation of channel sands similar to the dimensions observed near Agate results in sheet sand bodies that are up to 5000 feet wide with width/thickness ratios between 50 and 125.

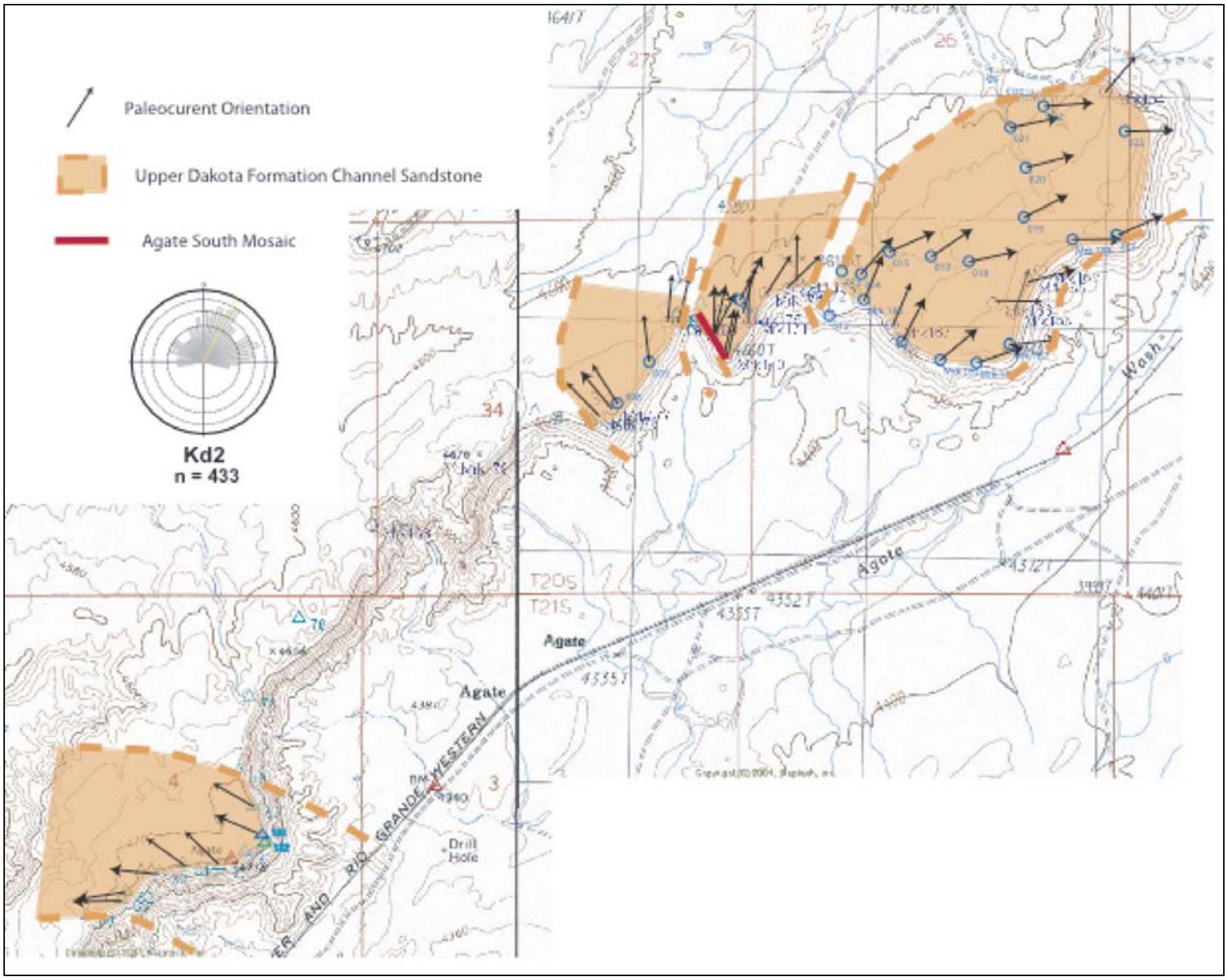

Figure 20. Map of South Agate outcrop area showing interpreted dimensions and paleocurrent orientations of basal upper Dakota Formation fluvial channels. Paleocurrent azimuths are averages of at least 10 measurements per station.

Architectural Profiles

Photo mosaics of well-exposed, vertical channel sandstone outcrops of the basal Dakota interval were constructed at both the Westwater West Point and South Agate outcrop localities. Descriptions and interpretations of these outcrop localities are listed in more detail below.

Westwater West Point (NW 1/4, Sec. 10, T. 20S, R. 25E)

Plate 1 shows a detailed photo mosaic of the lower part of the Dakota Formation from the western point of a ridge above Westwater Creek. At this location, about 40 feet of fluvial channel sandstones and conglomerates of the lower Dakota Formation rest unconformably above the Cedar Mountain Formation. The lower Dakota channel complex, however, is erosionally truncated by the basal channel conglomerates and sandstones of the upper Dakota Formation, which cut out all but the lower 3 feet of the lower Dakota in the center part of the outcrop.

Lower Dakota channel deposits consist of an overall upward-fining sequence of conglomerates and coarse- to fine-grained sandstones (plate 2). Sedimentary structures in the lower Dakota include trough- and planar-cross stratification, horizontal stratification and ripple-cross lamination (table 5). Paleocurrent orientations, measured from the orientation of trough axes and foresets, indicate an E-NE direction of paleo-flow. The orientation of surfaces bounding individual cross sets indicates deposition by in-channel dunes and downstream-accreting marcroforms (cf. Miall, 1996).

The basal channel sandstones of the upper Dakota Formation in the Westwater West Point outcrop contain at least three vertically amalgamated-channel complexes. Each channel complex contains a conglomeratic base with abundant chert and quartzite pebbles as well as mudstone and sandstone rip-up clasts. Sandstones are primarily coarse to medium grained, with sedimentary structures including trough-cross stratification, horizontal stratification and ripple-cross lamination. Paleocurrent orientations indicate a bimodal NW-SW direction of paleo-flow. The presence of silty, flaser-bedded ripples on trough foresets, as well as, herringbone-cross stratification from the middle part of the upper Dakota channel complex, may indicate a possible tidal influence on deposition. The orientation of surfaces bounding individual cross sets indicates deposition by migrating dunes and both downstream and lateral accreting marcroforms (cf. Miall, 1996).

South Agate (NE 1/4, Sec. 34, T. 20S, R. 24E)

Plate 3 shows a detailed photo mosaic of the lower part of the Dakota Formation from the South Agate outcrop locality. At this location, approximately 40 feet of fluvial-channel sandstones and conglomerates of the lower Dakota Formation rest unconformably above the Cedar Mountain Formation. Like the Westwater West Point locality, the lower Dakota channel complex at South Agate is truncated by the basal channel conglomerates and sandstones of the upper Dakota Formation. The upper Dakota channel erodes down through the entire lower Dakota Formation and into the Cedar Mountain Formation in the southeast part of the outcrop.

Table 5. Lithofacies documented at Westwater West Point and South Agate outcrop localities. See Plates 1-4 for distribution.

Lithofacies Code	Description
Fm/Sm	Interbedded, structureless sandstone and mudstone
Sr/Sh/Fm	Ripple–cross laminated and horizontally stratified sandstone with 1-3 cm thick beds of intercalated mudstone
Sr/Sh	Ripple–cross laminated and horizontally stratified sandstone
St/Sh, herringbone-cross stratification, flaser-bedded Sr	Intercalated trough–cross stratified/horizontally stratified/ herringbone-cross stratified sandstone; silt-draped ripple-cross laminations on trough foresets
St/Sh	Trough-cross bedded and horizontally bedded sandstone
St/Sh/Sm	Interbedded cross trough-stratified, horizontally stratified, and structureless sandstone
St/Sm/Sh, rip-up clasts, soft-sediment deformation	Interbedded horizontally laminated, trough-cross stratified, and structureless sandstone, with abundant mudstone/sandstone rip-up clasts, and liquefaction features
St w/ pebbles	Trough-cross bedded sandstone with scattered pebbles
Gm/Fm	Clast supported, structureless conglomerate overlain by structureless-laminated carbonaceous mudstone
Gcm/Gct	Clast supported, structureless and trough-cross bedded pebble-cobble conglomerate

Lower Dakota channel deposits consist of an overall upward-fining package of conglomerates and coarse- to fine-grained sandstones (plate 4, table 5). Sedimentary structures in the lower Dakota Formation include trough- and planar -cross stratification, horizontal stratification and ripple-cross lamination. Paleo-current orientations, measured from the orientation of trough axes and foresets, indicate a NE direction of paleo-flow. The orientations of surfaces bounding individual cross sets indicate deposition by in-channel dunes and both lateral- and downstream-accreting marcroforms (cf. Miall, 1996).

The basal sandstones of the upper Dakota Formation in the South Agate outcrop consist of one upward-fining channel form. The base of this channel contains abundant chert and quartzite pebbles, as well as mudstone and sandstone rip-up clasts. Sandstones are primarily coarse to fine grained, with sedimentary structures including trough-cross stratification, horizontal stratification and ripple-cross lamination. Paleocurrent orientations indicate a northeast paleo-flow direction. The orientation of surfaces bounding individual cross sets indicates that most of the upper Dakota channel was deposited by lateral accreting marcroforms, with downstream accreting bars and dunes comprising the upper 25% of the exposure (cf. Miall, 1996).

Paleocurrent Orientations

Paleocurrent orientations measured from Dakota Formation sandstones across the entire study area indicate an overall northeast direction of paleo-flow (figure 21). Orientations were measured from the dip direction of foresets in planar and trough cross-stratified sandstones or from the orientation of trough axes, where observed. Lower Dakota Formation channels in the study area have an average paleo-flow direction of 050° while Upper Dakota channels have an average paleo-flow direction of 025°.

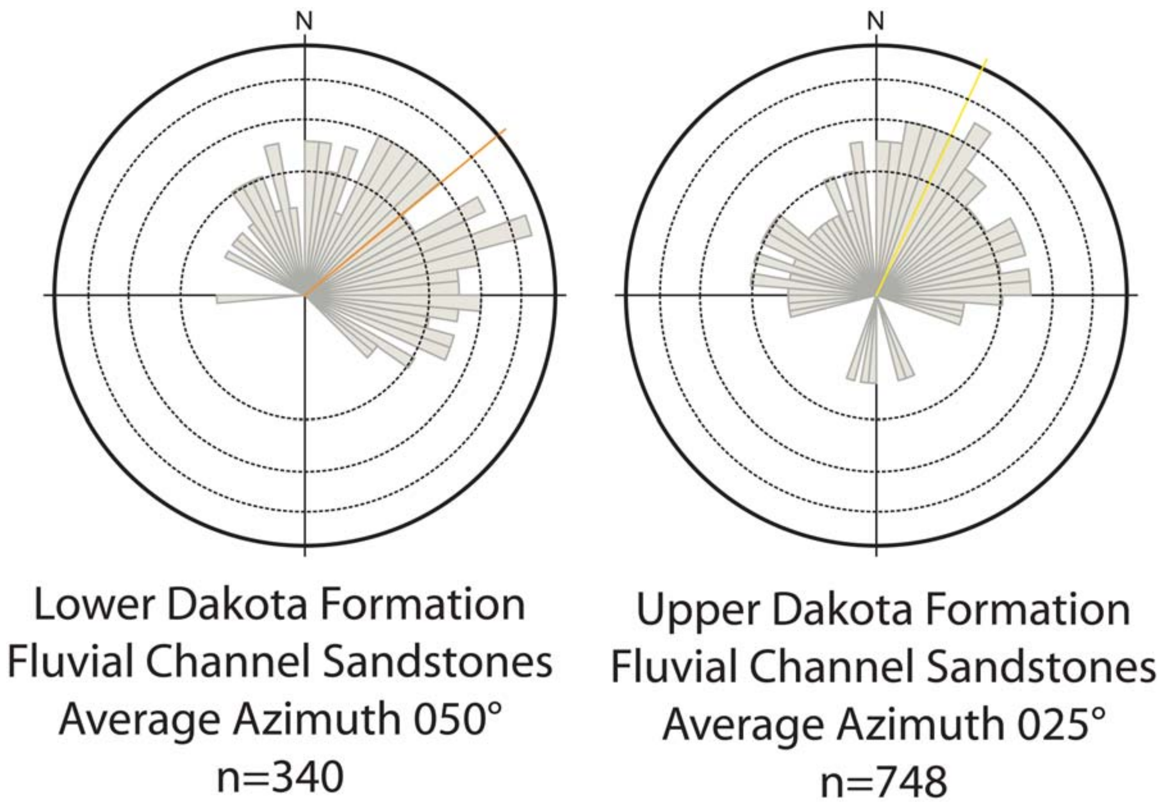

Figure 21. Paleocurrent orientations measured from Dakota Formation fluvial channel sandstones. Circular scale in 2% increments with 5° radial grid intervals. Rose diagrams constructed using the software of Thompson (2004).

POROSITY AND PERMEABILITY

A porosity and permeability database was constructed from ten conventional core analyses, one sidewall core analysis, and two plugs cut from outcrop locations within the CMD stratigraphic interval (Appendix 4). In addition, thin sections from four additional cores were visually inspected to provide porosity values. Data from wells near the study area in Utah and Colorado augmented the database as there is a lack of cored data within the study area. Figure 22 shows the well and outcrop locations where porosity and permeability data were acquired and table 6 lists the wells that were used in the analysis. The sources for this database include the USGS Colorado Core Research Center, the Utah Division of Oil, Gas and Mining, and the Colorado Oil and Gas Conservation Commission databases at their respective websites.

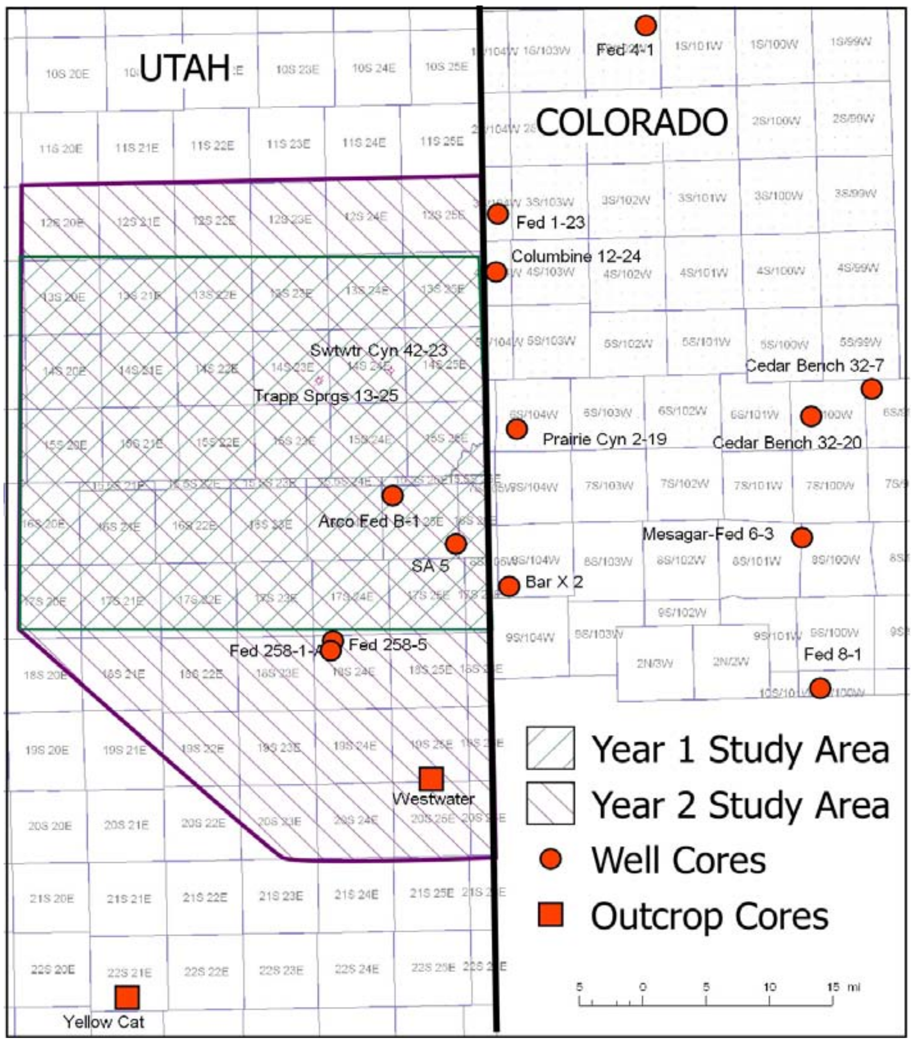

Figure 22. Map showing the locations of wells and outcrops with core data.

Table 6. Well information and production data for cores used to construct the porosity and permeability database.

Well ID	Original Operator	Well Name	Location	Core Type	Top Core Depth	Bottom Core Depth	KB	TD	Surf. Elev.	Comp. Date	Status	1st Prod	Cum Oil, BBLS	Cum Gas, MCF	Water, BBLS	Perforated/ Test Interval	Initial Production
05045060370000	Fuel Resource	Prairie Canyon 2-29	29-6S-104W	C	5325	5493	7012	5864	7001	Nov-73	G	Nov-86	0	554,686	0	5424-5745	130 MCFD
05045062620000	Dyco Petroleum	Mesa Gar Fed 6-3	6-8S-100W	C	7893	8029	7651	8125	7639	Nov-81	G, SI	Never				7877-7991	20 MCFD
05045067390000	NARCO	Cedar Bench 32-7	7-6S-99W	T	8990	9080	6222	9259	6624	Feb-91	P&A	Feb-91	0	31,267	1,690	8980-9030	75 MCFD
05045067600000	NARCO	Cedar Bench 32-20	20-6S-100W	T	7809	7884	6729	7997	6715	Aug-91	P&A	Nov-91	0	791,459	5,020	7798-7870	413 MCFD
05077050020000	American Metal	Bar X 2	8-8S-104W	C	3005	3027	5202	3687	5192	Nov-55	G	Oct-55	5,864	1,694,259	0	2970-3379	1.5 MMCFD
05077080260000	Mitchell Energy	Fed 8-1	8-10S-100W	C	2212	2494	4987	2500	4977	Aug-73	PA						
05103086780000	Coseka	Fed 1-23	23-3S-104W	T	6987	7121	6219	7255	6209	Jul-81	G	Sep-97	0	7,716	329	6931-69	120 MCFD
05103087150000	Coseka	Columbine 13-24	24-4S-104W	C	6348	6518	6218	6603	6208	Jun-81	G	Aug-82	6,377	2,377,643	6,649	6350-6536	595 MCFD
05103087190000	Coseka	Fed 4-1	1-1S-102W	T	5570	5689	5571	6112	5548	Jul-81	G	Mar-82	3,259	2,048,672	1,494	5484-89	2 MMCFD
43019158880000	Crescendo Energy	San Arroyo 5	25-16S-25E	C	4050	4143	5888	4940	5878	Sep-60	G, SI	Sep-60	20,194	6,145,022	371	4054-4834	2.4 MMCFD
43019303640000	Anschutz	Fed 258-5	8-18S-24E	C	3735	3748	5157	4419	5147	Jul-78	P&A						
43019304690000	Anschutz	Fed 258-1A	5-18S-24E	C	3898	3910	5218	4075	5208	Jan-79	O, P&A	Feb-79	2,455	200	13,050	3902-08	11 BOD+27 BWD
43019305520000	Lone Mt Prod.	Fed B1	6-16S-25E	C	6185	6187.5	7375	6730	7365	Feb-80	G	Feb-80	49	1,364,570	37	6090-6559	400 MCFD
43047309760000	PG&E Resources	Sweetwater Cyn 42-23	23-14S-24E	S	8384	8612	7348	8650	7360	Sep-90	P&A						
43047309780000	Coseka	Trapp Springs 13-25	25-14S-23E	C	8849	8890	7228	9125	7218	Aug-81	G, P&A	Jun-00				DST 8260-8414	Rec. 500 ft mud, no gas
43019001		Yellow Cat	28-22S-21E	OP					4700	Mar-06	OC						
43019004		Westwater	33-19S-25E	OP					4440	Mar-06	OC						

Abbreviations:

Abbreviations:	C = Conventional core analysis	P&A: plugged and abandoned	BBLS: barrels
	T = Thin section analysis	G: gas well	MCF: thousand cubic feet
	S = Sidewall core analysis	O: oil well	MCFD: thousand cubic feet/day
	OP = Outcrop plug	SI: shut in	BOD: barrels of oil/day
		OC: outcrop	DST: drill stem test

Methods for porosity and permeability data collection were not included with published core analyses, however well completion dates (table 6) can be used to infer standard laboratory methods utilized during the time of each analysis. Nelson and Kibler (2003) provide comprehensive references for core analysis techniques. Grain size data was included in all but four of the core analyses, however the accuracy of such data is unknown because reported grain sizes are dependant on the designations assigned by the original describer.

CMD core porosities range from 0.0 to 25.6 percent and core permeabilities range from <0.01 to 183 millidarcies. The 183 millidarcy measurement was obtained from an outcrop sample and likely reflects cement dissolution during weathering. In the subsurface, the maximum permeability is 105 millidarcies. Porosity values were compiled from 480 data points and have an arithmetic mean of 9.3 percent. Permeability values were compiled from 419 data points and have an arithmetic mean of 4.8 millidarcies and a geometric mean of 0.33 millidarcies.

Core data were available over the depth range of 0 to 9000 feet. This depth range was broken into 18 intervals of 500 feet each. For each well, an average porosity and permeability was calculated and then assigned to the 500-foot interval within which the core was obtained. The data were reviewed in depth versus porosity and depth versus permeability plots and two wells with deviant core analysis averages were identified: Bar-X 2 (8-8S-104W, Colorado), and Sweetwater Canyon 42-23 (23-14S-24E, Utah). Core analysis for the Bar-X well was conducted in 1955 and outdated laboratory methods are suspected as the source of discrepancy. Data for the Sweetwater Canyon 42-23 core was collected via sidewall coring and it is apparent that the sampling was high-graded. Therefore, these two wells were eliminated from the analysis. The outcrop samples have the highest average porosity and permeability measurements as expected. This is likely due to weathering of authigenic or detrital clays at the surface.

Figures 23 and 24 show the relationship of average porosity and average permeability versus depth, respectively. The relationship of porosity to depth is linear and a correlation coefficient of 0.76 was obtained in the analysis. This trend is consistent with other porosity versus depth studies: Atwater (1966), Magara (1980), Wendlandt and Bhuyan (1990), Ehrenberg and Nadeau (2005), and reflects the combined and interrelated effects of chemical compaction and cementation, and the dependence of both processes on thermal exposure (Ehrenburg and Nadeau, 2005). The relationship of permeability to depth is logarithmic with a correlation coefficient of 0.84. Porosity decreases with depth and is likely a function of increased cementation or precipitation of clays in the pore network, thereby decreasing pore throat size and permeability.

No petrographic analyses were conducted on CMD cored intervals, therefore a detailed description of diagenesis could not be inferred. Keighin et al. (1993) conducted a study on the Late Cretaceous Point Lookout Sandstone of the Mesaverde Group in the San Juan Basin of southwestern Colorado that included detailed core petrography. Findings of this paper include a paragenetic sequence for these rocks: compaction, quartz overgrowth, intergranular calcite cement, dissolution, and kaolinite precipitation. A similar pattern may have occurred for the CMD stratigraphic interval. More data needs to be collected to determine a detailed diagenetic history.

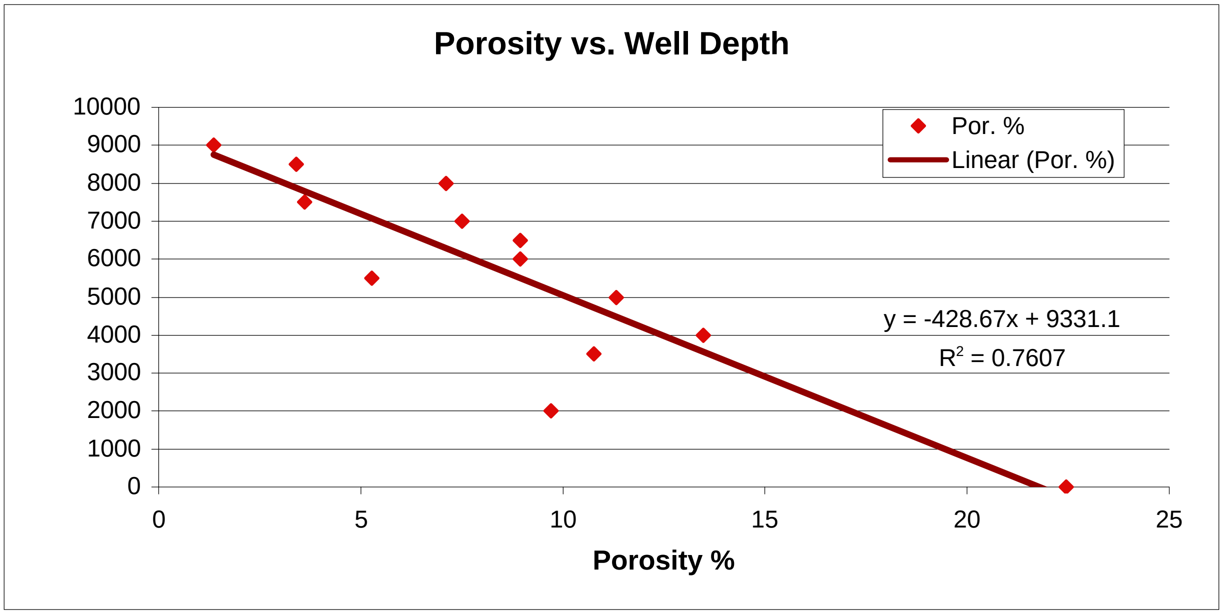

Figure 23. Plot of volume percent porosity versus well depth. Porosity values plotted are the averages of all porosity values that fall within preset 500-foot depth intervals.

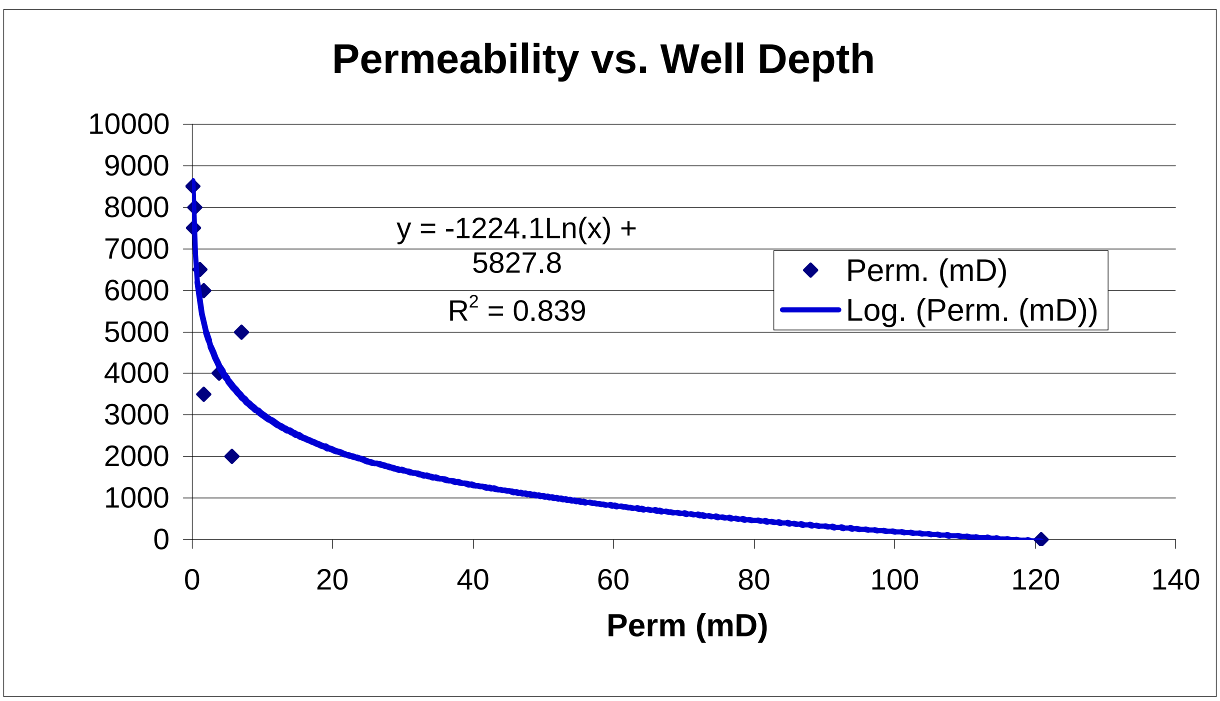

Figure 24. Plot of permeability versus well depth. Permeability values plotted are the arithmetic means of all permeability values that fall within preset 500-foot depth intervals.

To assess the grain size component in reservoir quality, all core porosity and permeability values were plotted against each other as a function of grain-size (figure 25). Although there is considerable scatter in the data, some general trends exist. Very-fine grained sands consistently plot with low porosity and permeability values. All grain sizes display a correlation between greater porosity and increasing permeability. Higher permeability corresponding to higher porosity is a fundamental characteristic of a porous media (Nelson, 1994). The strongest correlation for this trend exists in the fine to medium grained category with a correlation coefficient of 0.73. The graph also shows that coarser grain sizes cluster above the fine to medium-grained rocks indicating that permeability is related to grain size: the coarser the sandstone, the more likely it will be permeable. Figure 26 also illustrates this by comparing the arithmetic means of porosity to the arithmetic and geometric means of permeability for all grain size categories.

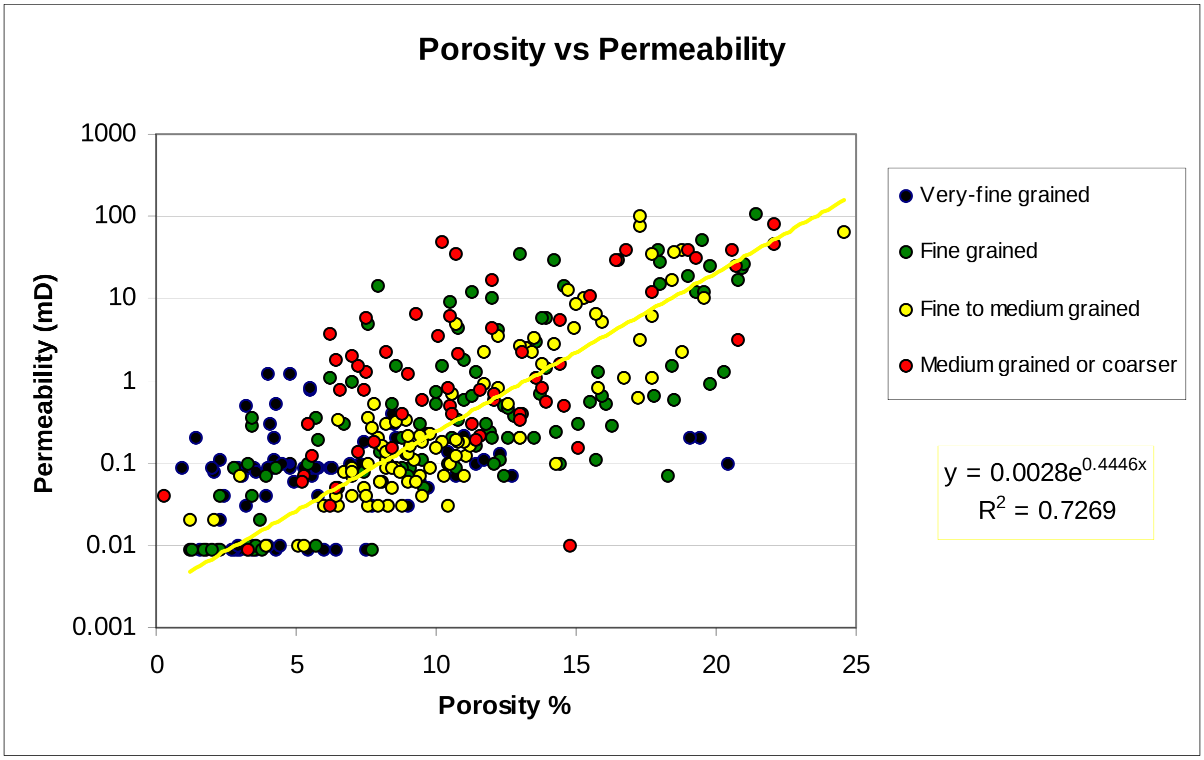

Figure 25. Plot of volume percent porosity versus permeability for 364 core data points. Values are color coded by grain size. Y-axis is a logarithmic scale. Yellow line represents exponential curve for fine to medium grained sandstone. Equation and R^2 value for curve are bordered by yellow box.

This trend between porosity, permeability, and grain size is consistent with other studies. Nelson and Kibler (2003) compiled porosity and permeability data from 70 studies conducted on cored samples from siliciclastic formations around the world. Four of these studies include data from nearby sandstone formations in the Piceance and Uinta Basins and attribute trends to depositional environment and responses of different grain sizes to compaction.

The data in this analysis are somewhat skewed as only three of the wells used in the analysis produced over 1 BCF. The majority of the data is from uneconomic or marginally economic wells. The core data analyzed in this study show a strong deterioration of reservoir-quality sandstone with depth. However, there are economic producers in the CMD interval that occur at 7000 feet or deeper. We assume that some porosity- and permeability-enhancing event has occurred in wells that are productive from greater than 7000 feet.

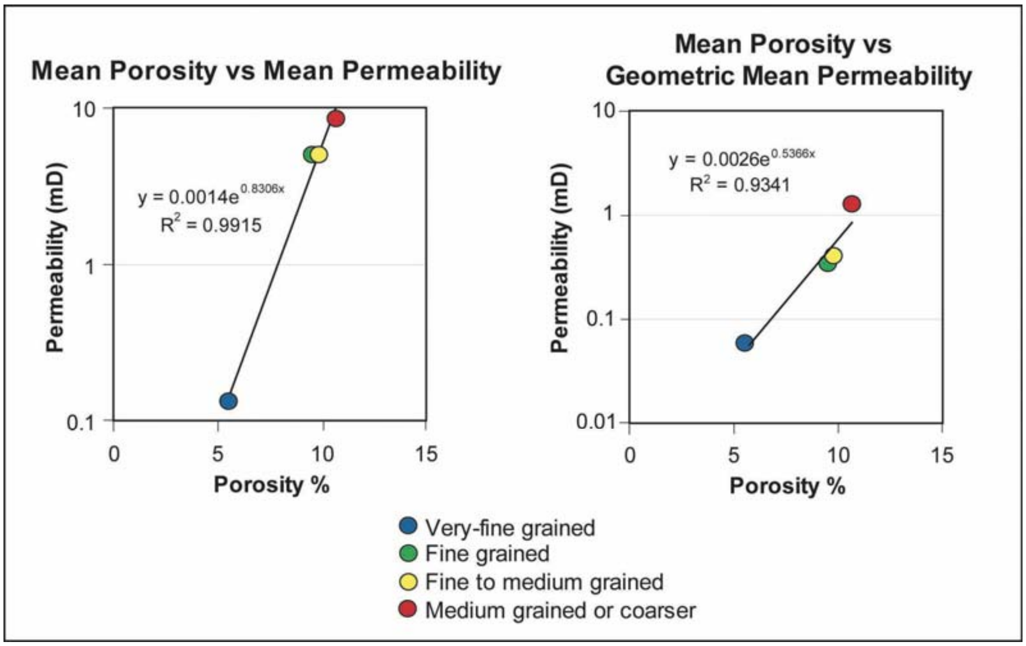

Figure 26. Plot of mean porosity versus mean permeability for grain size. Porosity and permeability values from 364 data points were divided into four grain size categories. All porosity values plotted are arithmetic means for each grain size category. Permeability values plotted are arithmetic means (left) and geometric means (right) for each grain size category.

RESERVOIR CONTROLS

A goal of this study was to identify parameters that control economic production in the CMD. The term “economic production” is applied loosely and is based on the drilling of a 9500 foot well in an area with developed infrastructure at mid-2007 Rocky Mountain gas prices of approximately $4 per MCF. At this depth, an economic well would be expected to have an initial potential of 2 MMCFD and cumulative gas production of 1.5 BCF over the life of the well (S. McPherson, Operations Manager, Natural Buttes Field, Anadarko Petroleum, Inc., personal communication, 2007). Parameters that control economic accumulations of gas include depth, stratigraphy, porosity, permeability, and reservoir architecture, which are documented in this report. Other factors such as structure, fracturing, and diagenesis can also influence the occurrence of economic accumulations of natural gas. Figure 27 is a portion of the oil and gas field map published by the Utah Geological Survey and shows the locations of fields that will be referred to in this section.

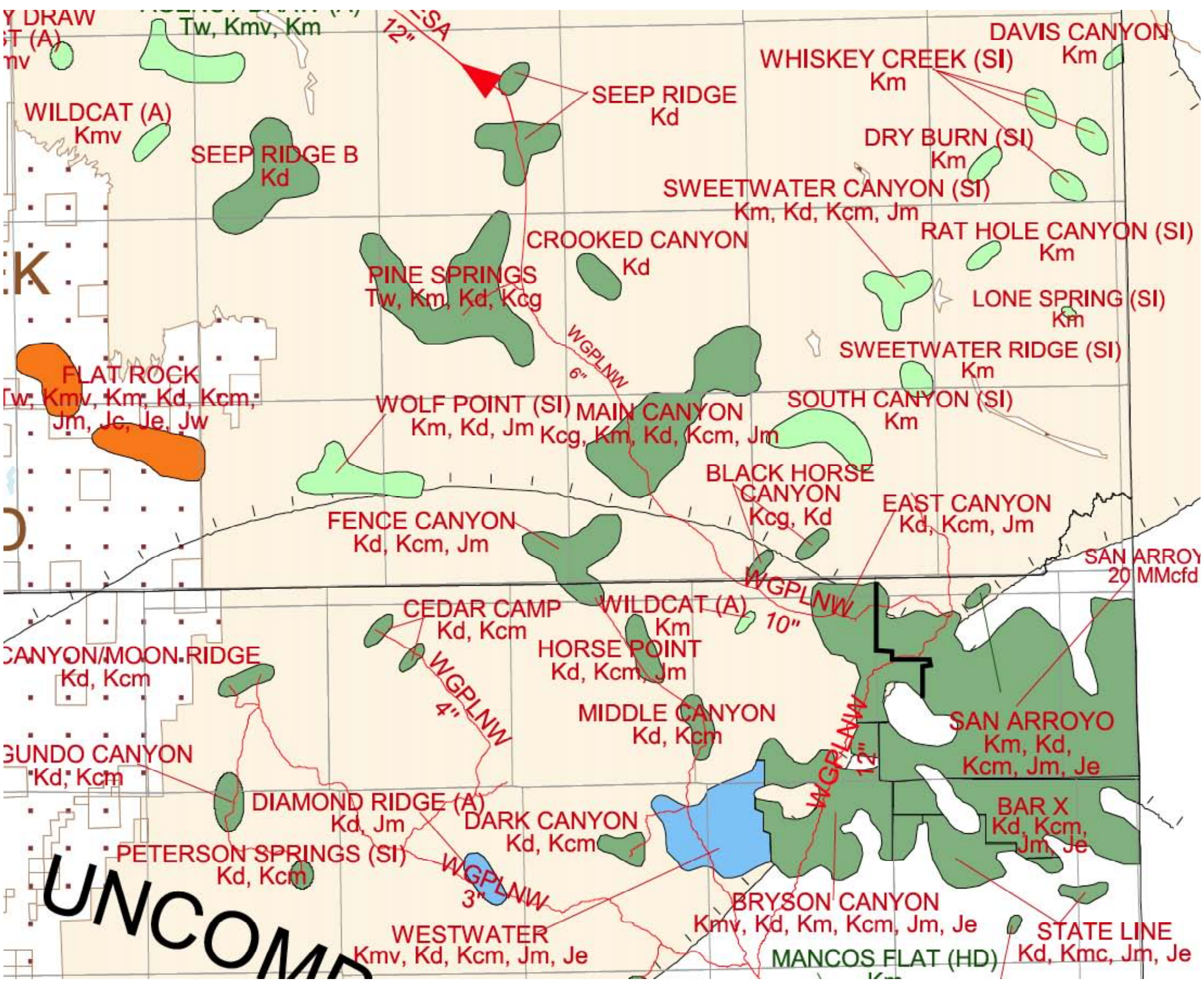

Figure 27. Map showing the locations of oil and gas fields in the study area (Chidsey et al., 2004). Some of these fields are referred to in this section of the report.

Depth

The porosity and permeability section of this report shows that reservoir quality evinces an overall deterioration with depth. Other influences aside, reservoir quality is very poor in wells >7000 feet and therefore, economic reserves risk increases below this depth. Figure 28 is a map of the measured depth to the top of the Dakota Formation. This map shows that the majority of economic producers from the CMD occur above measured depths of 7000 feet. However, depth is not the only factor, as wells that have economic cumulative production do occur below the 7000 foot contour. This indicates that there are other components influencing the occurrence of economic reserves. The remainder of this section will deal with potential reservoirs below 7000 feet.

Reservoir Architecture

Outcrop studies documenting the sedimentary architecture of potential Cedar Mountain Formation reservoir intervals have been presented by Harris (1980), Currie (1998 and 2002), Roca and Nadon (2007), and Stikes (2007). The reservoir architecture for the Dakota Formation is described in this report. Based on data from these studies, the width-to-thickness ratios of sandstone bodies within the formations can assist in reducing reservoir risk as some members or intervals of the CMD contain sandstone channels of too small dimension to provide economic reservoirs. Table 7 summarizes the width-to-thickness ratios of the CMD interval. Based on size only, the Buckhorn Conglomerate and Poison Strip Sandstone Members of the Cedar Mountain Formation, and the amalgamated channels of the Dakota Formation, are most likely to contain economic reserves.

Table 7. Width and thickness data for CMD sandstone bodies.

Interval	Width	Thickness	Width/Thickness Ratio
Dakota Formation			
Individual channels	500-750	</= 20 feet	24 - 35
Amalgamated channels	Up to 5000 feet	75-100 feet	100 - 125
Cedar Mountain Formation			
Ruby Ranch Member	300-750 feet	</= 30 feet	10 - 25
Poison Strip Ss Member	1000-4500 feet	6-45 feet	20 - 100
Yellow Cat Member		</= 6 feet	NA
Buckhorn Conglomerate	10,000 - 30,000 feet	</=100 feet	1000 - 3000

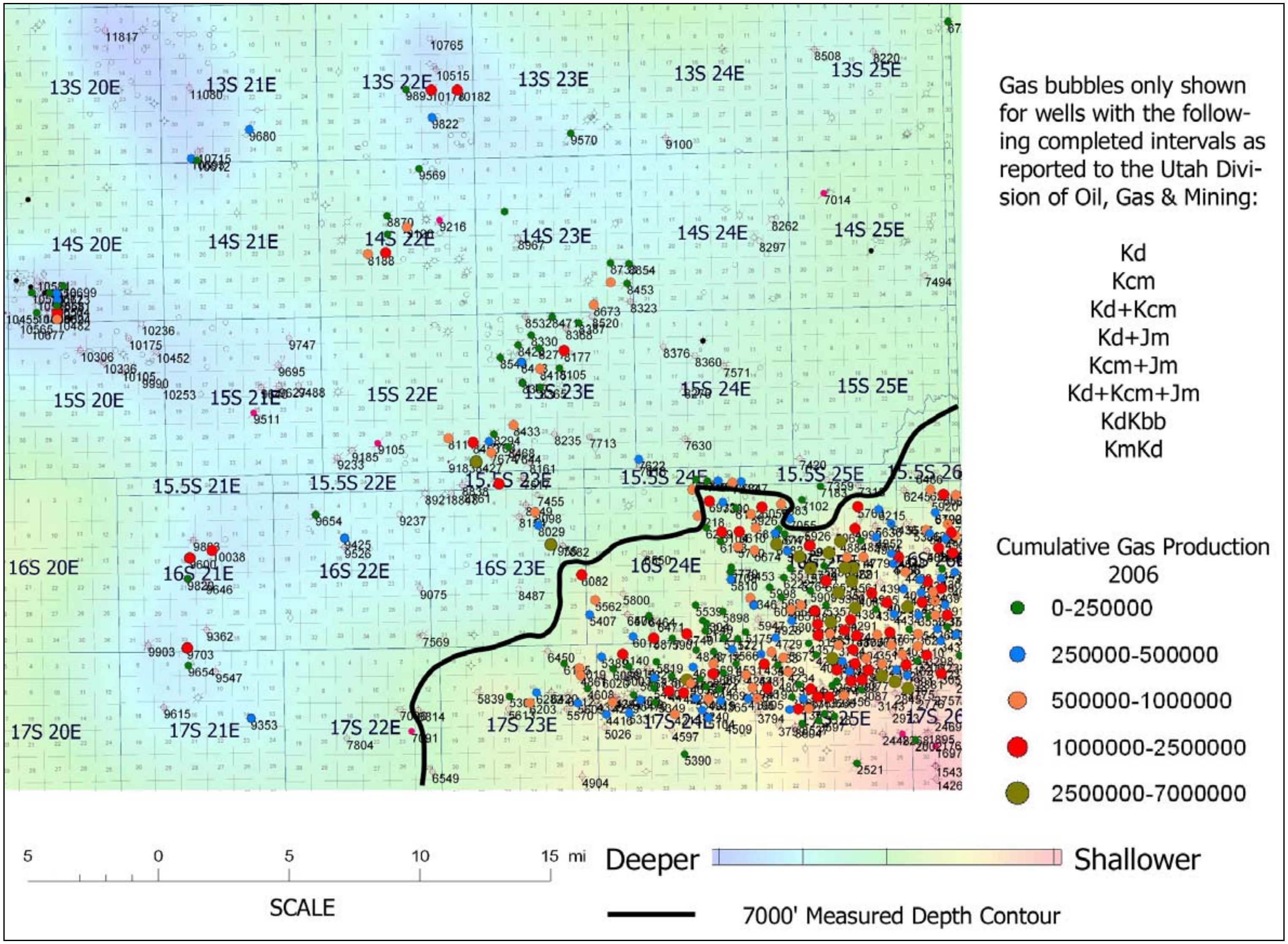

Figure 28. Map showing study area cumulative gas production for the CMD interval and top Dakota Formation 7000 foot measured depth contour. Map does not include production from the interval specified as "Mesozoic" in reports.

Stratigraphic Position

Cedar Mountain Formation

Buckhorn Conglomerate Member

The Buckhorn Conglomerate Member has the highest width-to-thickness ratio of all zones in the CMD and occurs in the northwest corner of the study area (see Buckhorn Conglomerate isopach in Appendix 2). It is productive in a few wells in the Flat Rock field and hydrocarbon accumulations appear to be structurally controlled. Figure 29 is a structural cross section of Buckhorn Conglomerate penetrations with fluid content noted. Few discreet tests of the Buckhorn Conglomerate exist and most operators did not perforate the interval.

The Buckhorn Conglomerate resistivity is high and seems to be an indicator of calcium carbonate cementation. Where effective reservoir occurs, it appears to be saturated with gassy salt water. The Buckhorn Conglomerate was not perforated in any other wells in the study area with the exception of the Chimney Rock 32-14 (32-13S-21E) and these perforations were excluded from production.

Poison Strip Sandstone Member

The Poison Strip Sandstone Member of the Cedar Mountain Formation also has sufficient width-to-thickness ratio to contain economic gas reserves. Although we were unable to correlate the Cedar Mountain Formation members (other than the Buckhorn Conglomerate Member) into the subsurface, the Cedar Mountain Formation does produce from sandstone intervals that are correlative between 640 acre or more offset wells. Based on our correlations, these sandstones are stratigraphically higher than the Buckhorn Conglomerate Member. Examples of Cedar Mountain Formation fields include Segundo Canyon, Peterson Springs, Moon Ridge and Seep Ridge; and the productive zone is probably the Poison Strip Sandstone Member. Figures 30 and 31 are stratigraphic cross sections over Segundo Canyon and Moon Ridge, and Seep Ridge fields showing the productive interval in the Cedar Mountain Formation. At Seep Ridge field, Seep Ridge 3 (22-13S-22E) is the structurally highest well but only produced approximately 4 MMCF. The Seep Ridge 4 (23-12S-22E) and Texaco Skyline B-NCT-1 (also known as the Gov Chorney B-NCT-1; 24-13S-22E) occupy flank positions on a small anticlinal nose but are the best producers, each with cumulative production over 1 BCF. Similarly, Cedar Mountain Formation production in 16S-21E and 17S-21E may not require a structural component. Where well-developed, the Poison Strip Sandstone Member appears to be a viable natural gas target.

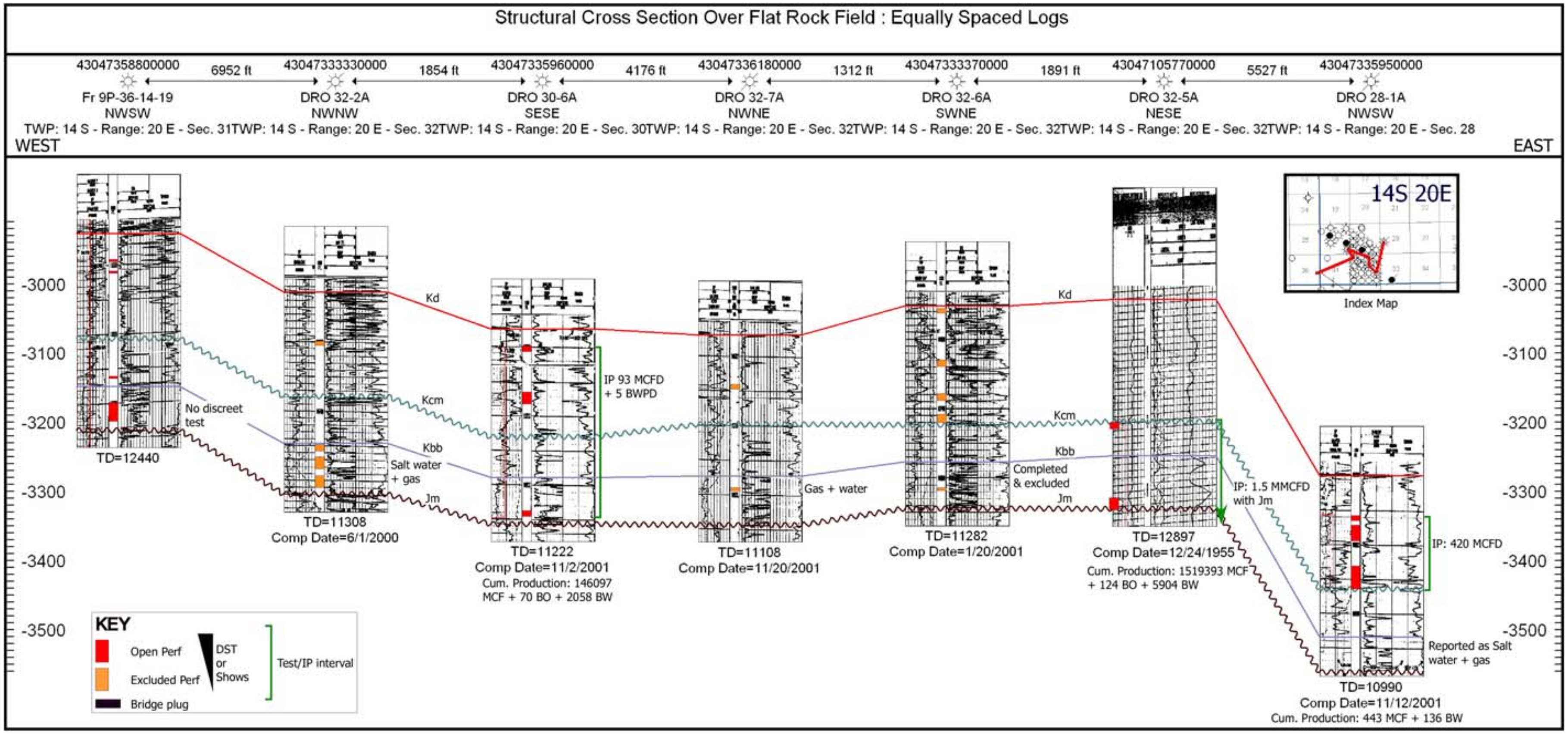

Figure 29. Structural cross section of the Flat Rock field showing Buckhorn Conglomerate completions.

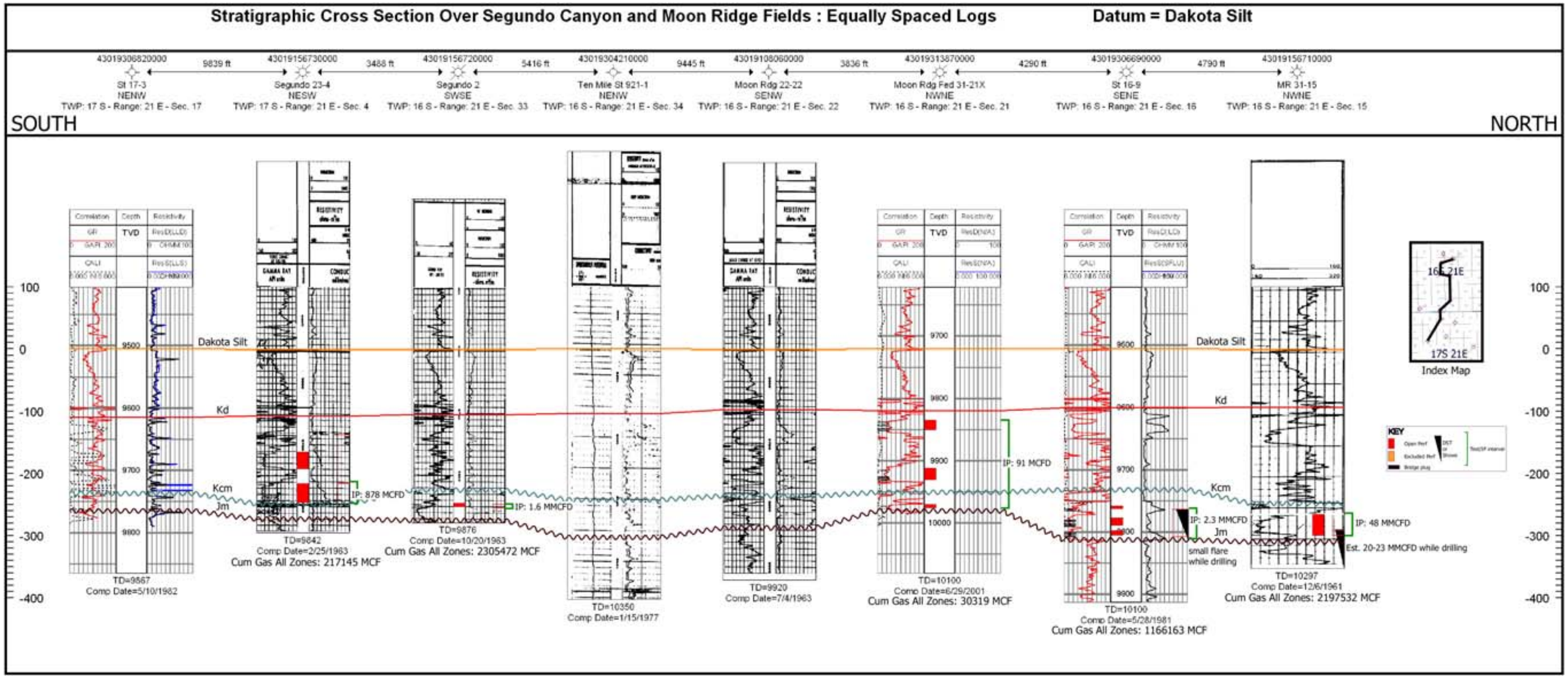

Figure 30. Cross section across the Segundo Canyon and Moon Ridge fields showing Cedar Mountain Formation reservoir intervals.

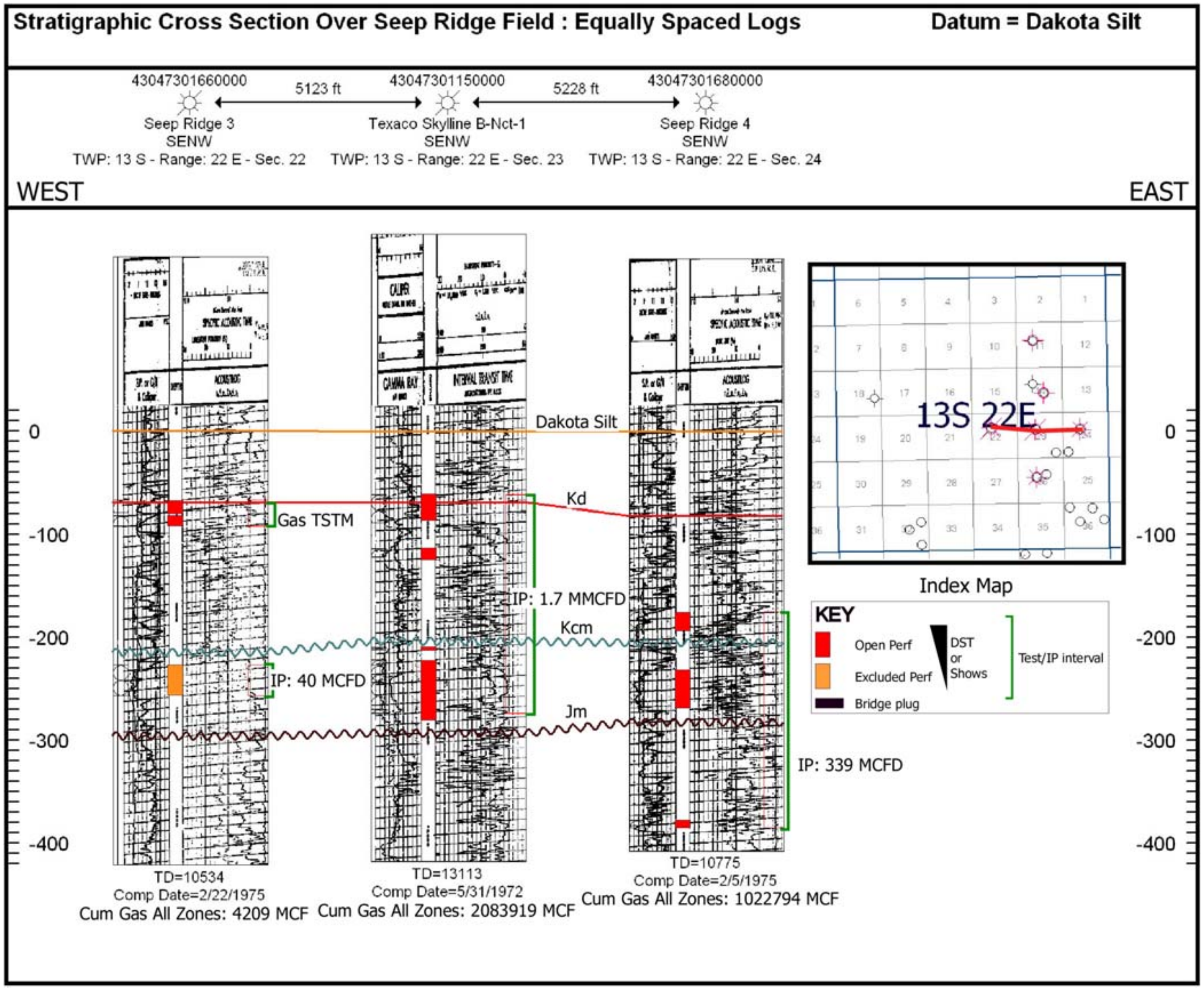

Figure 31. Cross section over Seep Ridge field showing possible Poison Strip Sandstone Member production.

Dakota Formation

Our outcrop study showed that amalgamated Dakota Formation sandstone channels have sufficient width-to-thickness ratios to be economic reservoirs. In the Westwater area, these amalgamated sandstones occur at the base of the Dakota Formation. During correlation of the Dakota Formation, it became apparent that high width-to-thickness ratio sandstones also occur at the top of this interval.

Figure 32 is a stratigraphic cross section over Fence Canyon Field and shows a well-developed basal sandstone interval. This sandstone is the primary producing interval in Middle Canyon, Horse Point and Fence Canyon fields. It commonly has a blocky signature and often fines upward at the very top. Other fields where this basal interval is productive include Pine Springs, Segundo Canyon and Main Canyon. The occurrence of this basal sandstone does not guarantee an economic gas producer as evidenced by several wells on the cross section in figure 32. However, there are wells where this basal sandstone is the sole completed interval and the well is economic as shown by the Fence Canyon 1 (36-15S-22E) with cumulative gas production in excess of 5 BCF.

Frequently, sandstone channels occur in the middle of the Dakota Formation with low width-to-thickness ratios. These sandstones are often completed for small cumulative production. An example is the shut-in Trapp Springs 16-25 (25-14S-23E) in Main Canyon field in figure 33 that has cumulative gas production of 23,334 MCF.

The upper sandstone with a high width-to-thickness ratio has been completed in many wells. Most Dakota Formation fields in the study area (figure 27) have this upper sandstone complex perforated in at least a few wells. Figures 33 and 34 show well-developed upper Dakota Formation sandstone in Main Canyon and Pine Spring fields. This upper sandstone interval is interpreted as a low sinuosity stream system (similar to the older Dakota channel deposits) with associated crevasse and overbank deposits. The log profile is generally fining upward but some blocky sandstone occurs. For wells where the depth to the Dakota is greater than 7000 feet, there is no economic production where the upper sand is the sole completion.

Structural Influence

A structure contour map (figure 35) was constructed on the top of the Dakota Silt using the faults interpreted by Stone (1977) and the Department of Energy funded study at North Hill Creek (Eckels et al., 2004). Figure 35 also includes cumulative gas production for CMD completions with the exclusion of wells reported as being completed in the "Mesozoic." Figure 36 is map of CMD producing gas fields (Chidsey et al., 2004) overlaying the structure map in figure 35. It also shows the 7000 foot measured depth contour to the top of the Dakota Formation.

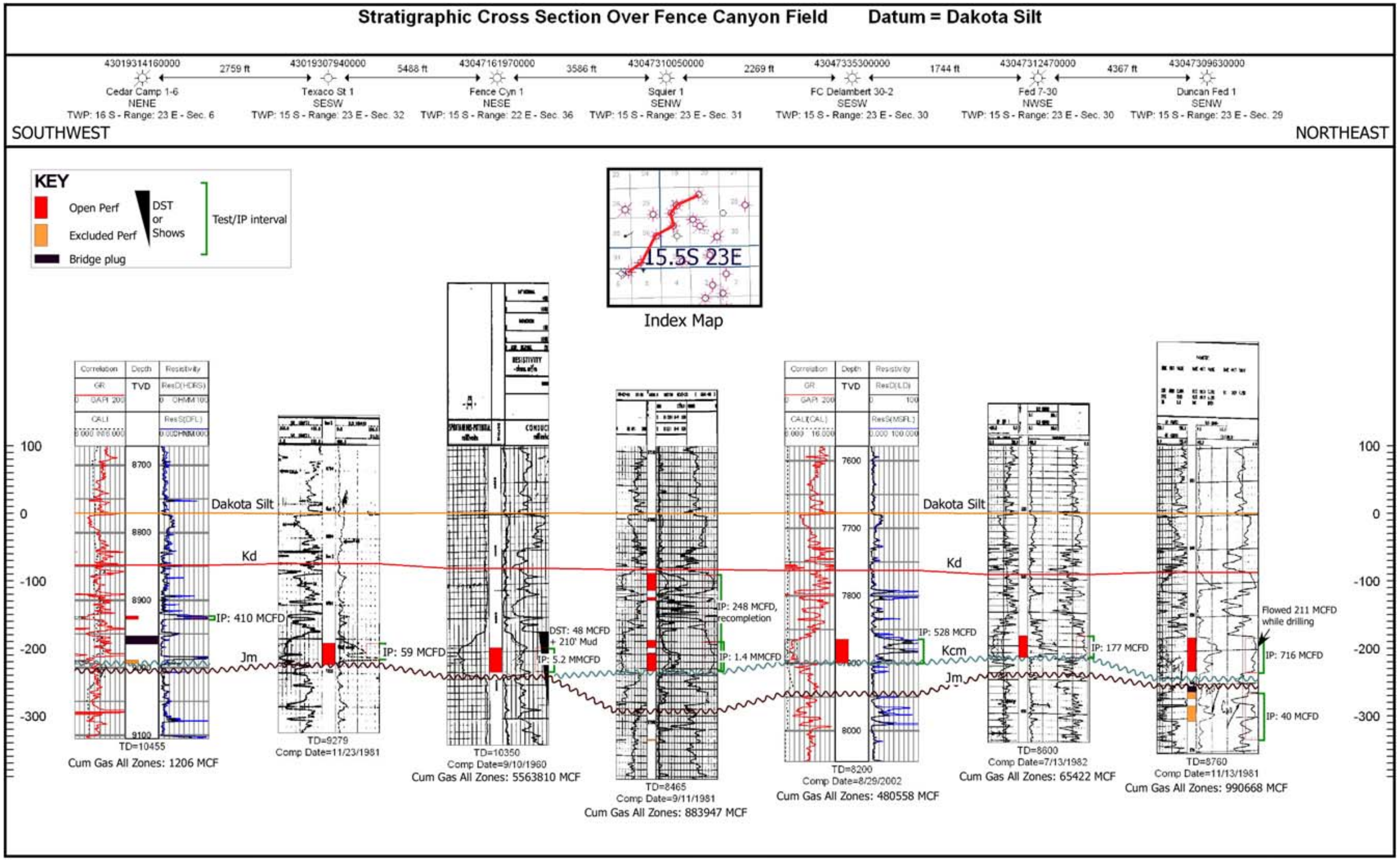

Figure 32. Stratigraphic cross section across Fence Canyon field showing well developed amalgamated sandstones of the basal Dakota Formation.

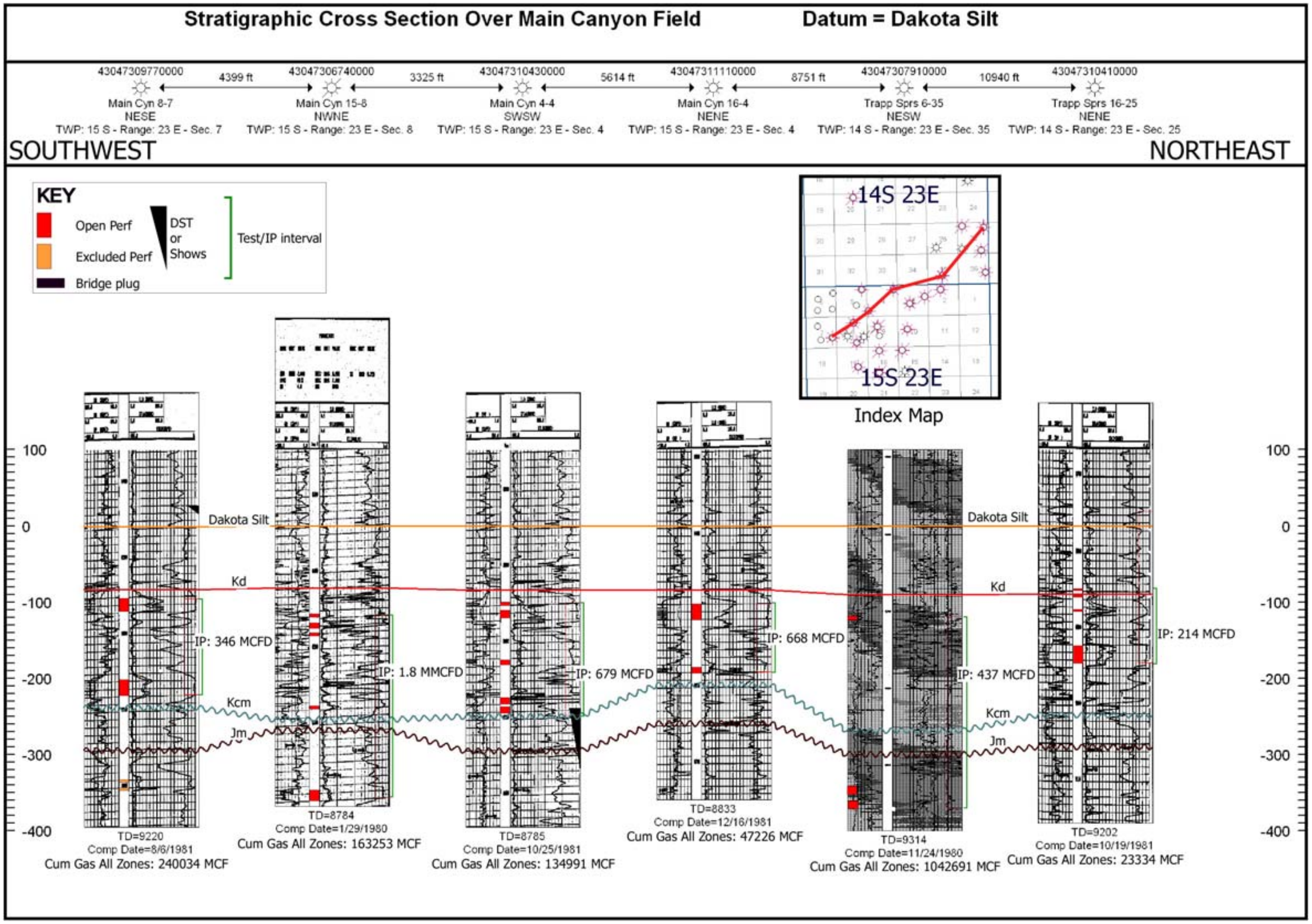

Figure 33. Stratigraphic cross section over Main Canyon field. The upper Dakota Formation sandstone is well-developed in this field. A middle Dakota channel with limited reservoir occurs in the Trapp Springs 16-25. The basal Dakota sandstone is developed in the southwest part of the field.

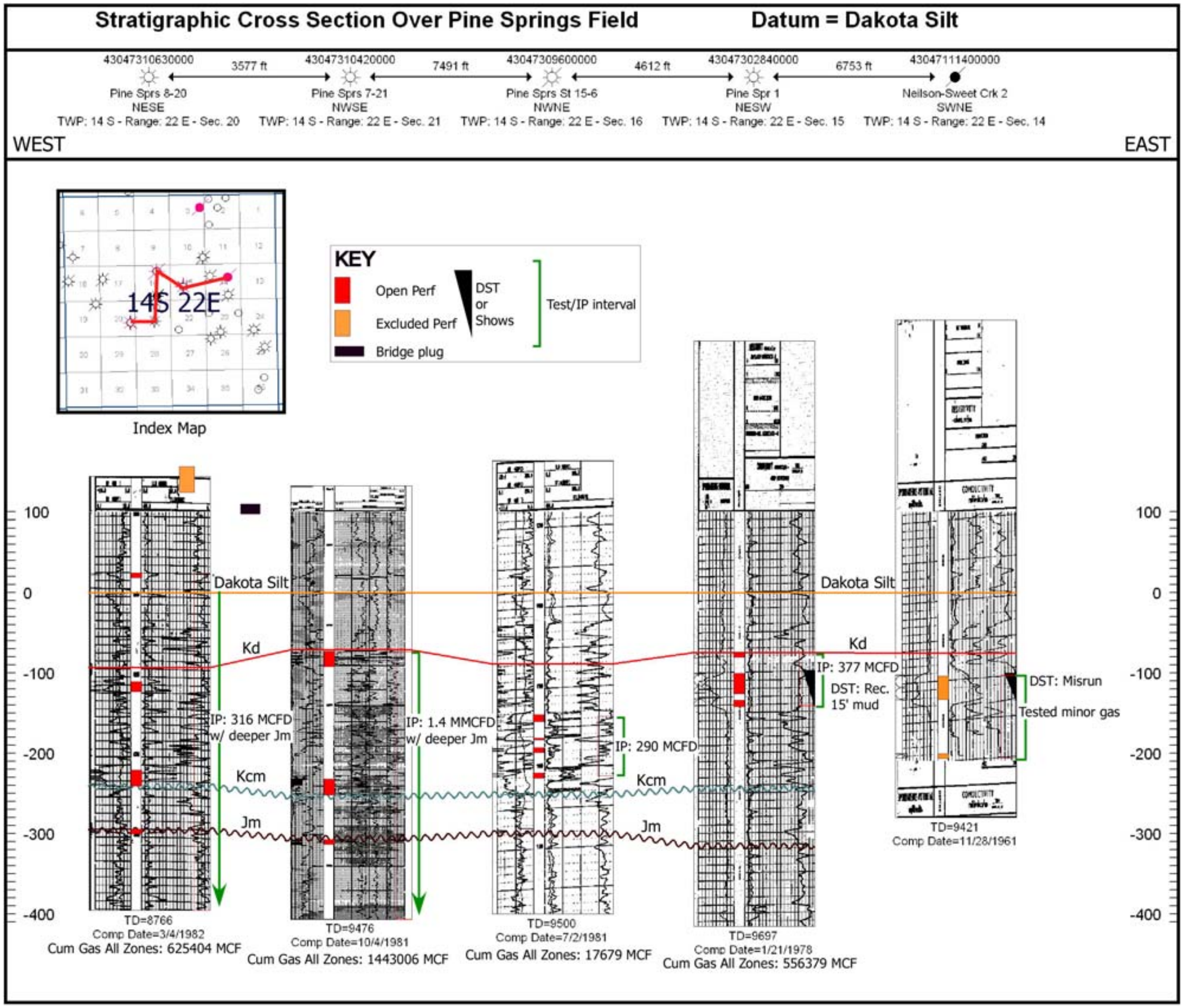

Figure 34. Stratigraphic cross section over Pine Springs field showing well-developed upper and basal Dakota Formation sandstones.

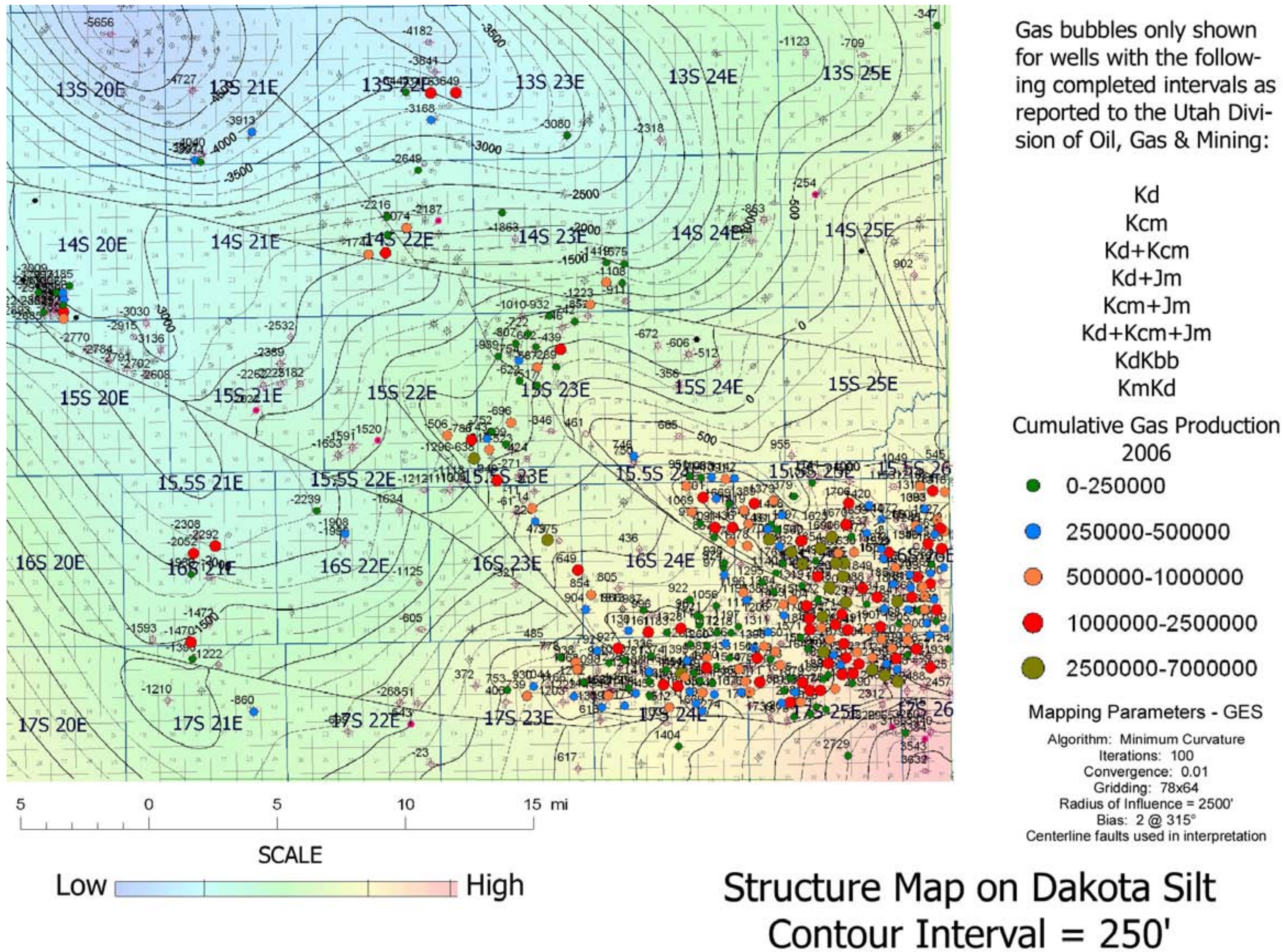

Figure 35. Structure contour (top Dakota Silt) and cumulative gas production map of the study area. Faults traces from Stone (1977) and Eckels et al. (2004).

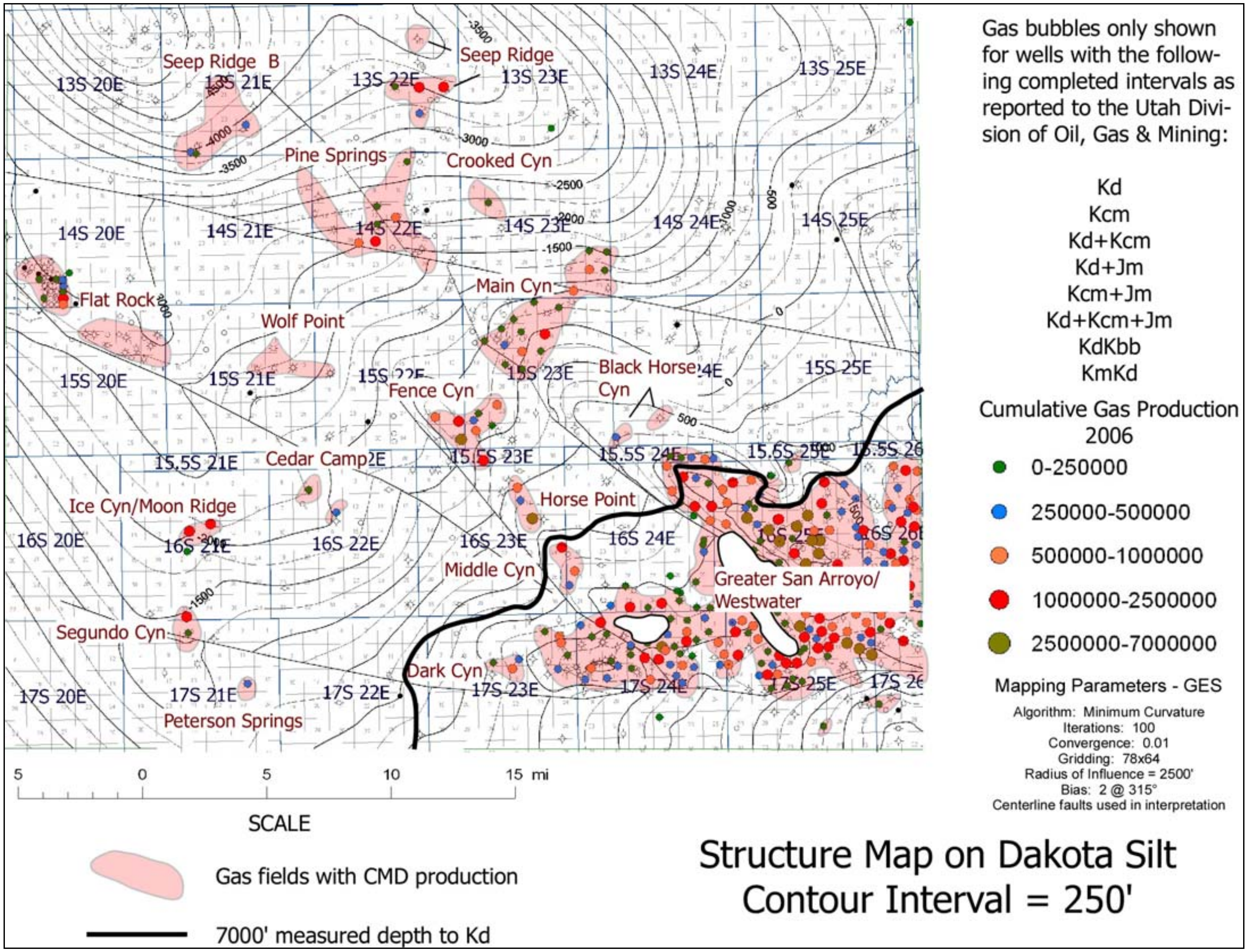

Figure 36. Structure contour map on the Dakota Silt showing locations of CMD production. The 7000 foot measured depth contour to the top of the Dakota Formation is also shown. Faults traces from Stone (1977) and Eckels et al. (2004).

Faults that exist in the study area are the result of Late Cretaceous-Eocene Laramide reactivation of structures associated with the Late Paleozoic Ancestral Rocky Mountains Uncompaghre Uplift. Faults within the study area are classified as left-lateral strike-slip or left-lateral high angle oblique-slip faults (Stone, 1977). Folds in the study area are linked to these regional, basement involved fault zones.

The primary CMD producing interval in the Peterson Springs, Segundo Canyon, Ice Canyon/Moon Ridge, and Seep Ridge fields is the probable Poison Strip Sandstone Member of the Cedar Mountain Formation. These gas accumulations do not appear to have a strong structural influence as shown in figure 35. However, the Buckhorn Conglomerate Member of the Cedar Mountain Formation (previously discussed) and the Dakota Formation producers do seem to require a structural component to be economic. The impact of structure on Dakota Formation production is illustrated by the 1 BCF and greater cumulative gas from wells at Horse Point, Fence Canyon and Main Canyon fields. The Pine Springs 7-21 (21-14S-22E) and Seep Ridge 4 (24-13S-22E) are the only two wells that have produced over 1 BCF of gas that are not near the crest of an anticlinal structure.

The faulting that formed the folds present in the study area may have also produced localized fracture systems proximal to individual fault segments. These fracture systems may have allowed for fluid migration into the CMD sandstone complexes that caused dissolution of the matrix system and enhanced the permeability and porosity of these rocks. A similar process has been documented in several studies. For example, the Jurassic Aztec Sandstone in southern Nevada displays a distribution of alteration patterns, including dissolution, that indicates regional-scale fluid migration pathways were controlled by stratigraphic contacts, thrust faults and high angle oblique faults (Eichhubl et al., 2005). In the highly indurated Eocene-Miocene sandstones in the San Joaquin Basin, California, fractures are through-going and alter the hydrologic regime by concentrating fluid movement and dissolution along fractures. With increasing depth porosity changes from an open, evenly distributed network dominated by intergranular pore spaces, through unevenly distributed intergranular porosity, to interconnected networks of secondary fracture-related porosity (Horton, 2001).

Zones of very high porosity in deeply buried (~13,000 feet) Cenozoic sandstones in the San Joaquin Basin follow fractures that act as conduits for diagenetic fluids which produce dissolution of silicate grains. Secondary porosity may exceed 50% immediately adjacent to these ‘channel ways’ but decreases to almost zero over very short distances at the edge of these zones (Horton and McCullough, 2000). Fracture enhanced porosity/permeability in CMD reservoir intervals may explain the occurrence of tight, low to no gas-bearing sandstones adjacent to economically-productive wells.

A recent study conducted on sandstones in an active thrust fault in the Wheeler oil field, California found that at depths less than about 8500 feet dissolution increases laterally toward fault zones, increasing fault conductivity. At depths greater than about 8500 feet post-fracture cement increases laterally toward the fault zone and decreases the fault conductivity, possibly creating local seals (Perez and Boles, 2004). The conductivity depth boundary identified in the Wheeler oil field is similar to the 7000-foot economic reserve boundary presented in this report. Faults or fracture systems within the study area may act as seals and conduits below and above 7000 feet, respectively.

Differences in the original cementing material of the upper and lower Dakota sandstones may also contribute to differences in reservoir quality within the formation. Secondary fluid chemistry may have controlled the degree of dissolution or further cementation that occurred. This could be another possible reason that the upper Dakota Formation sandstones do not contain economic reserves at depths greater than 7000 feet.

CONCLUSIONS

The Cedar Mountain and Dakota Formations in the southern Uinta Basin are economic gas producers. In the study area, the Neocomian-Albian Cedar Mountain Formation is comprised of the Buckhorn Conglomerate, Yellow Cat, Poison Strip Sandstone, and Ruby Ranch Members. Although the basal Buckhorn Conglomerate Member can be identified in the subsurface, the other members are identifiable only in outcrop. Based on the architectural arrangement of channel sandstones and overbank mudstones observed in outcrops, the Dakota Formation is comprised of upper and lower units. However, due to erosional truncation and superposition of upper Dakota channel complexes with those of the lower Dakota, the formation is undivided in the subsurface component of this investigation. Palynomorphs collected from the Dakota Formation and the overlying Mancos Shale indicate a Late Albian-Early Cenomanian age of deposition.

Studies of CMD fluvial channel architecture reveal that both formations mostly contain the deposits of northeast-flowing, low–sinuosity fluvial systems. Most observed channel deposits consist of an overall upward-fining sequence of conglomerates and coarse- to fine-grained sandstones. Sedimentary structures include trough- and planar-cross stratification, horizontal stratification and ripple-cross lamination. The orientation of internal bounding surfaces indicates deposition by in-channel dunes, and both lateral- and downstream-accreting marcroforms.

Economic gas production in the Cedar Mountain and Dakota Formations in the southern Uinta Basin is controlled by several different parameters including stratigraphic position, reservoir sandstone geometry, burial depth, and possible diagenetic controls associated with structural setting. Stratigraphically, amalgamated sandstone bodies in the middle part of the Cedar Mountain Formation (possibly correlative with the Poison Strip Sandstone Member) and the lower part of the Dakota Formation have the highest potential for economic natural gas production. These amalgamated channel sandstones tend to have relatively high width/thickness ratios (50 to 125) and are correlative between wells that are offset more than 640 acres.

Based on comparisons between our correlations, core porosity and permeability data from CMD sandstones and records of historical gas production in the study area, overall reservoir quality decreases in wells greater than 7000 feet deep. This is most likely due to decreased reservoir porosity and permeability due to burial diagenesis. In wells greater than 7000 feet measured depth, structural modification of reservoir sandstones, due to probable fracture enhanced porosity and permeability, seems to be required for economically-viable gas production from the Dakota Formation. Sandstones from the middle part of the Cedar Mountain Formation (likely correlative with the Poison Strip Sandstone Member) appear less reliant on structural overprinting to contain economic accumulations.

ACKNOWLEDGMENTS

We would like to thank the following for their assistance during this study: Gerald Waanders Consulting, Eddie Gudac of Gudac Brothers, Bill Barrett Corporation, Miller, Dyer and Co., Slate River Resources, QEP Uinta Basin, National Fuel Corporation, EOG Resources, Inc., and Jones Lease Service. Interpretation software used at Miami University was supplied by Landmark Graphics Corporation University Software Grant Program. MJ Systems provided raster log files to Miami University. Mark Kirschbaum of the USGS played an instrumental role in initial discussions on the stratigraphy of the Dakota Formation in eastern Utah. Discussions in the field with John Ladd of FIML Natural Resources, Inc. were also productive. We especially thank Dr. Donna Anderson of the Colorado School of Mines and Craig Morgan of the Utah Geological Survey for their insights, discussions, and support.

This study was funded, in part, by the Utah Geological Survey under the “Characterization of Utah’s Hydrocarbon Reservoirs and Potential New Reserves” program.

BIBLIOGRAPHY

Anderson, D.S., and Harris, N.B., 2006, Integrated sequence stratigraphic and geochemical resource characterization of the lower Mancos Shale, Uinta Basin, Utah. Utah Geological Survey Open-File-Report OFR-483, 130 p.

Anky-man, 2007, Exhumed River Channel. Web resource retrieved from http://en.wikipedia.org/wiki/Image:Exhumedchannel.jpg

Atwater, G. I., 1966, The effect of decrease in porosity with depth on oil and gas reserves in sandstone reservoirs. Houston Geological Society Bulletin, v. 8, no. 6, p. 20.

Aubrey, W.M., 1998, A newly discovered, widespread fluvial facies and unconformity marking the Upper Jurassic/Lower Cretaceous Boundary, Colorado Plateau. Modern Geology, v. 22, p. 209–233.

Bridge, J.S., Smith, N.D., Trent, F., Gabel, S.L., and Bernstein, P., 1986, Sedimentology and morphology of a low-sinuosity river: Calamus river, Nebraska Sand Hills. Sedimentology, v. 33, p. 851-870.

Carroll, R.E., 1992, Biostratigraphy and paleoecology of mid-Cretaceous sedimentary rocks, eastern Utah and western Colorado; a palynological interpretation. Ph.D. dissertation, Michigan State University, 423 p.

Chidsey, Jr., T.C., Wakefield, S. Hill, B.G., and Hebertson, M., 2004, Oil and gas fields map of Utah. Utah Geological Survey Online Geologic Map: http://geology.utah.gov/online/m/m-203.pdf

Conley, D.J., 1986, Stratigraphy and Depositional Environment of the Buckhorn Conglomerate Member of the Cedar Mountain Formation (Lower Cretaceous), Central Utah. M.S. Thesis, Fort Hays State University, 127 p.

Currie, B.S., 1997, Sequence stratigraphy of nonmarine Jurassic-Cretaceous rocks, central Cordilleran foreland basin. Geological Society of America Bulletin, v. 109, p. 1206-1222.

Currie, B.S., 1998, Upper Jurassic-Lower Cretaceous Morrison and Cedar Mountain Formations, NE Utah-NW Colorado: Relationships between nonmarine deposition and early Cordilleran foreland basin development. Journal of Sedimentary Research, v. 68, p. 632-652.

Currie, B.S., 2002, Structural configuration of the Late Jurassic-Early Cretaceous Cordilleran foreland-basin system and Sevier thrust belt, Utah and Colorado. Journal of Geology, v. 110, no. 6, p. 697-718.

Cushman, R.A., Jr., 1994, Palynostratigraphy of the Upper Cretaceous Mancos Shale in western Colorado. Ph.D. Dissertation, Colorado School of Mines, Golden, 686 p.

Demko, T.M., Currie, B.S., and Nicoll, K.A., 2004, Regional paleoclimatic and stratigraphic implications of paleosols and fluvial-overbank architecture in the Morrison Formation (Upper Jurassic), Western Interior, U.S.A. Sedimentary Geology, v. 167, p. 117-137.

Eberth, D.A., Britt, B.B., and Brinkman, D.B., 1997, Sedimentology, facies architecture, and stratigraphy of the Cedar Mountain Formation (Lower Cretaceous) at Dalton Wells Quarry, eastern Utah, U.S.A. Geological Society of America Abstracts with Programs, v. 29, p. 113.

Eckels, M.T., Suek, D.H., Harrison, D.H., and Harrison, P.J, 2004, North Hill Creek 3-D Seismic Exploration Project: Ute Indian Tribe, Uintah & Ouray Reservation, Uintah County, UT. US Department of Energy, Report DE-FG26-00BC15193.

Ehrenberg, S.N., and Nadeau, P.H., 2005, Sandstone vs. carbonate petroleum reservoirs; a global perspective on porosity-depth and porosity-permeability relationships. AAPG Bulletin, v. 89, no. 4, p. 435-445.

Eichhubl, P., Dehler, C.M., and Flodin, E., 2005, Brittle deformation, fluid flow, and diagenesis in sandstone at Valley of Fire State Park, Nevada. GSA Field Guide v. 6, p. 151-167.

Greenhalgh, B.W., Britt, B.B., and Kowallis, B.J., 2006, New U-Pb age control for the lower Cedar Mountain Formation and an evaluation of the Morrison Formation/Cedar Mountain Formation Boundary, Utah. Geological Society of America Abstracts with Programs, v. 38, no. 6, p. 7.

Gualtieri, J.L., 1988, Geologic map of Westwater 30’ x 60’ quadrangle, Grand and Uintah Counties, Utah and Garfield and Mesa Counties, Colorado; U.S. Geological Survey Miscellaneous Investigations Series Maps I-1765.

Harris, D.R., 1980, Exhumed paleochannels in the Lower Cretaceous Cedar Mountain Formation near Green River, Utah: Brigham Young University Geology Studies, v. 27, p. 51-66.

Horton, R.A., 2001, Depth-porosity relationships in Eocene through Miocene arkosic sandstones, San Joaquin Basin, California: Annual Meeting Expanded Abstracts - American Association of Petroleum Geologists, v. 2001, p. 92.

Horton, R. A., and McCullough, T., 2000, Porosity development in deeply buried sandstones, San Joaquin Basin, California. Annual Meeting Expanded Abstracts, American Association of Petroleum Geologists, v. 2000, p. 69.

Keighin, C.W., Dunbar, R.W., and Zech, R.S., 1993, The Point Lookout Sandstone; a tale of two cores, or petrology, diagenesis, and reservoir properties of Point Lookout Sandstone, southern Ute Indian Reservation, San Juan basin, Colorado. Mountain Geologist, v. 30, no. 1, p. 4-16.

Kirkland, J.I., 2005, Utah's newly recognized dinosaur record from the Early Cretaceous Cedar Mountain Formation. Utah Geological Survey, Survey Notes, v. 33, no. 1, p. 1-5.

Kirkland, J.I., and Madsen, S.K., 2007, The Lower Cretaceous Cedar Mountain Formation, eastern Utah: The view up always interesting learning curve, Geological Society of America Rocky Mountain Section Meeting Field Trip Guide Book, 108 p.

Kirkland, J.I., Britt, B.B., Burge, D.L., Carpenter, K., Cifelli, R., DeCourten, F., Eaton, J., Hasiotis, S., and Lawton, T., 1997, Lower to middle Cretaceous dinosaur faunas of the central Colorado Plateau: A key to understanding 35 million years of tectonics, sedimentology, evolution, and biogeography. Brigham Young University Geology Studies, v. 42, Part II, p. 69-103.

Magara, K., 1980, Comparison of porosity-depth relationships of shale and sandstone. Journal of Petroleum Geology, v. 3, no. 2, p. 175-185.

McPherson, M.L., Currie, B.S. and Pierson, J.S., 2006, Reservoir characterization of the Cretaceous Cedar Mountain and Dakota Formations, Southern Uinta Basin: Year One Report. Utah Geological Survey Open File Report OFR-492, 139 p.

Miall, A.D., 1996, The geology of fluvial deposits: sedimentary facies, basin analysis, and petroleum geology. Springer-Verlag, Berlin, 582 p.

Molenaar, C.M., and Cobban, W.A., 1991, Middle Cretaceous stratigraphy on the south and east sides of the Uinta Basin, northeastern Utah and northwestern Colorado. USGS Bulletin 1787-P, 34 p.

Munger, R.D., 1965, Subsurface exploration mapping, southern Uinta Basin, Castlegate and Dakota-Cedar Mountain Formations. The Mountain Geologist, v. 2, p. 141-166.

Nelson, P.H., 1994, Permeability/porosity relationships in sedimentary rocks. Log Analyst, v. 35, p. 38–62.

Nelson, P.H. and Kibler, J.E., 2003, A catalog of porosity and permeability from core plugs in siliciclastic rocks. United States Geological Survey Open File Report OFR 03-420. http://pubs.usgs.gov/of/2003/ofr-03-420/ofr-03-420.html

Nichols, D.J., and Jacobson, S.R., 1982, Palynostratigraphic Framework for the Cretaceous (Albian-Maastrichtian) of the Overthrust Belt of Utah and Wyoming. Palynology, v. 6., p. 119-147.

Perez, R. J., and Boles, R. 2004, Mineralization, fluid flow, and sealing properties associated with an active thrust fault; San Joaquin Basin, California. AAPG Bulletin, v. 88, no. 9, 1295-1314.

Quigley, M.D., 1959, Correlation of the Dakota-Cedar Mountain-Morrison sequence along the Douglas Creek Arch, *in* Haun, J.D., and Weimer, R.J., eds., Symposium on Cretaceous Rocks of Colorado and adjacent areas, 11th Field Conference Guidebook. Rocky Mountain Association of Geologists, p. 13-17.

Roca, X., and Nadon, G.C., 2007, Tectonic control and the sequence stratigraphy of nonmarine retro-arc foreland basin fills: insights from the Upper Jurassic of central Utah, U.S.A. Journal of Sedimentary Research, v. 77, p. 239-255.

Rose, K.K., Douds, A.S.B., Pancake, J.A., Pratt, H.R., III, and Boswell, R.M., 2004, Assessing technology needs of sub-economic natural gas resources: phase II - the Anadarko and Uinta Basins. GasTIPS, v. 10, no. 4.

Ryer, T.A., McClurg, J.J., and Muller, M.M., 1987, Dakota–Bear River paleoenvironments, depositional history and shoreline trends—implications for foreland basin paleotectonics, southwestern Green River basin and southern Wyoming overthrust belt: *in* Miller, W.R., ed. The thrust belt revisited. 38th Field Conference Guidebook. Casper, Wyoming Geological Association, p. 179–206.

Simmons, G.C., 1957, Contact of Burro Canyon Formation with Dakota Formation, Slick Rock district, Colorado and correlation of Burro Canyon Formations. American Association of Petroleum Geologists Bulletin, v. 41, p. 2519-2529.

Stikes, M.W., 2007, Fluvial facies and architecture of the Poison Strip Sandstone, Lower Cretaceous Cedar Mountain Formation, Grand County, Utah. Utah Geological Survey Miscellaneous Publication MP-06-2, 111 p.

Stokes, W.L., 1944, Morrison and related deposits in and adjacent to the Colorado Plateau. Geological Society of America Bulletin, v. 55, p. 951-992.

Stokes, W.L., 1952, Lower Cretaceous in Colorado Plateau. AAPG Bulletin, v. 36, p. 1766-1776.

Stone, D.S., 1977, Tectonic history of the Uncompaghre Uplift. 1977 Rocky Mountain Association of Geologists Symposium, p. 23-30.

Thompson, T.A., 2004, Rose. (Version 2.1.0), Freeware download http://mypage.iu.edu/~tthomps/programs/html/tntrose.htm. Bloomington: Todd A Thompson Software.

Wendlandt, R. F., and Bhuyan, K., 1990, Estimation of mineralogy and lithology from geochemical log measurements. AAPG Bulletin, v. 74, no. 6, p. 837-856.

Willis, G.C., 2005, Simplified Geologic Map of Utah, Utah Geological Survey Online Geologic Map: http://geology.utah.gov/maps/geomap/statemap/pdf/geoutah_1.pdf

Yingling, V. L. 1987. Timing and initiation of Sevier orogeny: Morrison and Cedar Mountain Formations and Dakota Sandstone, east-central Utah. M.S. thesis, University of Wyoming, Laramie, 169 p.

Young, R.G., 1960, The Dakota Group of the Colorado Plateau. AAPG Bulletin v. 44, p. 156-194.

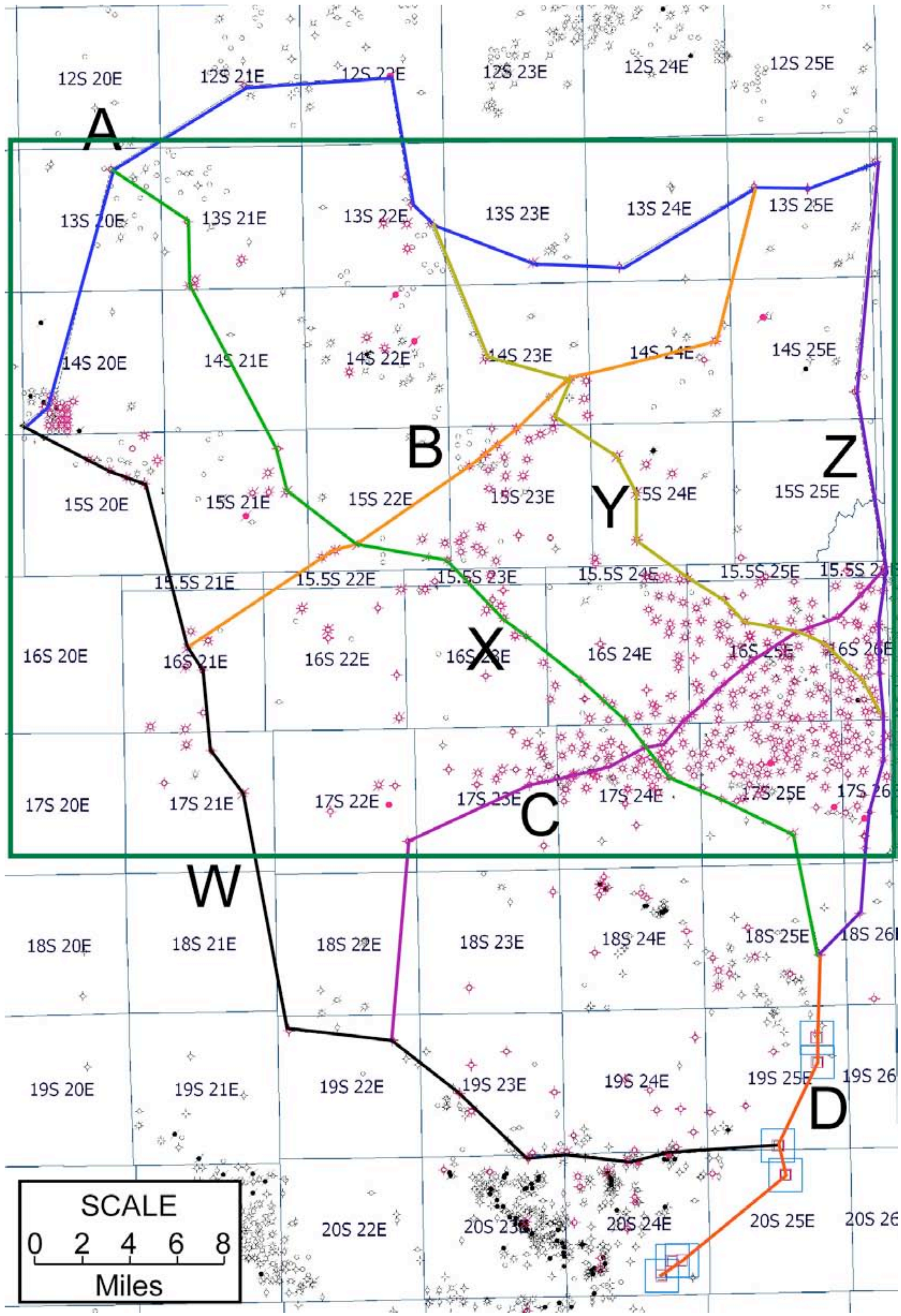

APPENDIX 1: Location Map for Cross Sections


Stratigraphic Cross Section A : Equally Spaced Logs
Datum = Dakota Silt
Vertical Scale = 2 in per 100 ft
43047358800000
9218 ft
43047341020000
53221 ft
43047315100000
35043 ft
43047302260000
32580 ft
43047303570000
29009 ft
43047303230000
6002 ft
43047301680000
24522 ft
43047303860000
19186 ft
43047307730000
34913 ft
43047109600000
11894 ft
43047312310000
16233 ft
43047311340000
Fr 9P-36-14-19
NWSW
TWP: 14 S - Range: 20 E - Sec. 31
DRO 29-6A
NESW
TWP: 14 S - Range: 20 E - Sec. 29
Agency Draw 16-3
SESE
TWP: 13 S - Range: 20 E - Sec. 3
Gray Knoll Fed 1
SWNE
TWP: 12 S - Range: 21 E - Sec. 22
Buck Camp 1
NENE
TWP: 12 S - Range: 22 E - Sec. 22
Seep Ridge 8
NWSE
TWP: 13 S - Range: 22 E - Sec. 14
Seep Ridge 4
SENW
TWP: 13 S - Range: 22 E - Sec. 24
Crooked Cyn 2
E/2 NWN
TWP: 13 S - Range: 23 E - Sec. 34
Crooked Cyn 3
SENW
TWP: 13 S - Range: 24 E - Sec. 32
Gov 1
NWNW
TWP: 13 S - Range: 25 E - Sec. 17
Eni-Hatch 15-6
NENW
TWP: 13 S - Range: 25 E - Sec. 15
Fed Eni 7-1
NENE
TWP: 13 S - Range: 26 E - Sec. 7
WEST
EAST
100
0
-100
-200
-300
-400
-500
Dakota Silt
Kd
Kcm
Kbb
Jm
Test 6.9 MMCFD with Je; IP: 745 MCFD against line Pressure
IP: 64 MCFD + 5 BOPD + 10 BWPD
Never Produced
IP: 399 MCFD
IP: 66 MCFD
IP: 399 MCFD
Correlation
Depth
Resistivity
GR
TVD
ResD(ILD)
GAPI 200
OHMM 100
CALI(CAL)
ResS(N/A)
6.000 IN 16.000
0.000 100.000
CALI
12300
12400
12500
12600
12700
12800
11300
11400
11500
11600
11700
11800
TD=12440
Cum Gas All Zones: 1399791 MCF
Also produces from deeper zones
TD=11780
Comp Date=1/9/2002
Cum Gas All Zones: 3596995 MCF
Produces from deeper zones
TD=12512
Comp Date=3/14/1985
TD=15666
Comp Date=4/29/1977
TD=15082
Comp Date=6/15/1978
TD=10789
Comp Date=5/17/1978
TD=10775
Comp Date=2/5/1975
Cum Gas All Zones: 1022794 MCF
TD=9800
Comp Date=11/17/1981
Cum Gas All Zones: 518 MCF
TD=9470
Comp Date=6/6/1981
TD=8840
Comp Date=1/19/1963
TD=8562
Comp Date=7/1/1982
TD=6990
Comp Date=6/17/1982
Cum Gas All Zones: 94716 MCF
Index Map
A
B
Y
Z
X
C
W
D
KEY
Open Perf
Excluded Perf
Bridge plug
DST or Shows
Test/IP interval
Cumulative Production from Utah Division of Oil, Gas & Mining web site, 6-07

Stratigraphic Cross Section B : Equally Spaced Logs
Datum = Dakota Silt
Vertical Scale = 2 in per 100 ft
43019306690000
36024 ft
43047310940000
3308 ft
43047306440000
5415 ft
43047301260000
30166 ft
43047309770000
4399 ft
43047306740000
3325 ft
43047310430000
5614 ft
43047311110000
16048 ft
43047309780000
33709 ft
43047310400000
35350 ft
43047109600000
St 16-9
SENE
TWP: 16 S - Range: 21 E - Sec. 16
Meadow Crk 1
SWNE
TWP: 15 S - Range: 22 E - Sec. 31
Winter Rdg St 11-32
NWNW
TWP: 15 S - Range: 22 E - Sec. 32
SE Flank Uintah 28-1
SWSW
TWP: 15 S - Range: 22 E - Sec. 28
Main Cyn 8-7
NESE
TWP: 15 S - Range: 23 E - Sec. 7
Main Cyn 15-8
NWNE
TWP: 15 S - Range: 23 E - Sec. 8
Main Cyn 4-4
SWSW
TWP: 15 S - Range: 23 E - Sec. 4
Main Cyn 16-4
NENE
TWP: 15 S - Range: 23 E - Sec. 4
Trapp Sprs 13-25
NWNW
TWP: 14 S - Range: 23 E - Sec. 25
Sweet 13-6
NESW
TWP: 14 S - Range: 24 E - Sec. 13
Gov 1
NWNW
TWP: 13 S - Range: 25 E - Sec. 17
SOUTHWEST
NORTHEAST
KEY
Open Perf
Excluded Perf
Bridge plug
DST or Shows
Test/IP interval
Index Map
Correlation
Depth
Resistivity
GR
TVD
ResD(ILD)
GAPI 200
OHMM 100
CALI
ResS(SFLU)
100
0
-100
-200
-300
-400
9500
9600
9700
9800
9900
Dakota Silt
Kd
Kcm
Jm
IP: 2.25 MMCFD
Small flare gas while drilling
IP: 223 MCFD
IP: 900 MCFD
DST: Recover 20' mud
Tested water
IP: 346 MCFD
IP: 1.8 MMCFD + 6 BOPD
IP: 679 MCFD
354 u gas inc over background
IP: 668 MCFD
IP: 274 MCFD
TD=10100
Comp Date=5/28/1981
Cum Gas All Zones: 1166163 MCF
TD=9571
Comp Date=11/25/1981
TD=9908
Comp Date=12/9/1988
TD=10018
Comp Date=6/17/1972
TD=9220
Comp Date=8/6/1981
Cum Gas All Zones: 240034 MCF
TD=8784
Comp Date=1/29/1980
Cum Gas All Zones: 163253 MCF
TD=8785
Comp Date=10/25/1981
CCum Gas All Zones: 134991 MCF
TD=8833
Comp Date=12/16/1981
Cum Gas All Zones: 47226 MCF
TD=9069
Comp Date=8/5/1981
Cum Gas All Zones: 18248 MCF
TD=8950
Comp Date=12/18/1981
TD=8840
Comp Date=1/19/1963
Cumulative Production from Utah Division of Oil, Gas & Mining web site, 6-07

Stratigraphic Cross Section C : Equally Spaced Logs
Datum = Dakota Silt
Vertical Scale = 2 in per 100 ft
43019307320000
44385 ft
43019111650000
29923 ft
43019156590000
10144 ft
43019156570000
7951 ft
43019113090000
8996 ft
43019304630000
4100 ft
43019305710000
7054 ft
43019306060000
5727 ft
43019311670000
6448 ft
43019308590000
7943 ft
43019158890000
11774 ft
43019305410000
9837 ft
43019312040000
6995 ft
43019313840000
8217 ft
43019311710000
Tenneco USA 11-1
NENE
TWP: 19 S - Range: 22 E - Sec. 11
Diamond Rdg 3
NESE
TWP: 17 S - Range: 22 E - Sec. 25
WwE 4
SENE
TWP: 17 S - Range: 23 E - Sec. 14
Ww E2
SWSE
TWP: 17 S - Range: 24 E - Sec. 7
Bryson Cyn 29-1
NWSW
TWP: 17 S - Range: 24 E - Sec. 9
Fed 3-15
SWSE
TWP: 17 S - Range: 24 E - Sec. 3
St 2-14
SESW
TWP: 17 S - Range: 24 E - Sec. 2
St 36-16
SESE
TWP: 16 S - Range: 24 E - Sec. 36
SAGE Fed 31-31
NWNE
TWP: 16 S - Range: 25 E - Sec. 31
Lauck Fed 1
SWNE
TWP: 16 S - Range: 25 E - Sec. 29
SA 6
SWNE
TWP: 16 S - Range: 25 E - Sec. 21
Fed 14-2
NWNE
TWP: 16 S - Range: 25 E - Sec. 14
BMG Fed 8
SWNW
TWP: 16 S - Range: 26 E - Sec. 7
Credo Fed 3
NESW
TWP: 16 S - Range: 26 E - Sec. 5
N Credo Fed 1
SWSW
TWP: 15 S - Range: 25 E - Sec. 33
SOUTHWEST
NORTHEAST
KEY
Open Perf
Excluded Perf
Bridge plug
DST or Shows
Test/IP interval
Index Map
100
0
-100
-200
-300
-400
Dakota Silt
Kd
Kcm
Jm
Flowed 1.4 MMCFD with drilling with air
Casing collapsed and twisted off in hole, drilled offset
No info
IP: 10.5 MMCFD with deeper Jm + Je perfs
IP: 3.5 MMCFD with deeper Jm perfs
IP: 2.8 MMCFD
IP: 1.1 MMCFD
Produced from deeper Jm perfs
IP: 3 MMCFD; AOF = 6 MMCFD
DST: Recover 100 MCFD + 900' mud + 900' sl GWCM
IP: 990 MCFD
IP: 1.2 MMCFD
TD=4900
Comp Date=12/1/1981
TD=7633
Comp Date=12/31/1960
TD=6471
Comp Date=5/28/1962
TD=5289
Comp Date=1/26/1959
Cum Gas All Zones: 9753476 MCF
TD=6224
Comp Date=6/15/1963
TD=5224
Comp Date=10/6/1978
Cum Gas All Zones: 497723 MCF
TD=6450
Comp Date=8/15/1983
Cum Gas All Zones: 574918 MCF
TD=6445
Comp Date=10/1/1980
Cum Gas All Zones: 7600 MCF
TD=6563
Comp Date=10/9/1984
Cum Gas All Zones: 49935 MCF
TD=5860
Comp Date=6/23/1983
TD=6575
Comp Date=11/15/1961
Cum Gas All Zones: 12276656 MCF
Production from Je
TD=5512
Comp Date=1/31/1980
Cum Gas All Zones: 176255 MCF
TD=5860
Comp Date=12/7/1985
TD=6350
Comp Date=10/20/2006
TD=6755
Comp Date=11/17/1984
Cumulative Production from Utah Division of Oil, Gas & Mining web site, 6-07

Stratigraphic Cross Section D : Equally Spaced Logs   Datum = Cedar Mountain Fm   Vertical Scale = 2 in per 100 ft

Stratigraphic Cross Section W : Equally Spaced Logs   Datum = Dakota Silt   Vertical Scale = 2 in per 100 ft

Stratigraphic Cross Section X : Equally Spaced Logs **Datum = Dakota Silt** **Vertical Scale = 2 in per 100 ft**

Cumulative Production from Utah Division of Oil, Gas & Mining web site, 6-07

Stratigraphic Cross Section Y : Equally Spaced Logs **Datum = Dakota Silt** **Vertical Scale = 2 in per 100 ft**

Cumulative Production from Utah Division of Oil, Gas & Mining web site, 6-07

Stratigraphic Cross Section Z : Equally Spaced Logs   Datum = Dakota Silt   Vertical Scale = 2 in per 100 ft

43047311340000	51466 ft	43047318940000	39614 ft	43019311710000	14241 ft	43019313510000	9810 ft	43019313000000	9681 ft	43019304160000	9679 ft	43019305970000	11921 ft	43019109980000	8085 ft	43019304150000	14525 ft	43019304140000	12988 ft	43019304130000
Fed Eni 7-1		Bitter 1-25-14-25		N Credo Fed 1		Fed 9		SA 46		Fed 33-13		Bar X 12		Fed 5		Fed 3-31		Fed 2-18		Fed 1-23
NENE		SWSW		SWSW		NENE		NWNW		SWSW		NWSE		SWSW		SENE		NWNE		SESE
TWP: 13 S - Range: 26 E - Sec. 7		TWP: 14 S - Range: 25 E - Sec. 25		TWP: 15 S - Range: 26 E - Sec. 33		TWP: 16 S - Range: 26 E - Sec. 17		TWP: 16 S - Range: 26 E - Sec. 28		TWP: 16 S - Range: 26 E - Sec. 33		TWP: 17 S - Range: 26 E - Sec. 8		TWP: 17 S - Range: 26 E - Sec. 20		TWP: 17 S - Range: 26 E - Sec. 31		TWP: 18 S - Range: 26 E - Sec. 18		TWP: 18 S - Range: 25 E - Sec. 23

NORTH SOUTH

Cumulative Production from Utah Division of Oil, Gas & Mining web site, 6-07

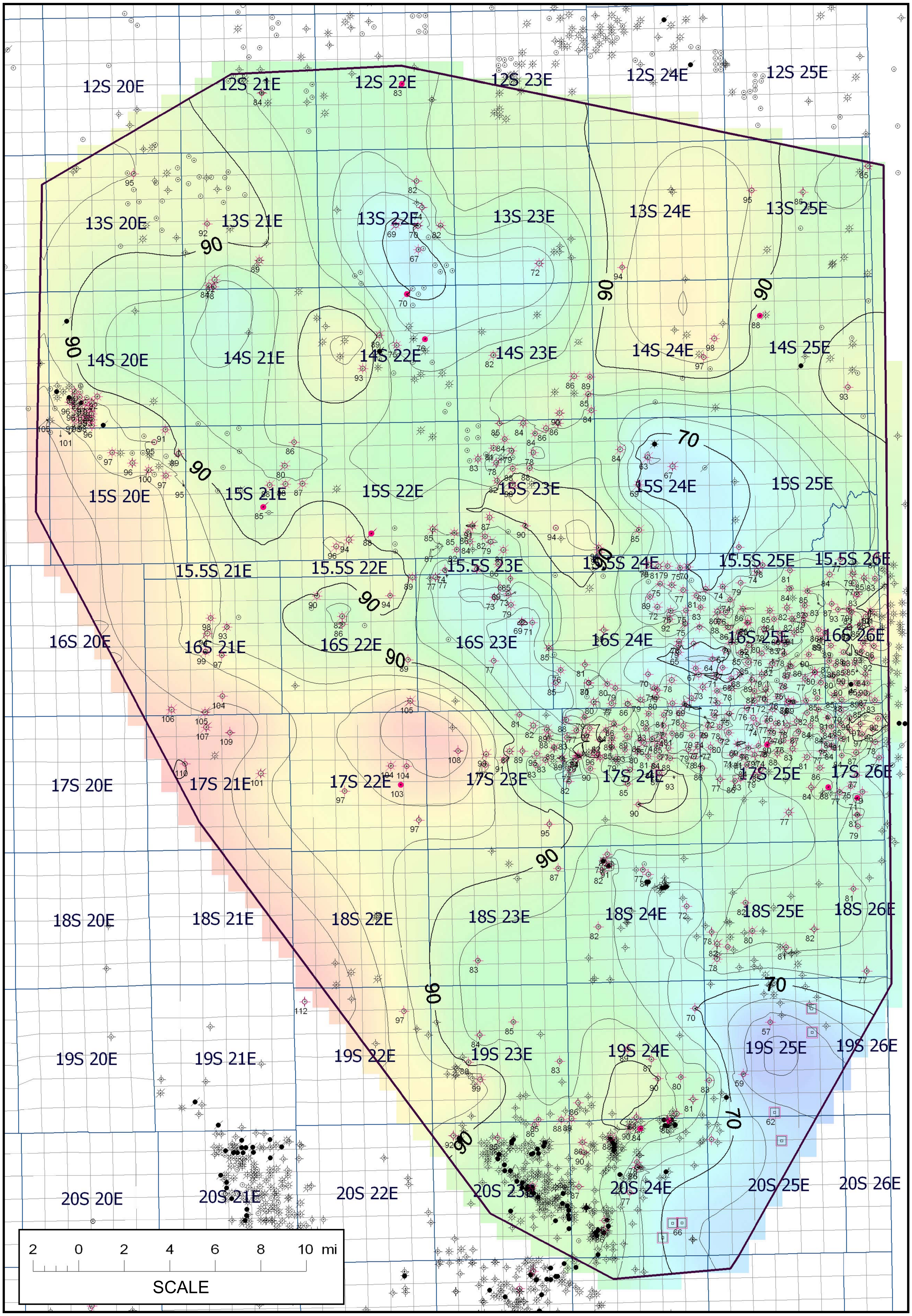

WELL KEY

- Dry Hole
- Gas Well
- Oil & Gas Well
- SI Gas Well
- P&A Gas Well
- SI Oil Well
- P& A Oil & Gas Well
- P&A Oil Well
- Proposed Location
- Outcrop

NORTH

Max

THICKNESS SPECTRUM

Min

Mapping Parameters - GES

Algorithm: Minimum Curvature
Data Honoring Forced
Iterations: 100
Convergence: 0.01
Gridding: Simplified Defaults
Bias: None

ISOPACH MAP

Dakota Silt to Dakota Fm
Data Range 57 - 112'

CONTOUR INTERVAL = 20'

Red Wells are Data Points

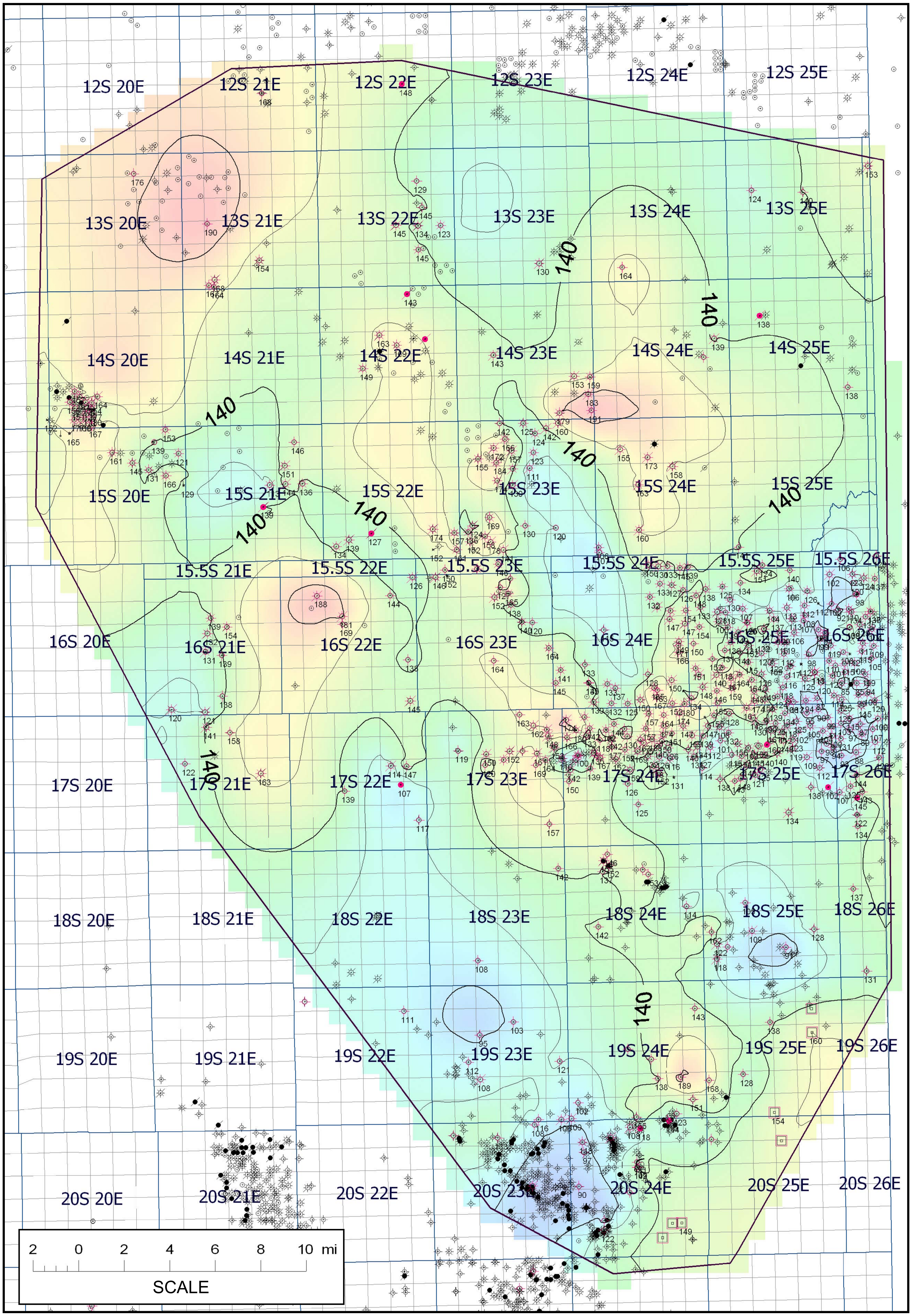

WELL KEY

- Dry Hole
- Gas Well
- Oil & Gas Well
- SI Gas Well
- P&A Gas Well
- SI Oil Well
- P& A Oil & Gas Well
- P&A Oil Well
- Proposed Location
- Outcrop

NORTH

Max

THICKNESS SPECTRUM

Min

Mapping Parameters - GES

Algorithm: Minimum Curvature
Data Honoring Forced
Iterations: 100
Convergence: 0.01
Gridding: Simplified Defaults
Bias: None

ISOPACH MAP

Dakota Fm
Data Range 82 - 191'

CONTOUR INTERVAL = 20'

Red Wells are Data Points

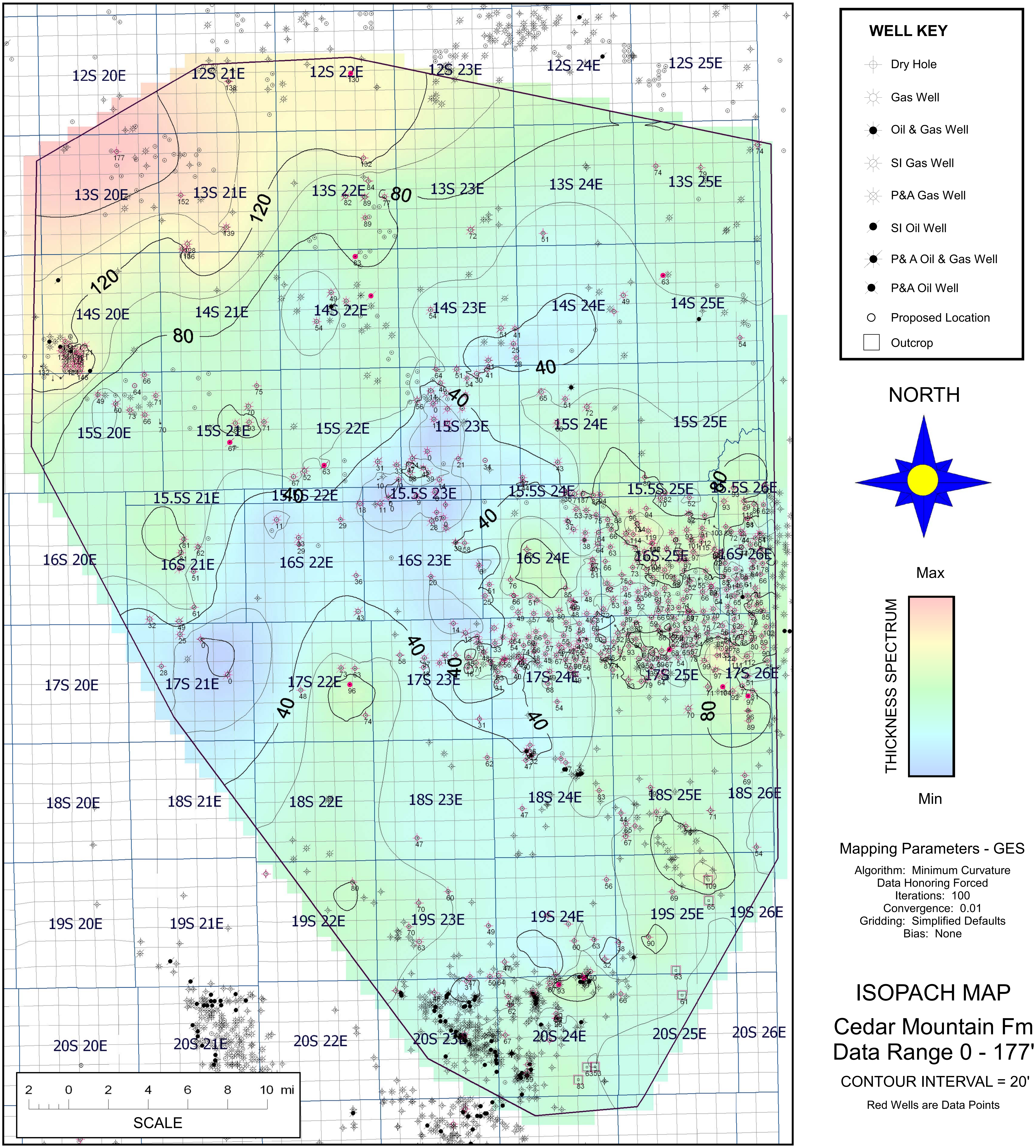
WELL KEY
Dry Hole
Gas Well
Oil & Gas Well
SI Gas Well
P&A Gas Well
SI Oil Well
P & A Oil & Gas Well
P&A Oil Well
Proposed Location
Outcrop
NORTH
Max
THICKNESS SPECTRUM
Min
Mapping Parameters - GES
Algorithm: Minimum Curvature
Data Honoring Forced
Iterations: 100
Convergence: 0.01
Gridding: Simplified Defaults
Bias: None
ISOPACH MAP
Cedar Mountain Fm
Data Range 0 - 177'
CONTOUR INTERVAL = 20'
Red Wells are Data Points
2 0 2 4 6 8 10 mi
SCALE

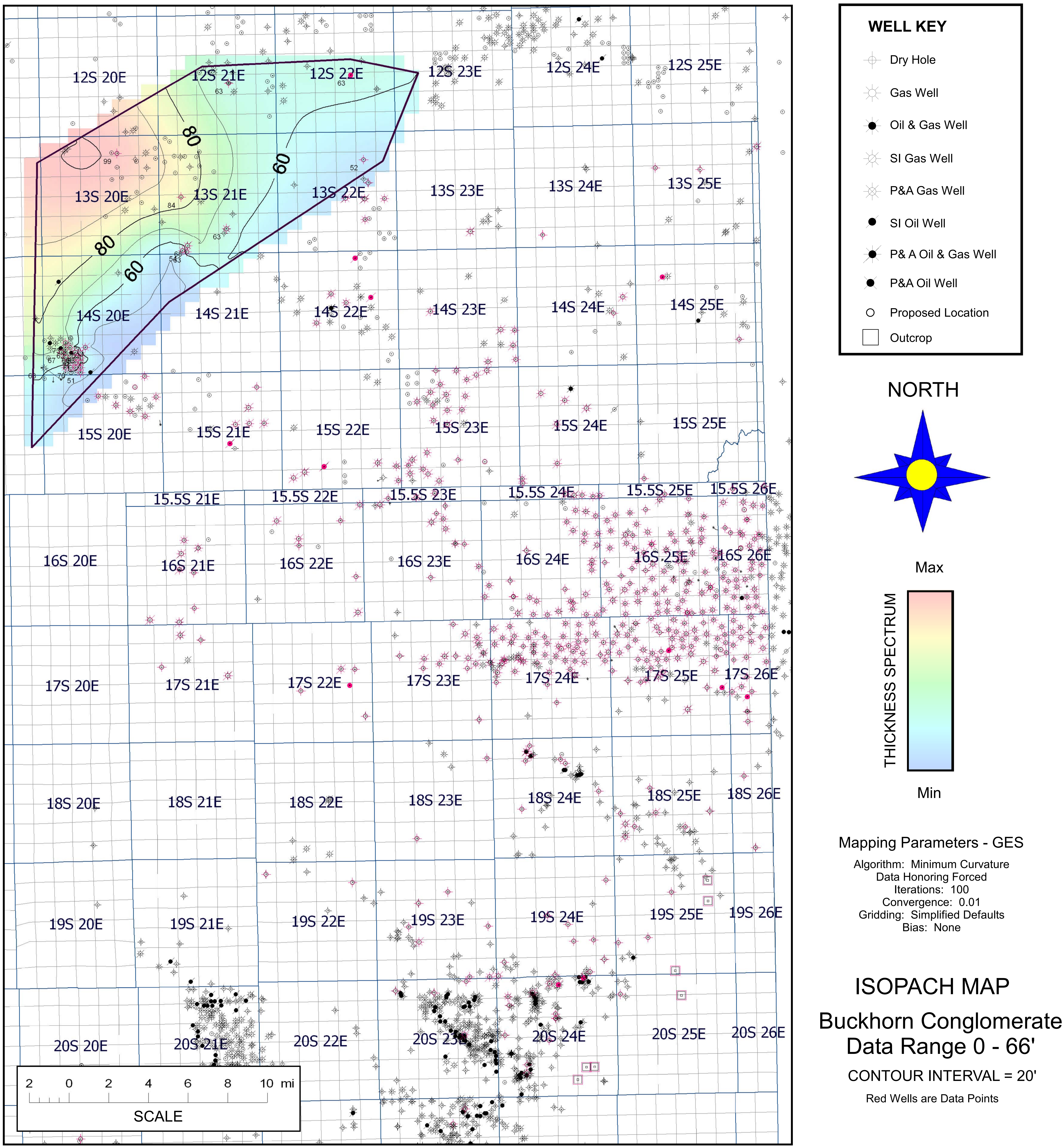
WELL KEY
Dry Hole
Gas Well
Oil & Gas Well
SI Gas Well
P&A Gas Well
SI Oil Well
P& A Oil & Gas Well
P&A Oil Well
Proposed Location
Outcrop
NORTH
Max
THICKNESS SPECTRUM
Min
Mapping Parameters - GES
Algorithm: Minimum Curvature
Data Honoring Forced
Iterations: 100
Convergence: 0.01
Gridding: Simplified Defaults
Bias: None
ISOPACH MAP
Buckhorn Conglomerate
Data Range 0 - 66'
CONTOUR INTERVAL = 20'
Red Wells are Data Points
2 0 2 4 6 8 10 mi
SCALE
12S 20E
12S 21E
12S 22E
12S 23E
12S 24E
12S 25E
13S 20E
13S 21E
13S 22E
13S 23E
13S 24E
13S 25E
14S 20E
14S 21E
14S 22E
14S 23E
14S 24E
14S 25E
15S 20E
15S 21E
15S 22E
15S 23E
15S 24E
15S 25E
15.5S 21E
15.5S 22E
15.5S 23E
15.5S 24E
15.5S 25E
15.5S 26E
16S 20E
16S 21E
16S 22E
16S 23E
16S 24E
16S 25E
16S 26E
17S 20E
17S 21E
17S 22E
17S 23E
17S 24E
17S 25E
17S 26E
18S 20E
18S 21E
18S 22E
18S 23E
18S 24E
18S 25E
18S 26E
19S 20E
19S 21E
19S 22E
19S 23E
19S 24E
19S 25E
19S 26E
20S 20E
20S 21E
20S 22E
20S 23E
20S 24E
20S 25E
20S 26E
80
60

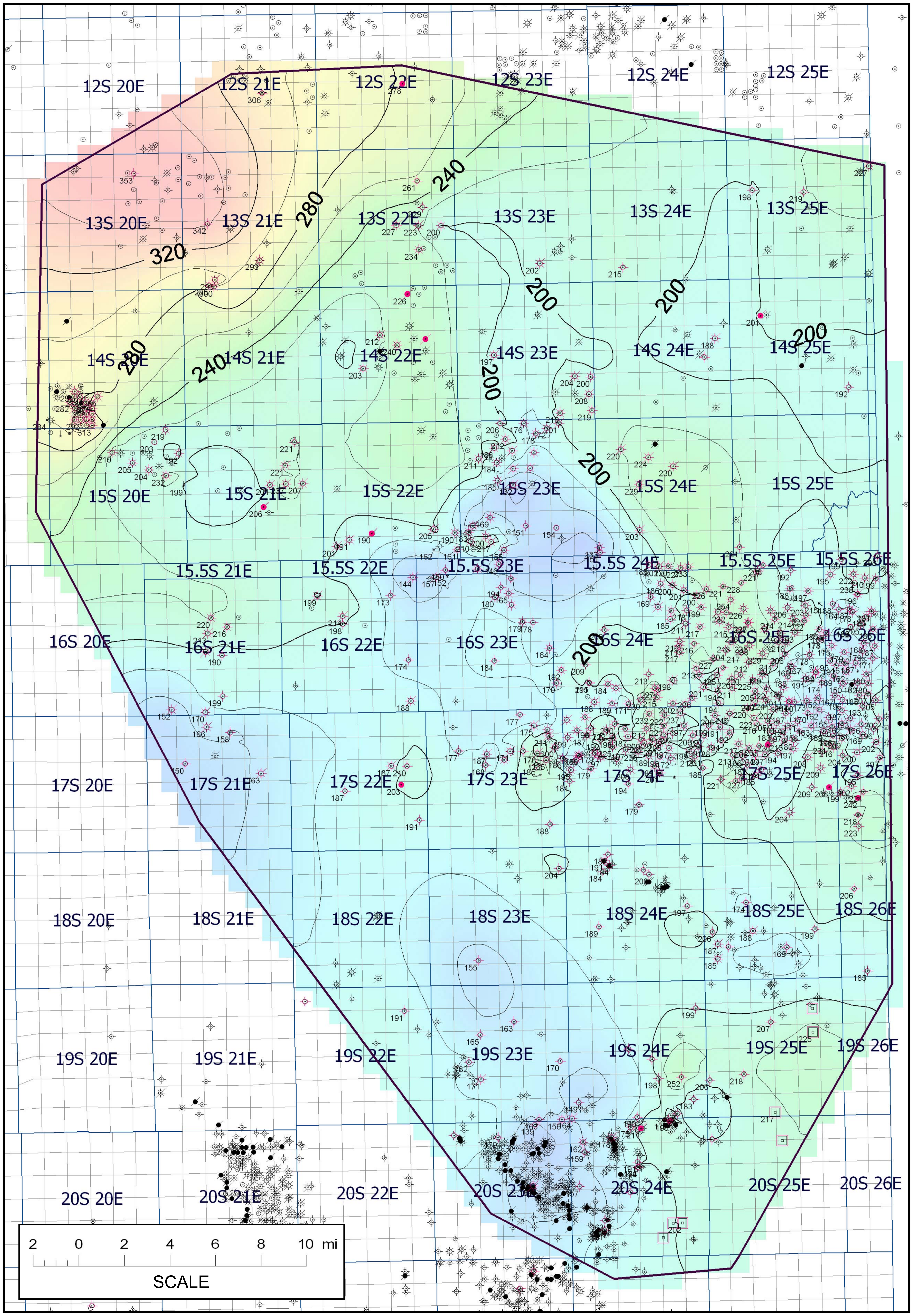

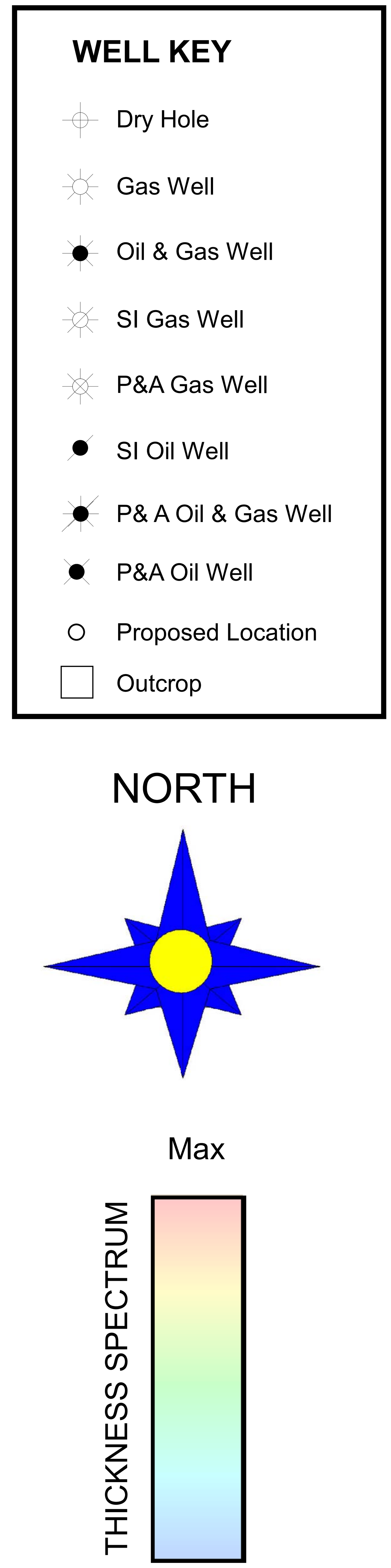

Mapping Parameters - GES

Algorithm: Minimum Curvature
Data Honoring Forced
Iterations: 100
Convergence: 0.01
Gridding: Simplified Defaults
Bias: None

ISOPACH MAP
Dakota Fm + Cedar Mt. Fm
Data Range 132-353'

CONTOUR INTERVAL = 20'

Red Wells are Data Points

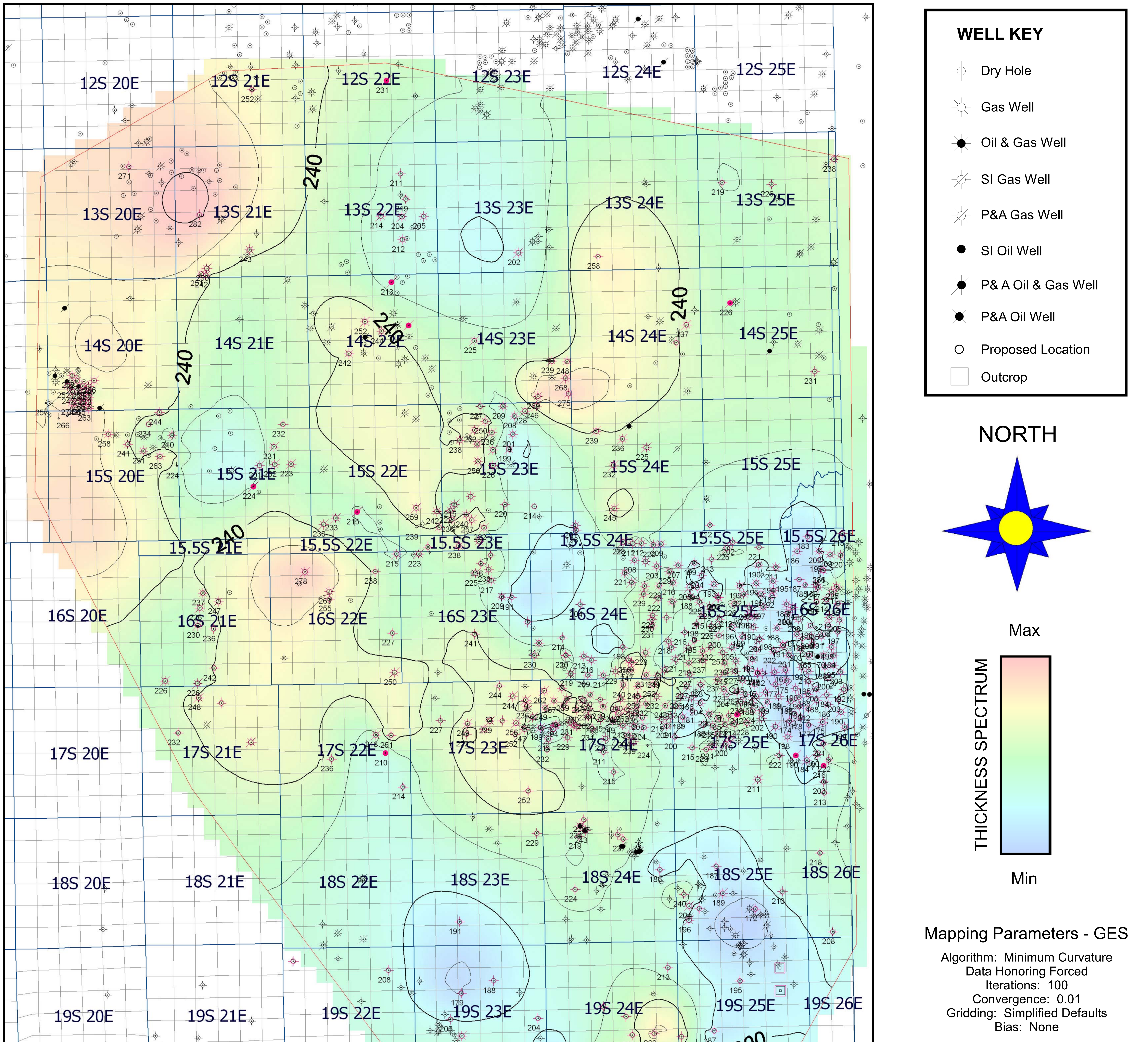

ISOPACH MAP

Dakota Silt to top of Cedar Mountain Fm
Data Range 165 - 282'

Red Wells are Data Points

CONTOUR INTERVAL = 20'

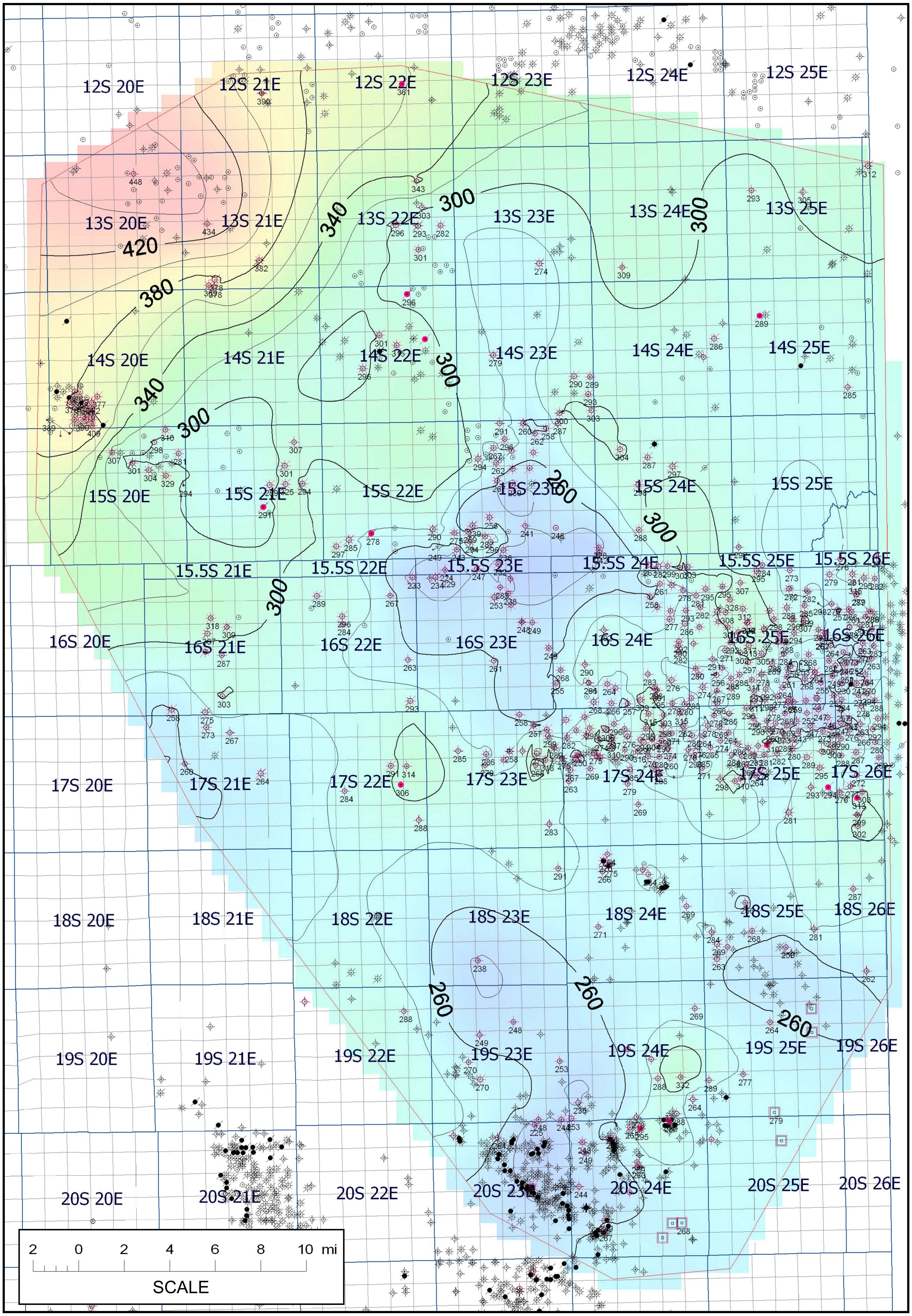

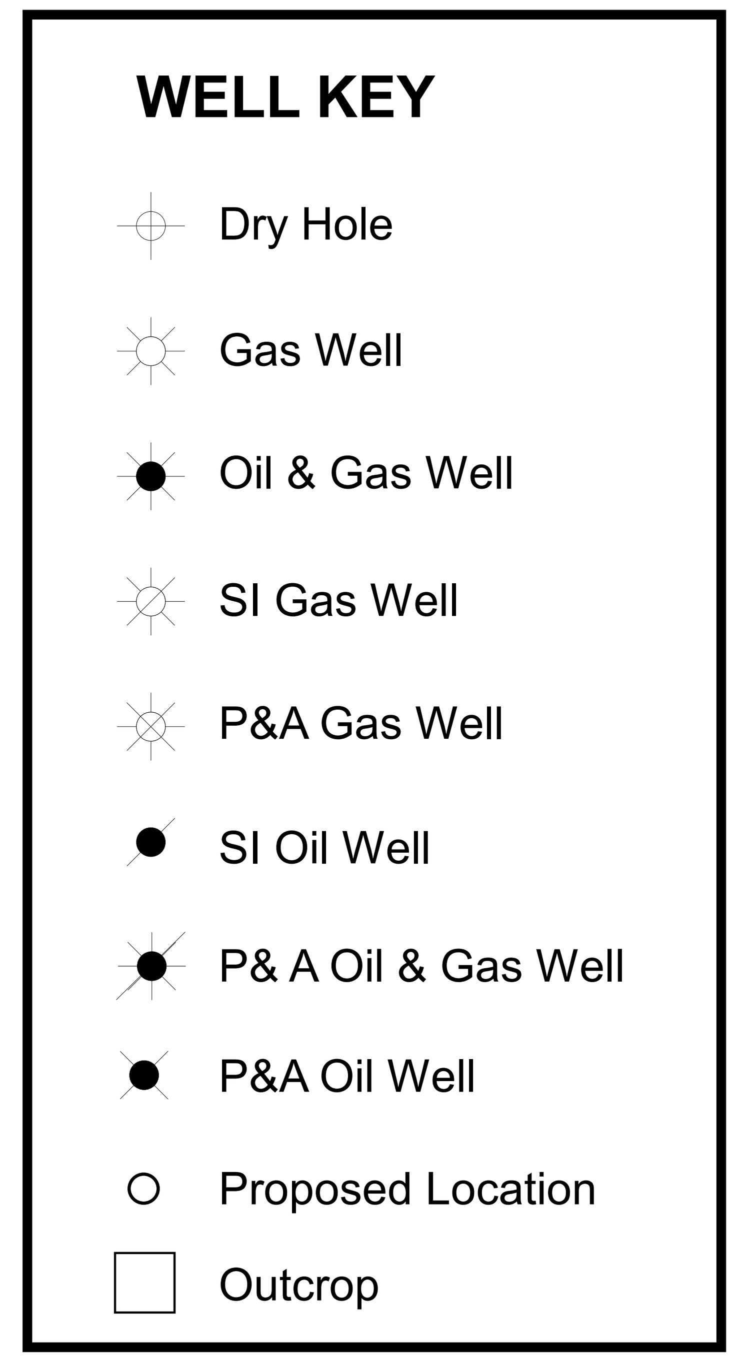

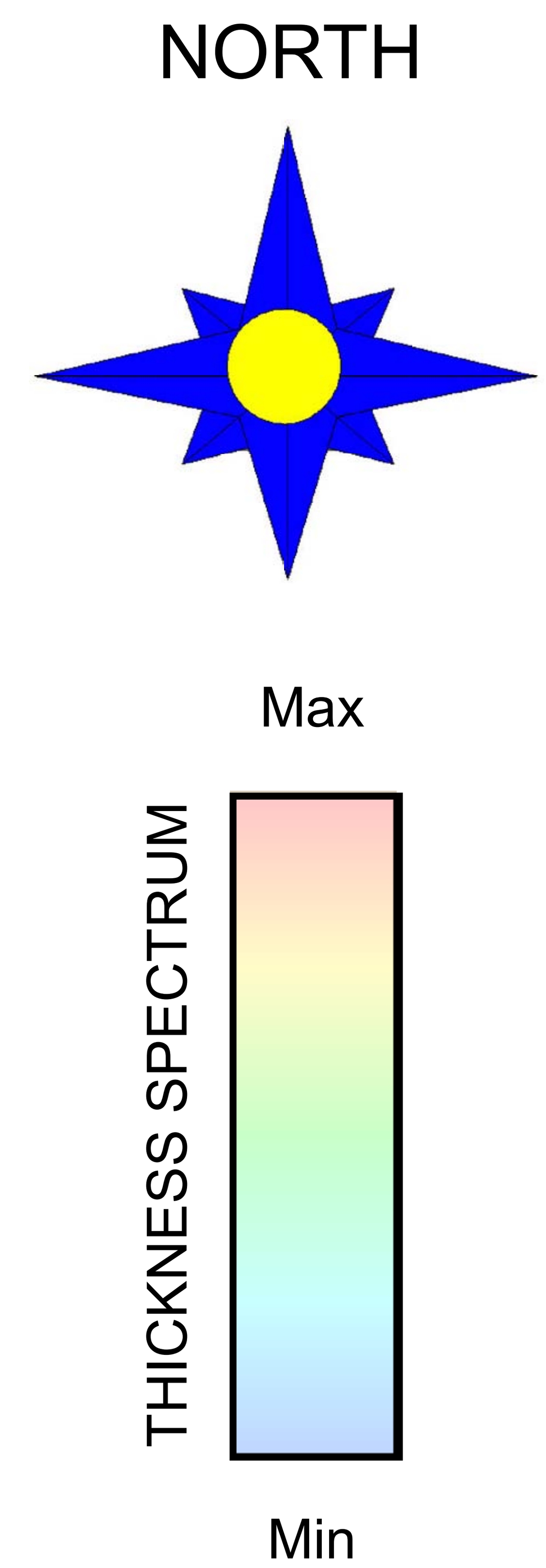

Mapping Parameters - GES

Algorithm: Minimum Curvature
Data Honoring Forced
Iterations: 100
Convergence: 0.01
Gridding: Simplified Defaults
Bias: None

ISOPACH MAP

Dakota Silt to Morrison Fm
Data Range 224 - 448'

CONTOUR INTERVAL = 20'

Red Wells are Data Points

Well ID	Well Name	Well Number	Quarter	Location	Dakota Silt Top TVD	KD Top TVD	Kcm Top TVD	Kbb Top TVD	Jm Top TVD
43019100140000	Wild Cow Gov	1	SWSE	4-17E-25S	4012	4086	4216		4302
43019100240000	S Bar X Gov	3	NENE	19-17E-26S	2392	2469	2613		2664
43019100430000	Larson	1	NWNE	29-19E-25S	343	402	530		620
43019100850000	E Cyn Gov	1	SESW	25-17E-23S	4809	4904	5061		5092
43019100890000	Westbit	3	C-SW	31-15E-25S	7349	7420	7561		7641
43019101070000	Norton	1	SWNW	13-16E-25S	4909	4994	5101		5216
43019103940000	Gov Fed	1A	SESE	30-17E-26S	1462	1543	1665		1761
43019104580000	Dutch Fed	2	SESW	29-20E-24S	376	462	584		643
43019107130000	St	2	NENW	2-20E-24S	1042	1133	1243		1310
43019108040000	Cherry Cyn	1	SESE	2-16E-22S	9143	9237	9381		9410
43019108060000	Moon Rdg	22-22	SENW	22-16E-21S	9549	9646	9785		9836
43019108900000	Jones Fed	1	SWSE	4-17E-24S	5640				
43019109910000	Fed	1	SWSW	19-17E-26S	1925	2002	2109		2201
43019109980000	Fed	5	SWSW	20-17E-26S	1687	1766	1909		1990
43019110100000	E Cyn Fed	1	NWNE	35-16E-24S	5170	5249	5432		5471
43019110110000	E Cyn Fed	2	SWNE	24-16E-24S	5629	5708	5879		5919
43019110120000	E Cyn Fed	3	NWSW	26-16E-24S	5469	5539	5667		5752
43019110900000	SA	35	SESW	24-16E-25S	4306	4396	4494		4574
43019110910000	SA	34A	NESW	21-16E-25S	5679	5764	5905		5981
43019110930000	S SA	1	SWSE	35-16E-25S	3687	3756	3869		3946
43019111520000	Stadia-Larsen	1	SESE	9-19E-25S	779	836	974		1043
43019111650000	Diamond Rdg	3	NESE	25-17E-22S	6452	6549	6666		6740
43019111660000	Diamond Rdg	4	NWSE	36-16E-22S	7464	7569	7714		7757
43019111670000	Diamond Rdg	5	SENW	21-17E-22S	7707	7804	7943		7991
43019112810000	Fed	1-C	SWNW	30-20E-26S	922	1005	1173		1211
43019112830000	Fed	E-1	NWSE	27-18E-25S	1118	1199	1290		1368
43019113060000	Bryson Cyn	4	NWNW	14-17E-24S	4831	4915	5041		5111
43019113080000	Bryson Cyn	5-A	SWSE	12-17E-24S	4217	4296	4436		4495
43019113090000	Bryson Cyn	29-1	NWSW	9-17E-24S	5335	5420	5597		5645
43019113190000	Fed-Gibbs	1-29	NENW	29-16E-24S	5719	5800	5933		6009
43019113200000	Murphy St	16-1	NESW	16-16E-24S	6461	6550	6665		6753
43019114330000	Fed	1	NENW	10-18E-24S	2820	2897			
43019114840000	Lansdale Gov	12-X	NWNE	31-18E-25S	717	795	913		980
43019115720000	Bryson Cyn	1	NWSW	18-17E-25S	3708	3794	3908		3979
43019115770000	Henroid-Fed	1	SWSE	35-19E-24S	1047	1132	1255		1335

Well ID	Well Name	Well Number	Quarter	Location	Dakota Silt Top TVD	KD Top TVD	Kcm Top TVD	Kbb Top TVD	Jm Top TVD
43019150230000	Bar X	4	NENE	18-17E-26S	2670	2757	2845		2957
43019150240000	Bar X	5	SENE	17-17E-26S	2756	2828	2950		3025
43019150260000	Bar X	7	NWNE	7-17E-26S	3041	3132	3229		3317
43019150270000	Crittenden	1	SESE	12-17E-25S	2691	2775	2869		2991
43019150460000	Harley Gov	1	SWNE	30-18E-25S	689	771	893		958
43019150470000	Westbit	1	SWSE	10-16E-25S	4978	5063	5177		
43019150480000	Westbit	2	SESW	9-16E-25S	5840	5926	6033		6152
43019150920000	Hatch	1	SWSW	18-16E-26S	4558	4648	4742		4833
43019153170000	Larsen St	1	NENW	2-20E-24S	1013	1098	1212		1293
43019153730000	CSV Hancock	2	NWSE	10-17E-25S	3192	3268	3416		3481
43019154810000	West Bar X	1	NENW	21-17E-25S	3518	3597	3718		3782
43019154820000	Fed Gov	1	SESE	3-17E-25S	3236	3314	3432		3505
43019154830000	Hancock Gov	4	SWSW	9-17E-25S	3726	3802	3911		4008
43019154840000	USA-WA Peterson	A1	NWNE	8-17E-26S	3085	3181	3288		3377
43019156480000	Fed	1	NENE	13-17E-23S	4266	4355	4465		4541
43019156540000	Ww Fed	C9-10	SWSE	10-17E-23S	6195	6282	6434		6453
43019156560000	Castlegt	D2	NWNE	18-17E-24S	4210	4284			
43019156570000	Ww	E2	SWSE	7-17E-24S	4247	4341	4441		4497
43019156580000	Ww	E3	NENW	17-17S-24E	5281	5369	5511		5553
43019156590000	WwE	4	SENE	14-17E-23S	5487	5570	5739		5755
43019156600000	Ww	M1	SESW	1-17E-23S	4930	5019			
43019156610000	Ww	M2	NWSE	12-17E-23S	4519	4608	4760		4808
43019156620000	Ww	M3	NWNW	7-17E-24S	5937	6020	6186		6219
43019156710000	MR	31-15	NWNE	15-16E-21S	9945	10038	10192		10254
43019156720000	Segundo	2	SWSE	33-16E-21S	9598	9703	9824		9873
43019156730000	Segundo	23-4	NESW	4-17E-21S	9547	9654	9795		9820
43019156960000	East Cyn	41-20	NENE	20-16E-25S	5436	5515	5651		5728
43019156970000	Gov Fed	1-A	SWNW	8-17S-24E	4911	5003	5136		5190
43019157000000	Jones Fed	2	SESE	5-17E-24S	5739	5823	5985		6045
43019158840000	Fed	174	SESW	11-16E-25S	4917	4999	5112		5205
43019158860000	SA	3	SENW	23-16E-25S	4619	4691	4810		4907
43019158870000	SA	4	SESW	30-16E-26S	3802	3882	4005		4051
43019158880000	SA	5	NWSE	25-16S-25E	3952	4033	4146		4215
43019158890000	SA	6	SWNE	21-16E-25S	5639	5714	5866		5952
43019158900000	SA	8	SWSW	16-16E-25S	5498	5577	5726		5815

Well ID	Well Name	Well Number	Quarter	Location	Dakota Silt Top TVD	KD Top TVD	Kcm Top TVD	Kbb Top TVD	Jm Top TVD
43019158910000	SA	9	NWNE	27-16E-25S	5278	5360	5469		5567
43019158920000	SA	11	NESW	15-16E-25S	5680	5759	5906		
43019158930000	SA	12	SWSW	23-16E-25S	4483	4561	4673		4767
43019158940000	SA	13	C-SW	22-16E-25S	5579	5655	5775		5884
43019158950000	SA	14	SWNE	16-16E-25S	5883	5966	6086		6191
43019158960000	SA	16	SESW	26-16E-25S	4303	4381	4497		4564
43019158970000	SA	17	NENE	24-16E-25S	4317	4406	4517		4579
43019158980000	SA	18	NWNW	30-16E-26S	3935	4022	4132		4217
43019158990000	SA	19	SWSE	14-16E-25S	4688	4779	4885		4982
43019159000000	SA	20	SENE	26-16E-25S	4877	4963	5075		5130
43019159010000	SA	21	NWSE	25-16E-25S	3958	4038	4149		4222
43019159020000	SA	22	NENE	15-16E-25S	4800	4884	5021		5098
43019159030000	SA	24	SENW	19-16E-26S	4314	4403	4522		4578
43019159040000	SA	25	SWNE	21-16E-25S	5645	5727	5858		5962
43019159050000	SA	26	SWSW	20-16E-26S	4101	4194	4306		4374
43019159080000	SA	29	NENE	22-16E-25S	4939	5022	5137		
43019159090000	SA	30	NWSW	21-16E-26S	3817	3913	4022		4100
43019159330000	Diamond Rdg	1	NESW	8-17E-23S	5731	5839	5958		6016
43019159340000	Diamond Rdg	2	NENE	23-17E-22S	6988	7091	7198		7294
43019159350000	Diamond Rdg	6	SENW	14-17E-22S	6932	7036	7150		7223
43019160460000	Fence Cyn	3	SWSE	33-15.5E-23S	7865	7952	8103		8112
43019162020000	East Cyn	B22-17	SENW	17-16E-25S	6594	6682	6782		
43019162030000	East Cyn	33-18	NWSE	18-16S-25E	6596	6674	6828		6891
43019162040000	E Cyn A	42-13	SENE	13-16E-24S	5685	5760	5907		5971
43019162050000	E Cyn	A44-12	SESE	12-16E-24S	5535	5610	5764		5828
43019162060000	HP	1X	NWNE	14-16E-23S	7886	7955	8095		8134
43019162090000	Bryson Cyn	1	SESW	10-17E-24S	4142	4222	4391		4458
43019162100000	Bryson Cyn	2	SENW	10-17E-24S	4357	4442	4605		4651
43019162110000	Bryson Cyn	3	SESW	8-17E-24S	5364	5460	5595		5639
43019162120000	Bryson Cyn	6-A	SWSE	9-17E-24S	4382	4475	4627		4672
43019162140000	Bryson Cyn	9	NWSE	10-17E-24S	4578	4653	4828		4875
43019162600000	Gretchen St	1	NENE	16-20E-24S	1410	1485	1587		1683
43019165320000	SA	1	SENW	26-16E-25S	4000	4087	4204		4256
43019201540000	HP	M4	SENE	6-17E-24S	6061	6140			
43019202040000	Douglas St	1	SW	32-18E-26S	52	129	260		314

Well ID	Well Name	Well Number	Quarter	Location	Dakota Silt Top TVD	KD Top TVD	Kcm Top TVD	Kbb Top TVD	Jm Top TVD
43019300130000	HP	M6	NESE	32-16E-24S	5932	6012	6151		6200
43019300180000	Huskey St	1	NENW	36-19E-24S	1012	1093	1244		1276
43019300470000	Bitter Crk	1	SWSE	2-16E-25S	5679	5763	5869		5951
43019300490000	HP	M7	SWNW	6-17E-24S	5301	5389	5563		
43019300610000	Bitter Crk St	2	NWNE	2-16E-25S	7232	7313	7453		7505
43019300660000	HP	M9	SWSE	29-16E-24S	6402	6473	6612		6668
43019300770000	Ww	E5	NWNE	18-17E-24S	4210	4289			
43019301350000	Anderson Fed	1	SESW	8-16E-25S	6794	6874	7002		
43019301360000	Anderson Fed	2	SWSW	12-16E-24S	6029	6104			
43019301690000	Cherry Cyn St	428-1	SWSE	5-16E-22S	9564	9654	9842		9853
43019301710000	Fed	915-1	SWNW	13-17E-22S	6710	6814	6961		7024
43019301720000	Fed	051-1	SESW	22-16E-23S	8410	8487	8651		8671
43019301790000	Fed	33-11-428	NWSE	11-16E-24S	6227	6299			
43019301930000	St	913-1A	C-SE	9-16E-22S	9343	9425	9606		9639
43019302040000	Fed	614-1	SESW	3-17E-21S	9438	9547			9705
43019302180000	Hancock Gov	10A	NESE	4-17E-25S	3735	3812	4002		4017
43019302250000	Hancock Gov	20	NESE	9-17E-25S	3596	3674			
43019302400000	Arco St	2-1	NESE	2-16E-24S	6858	6933	7066		7119
43019302550000	Kewanee	1-28	NWNW	28-19E-23S	2454	2553	2661		2724
43019302750000	Ww	M10	SWSE	6-17E-24S	6011	6088	6268		
43019302790000	Lansdale Fed	14-1	SWNE	14-17E-25S	3062	3143	3252		3351
43019302880000	Fed	M11	NWNW	19-17E-24S	4944	5026	5176		5207
43019302890000	Hancock-Gov	14	SWNE	20-17E-25S	3518	3604	3747		
43019303100000	Hancock St	7	NESW	2-17S-25E		3377	3502		3548
43019303170000	Ww St	M15	NESE	2-17E-23S	6093	6175	6337		6350
43019303180000	Ww St	M14	NWNW	2-17E-23S	6369	6450	6613		6627
43019303210000	Fed	M12	SWSW	11-17E-23S	6331	6420			
43019303230000	Fed	6-1	NESW	6-19E-22S	5990	6102			
43019303350000	Bar Crk	1	NWSE	19-17E-26S	1820	1895	2020		2097
43019303380000	Fed	266-1	SWNE	24-19E-23S	2496	2579	2700		2749
43019303400000	Fed	263-1	NWSE	10-19E-23S	3453	3538	3641		3701
43019303430000	Fed	258-1	NWSE	5-18E-24S	3812	3891	4046		4082
43019303440000	Anschutz	2	NWSE	24-17E-25S	2180	2268	2370		2474
43019303460000	Fed	273-1	SWSW	28-18E-23S	4522	4605	4713		4760
43019303600000	Anschutz	B385-3	NESE	23-17E-25S	2364	2448	2586		2657

Well ID	Well Name	Well Number	Quarter	Location	Dakota Silt Top TVD	KD Top TVD	Kcm Top TVD	Kbb Top TVD	Jm Top TVD
43019303620000	Fed	258-3	SENE	5-18E-24S	3690	3772	3918		3954
43019303640000	Fed	258-5	NWNE	8-18E-24S	3521	3603	3740		3787
43019303860000	Fed	335-1	SWNE	20-19E-23S	2758	2846	2958		3028
43019303900000	Hancock Gov	44	NENE	19-17E-25S	3722	3799	3937		4020
43019304100000	Joyce St	1	NENE	16-20E-24S	785	871	1020		1045
43019304110000	Bowers Fed	1-6	SWSE	6-20E-24S	1506	1592	1710		1754
43019304120000	Lansdale Gov	13-13	SWSW	13-17E-25S	2887	2973	3085		3182
43019304130000	Fed	1-23	SESE	23-18E-25S	977	1059	1187		1258
43019304140000	Fed	2-18	NWNE	18-18E-26S	794	875	1012		1081
43019304150000	Fed	3-31	SENE	31-17E-26S	1347	1426	1560		1649
43019304160000	Fed	33-13	SWSW	33-16E-26S	3468	3551	3671		3756
43019304210000	Ten Mile St	921-1	NENW	34-16E-21S	9258	9362	9500		9561
43019304250000	Bar Crk	5	NENE	30-17E-26S	1626	1697	1842		1939
43019304270000	Hancock	33	SWSE	16-17E-25S	3433	3518	3643		3709
43019304510000	st	32-1	NENE	32-16E-26S	3667	3757	3851		3937
43019304590000	CSV Fed	1-31	NESW	31-16E-26S	3669	3754	3868		3921
43019304600000	Fed	1-20	NWSE	20-16E-25S	6155	6222	6353		6426
43019304620000	Fed	6-14	SESW	6-17E-25S	4270	4349	4496		4548
43019304630000	Fed	3-15	SWSE	3-17E-24S	4536	4619	4776		4831
43019304680000	Fed	13-9	NESE	13-16E-25S	4647	4733	4836		4928
43019304720000	Fed	17-9	NESE	17-16E-25S	5611	5697	5836		5912
43019304910000	Bowers St	1-36	SWSE	36-19E-23S	1931	2019	2125		2175
43019304930000	Fed	258-6	SESE	5-18E-24S	3577	3668	3820		3852
43019304940000	Bar X	8	NENW	11-17E-25S	3114	3201	3303		3357
43019304970000	Fed	5-4	NWNW	5-17E-26S	3350	3435	3550		3628
43019304990000	Fed	8-5	SWNW	8-17E-26S	2960	3057	3146		3226
43019305000000	st	32-11	NESW	32-16E-26S	3541	3630	3729		3815
43019305050000	Bowers Fed	1-35	SWSE	35-19E-23S	2090	2175	2291		2338
43019305060000	Fed	5-9	NESE	5-17E-26S	3194	3286	3386		3488
43019305070000	Hogle USA	14-4	NWNW	14-17S-24E	4830	4919	5034		5100
43019305160000	Fed	6-7	SWNE	6-17E-25S	4461	4533	4688		4739
43019305170000	Fed	7-4	SWNW	7-17E-25S	4207	4281	4420		4471
43019305190000	Fed	29-15	SWSE	29-16E-24S	6426	6506	6651		6717
43019305200000	Wilson	33-15	SWSE	33-16E-24S	5800	5877	6009		6066
43019305210000	Fed	3-8	SENE	3-17E-24S	4745	4828	4985		5060

Well ID	Well Name	Well Number	Quarter	Location	Dakota Silt Top TVD	KD Top TVD	Kcm Top TVD	Kbb Top TVD	Jm Top TVD
43019305220000	Fed	4-12	NWSW	4-17E-24S	5733	5819	5963		6029
43019305270000	SA	31	NWNW	22-16E-25S	5803	5883	6015		
43019305280000	SA	32	SWSW	14-16E-25S	4528	4614	4734		4807
43019305330000	Fed	27-1	NENE	27-19E-24S	1762	1852	1990		2050
43019305380000	Fed	35-10	NWSE	35-16E-24S	5042	5122	5289		5337
43019305410000	Fed	14-2	NWNE	14-16E-25S	4775	4857	4970		5071
43019305440000	Fed	5-13	SWSW	5-17E-24S	5817	5914	6056		6110
43019305450000	Fed	28-15	SESW	28-16E-24S	6384	6464	6597		6648
43019305490000	Fed	10-1	SWNE	10-18E-24S	2652	2736	2889		2936
43019305500000	Fed	13-2	NESW	13-18E-24S	1442	1514	1628		1711
43019305520000	Arco Fed	B1	SESE	6-16E-25S	5986	6055	6193		6281
43019305540000	Fed	12-1	NWNE	12-19E-24S	1364	1434	1577		1633
43019305640000	Fed	26-1	NENE	26-19E-24S	1408	1488	1677		1740
43019305700000	Arco	27-1	NWSW	27-16E-25S	5278	5357	5483		5556
43019305710000	St	2-14	SESW	2-17E-24S	5614	5691	5865		5912
43019305720000	Arco Fed	C1	NWNW	35-16E-25S	4216	4291	4409		4480
43019305780000	Arco Fed	D1	NESE	34-16E-25S	4148	4224	4348		4425
43019305920000	Bar X	11	NWNW	18-17E-26S	2692	2776	2869		2980
43019305970000	Bar X	12	NWSE	8-17E-26S	2910	2988	3100		3190
43019305980000	Bar X	13	NWSW	7-17E-26S	2800	2881	3012		3090
43019306040000	St	2-7	SENW	2-17E-24S	5637	5718	5882		5940
43019306050000	St	36-14	SESW	36-16E-24S	5633	5712	5864		5912
43019306060000	St	36-16	SESE	36-16E-24S	5652	5721	5901		5932
43019306080000	SA	33	SWSW	25-16E-25S	4255	4332	4457		4523
43019306170000	Carlson USA	13-4	NWNW	13-16E-25S	4873	4952	5060		5172
43019306240000	TXO-Arco Fed	G1	NWNW	19-16S-25E	6382	6453	6603		6669
43019306300000	Ambra-Bowers	7-3	SWNE	7-20E-24S	1358	1448	1545		1607
43019306320000	McCormick St	16-9	NESE	16-17E-24S	4138	4215	4374		4423
43019306340000	Texas Texas	1	NWSE	36-16E-25S	3682	3767	3849		3919
43019306390000	Valentine Fed	4	SESW	35-16E-25S	3797	3867	3975		4064
43019306400000	Valentine Fed	2	SENW	34-16E-25S	4328	4398	4547		4620
43019306410000	Mid Cyn	4-30	SWSW	30-16E-24S	5322	5407	5552		5577
43019306450000	Fed	6-4	NESW	4-16E-25S	7023	7102	7236		7330
43019306460000	Fed	13-3	NWNW	3-16E-25S	7109	7183	7334		7404
43019306480000	St	16-7	SWNE	16-17E-23S	5511	5613	5733		5781

Well ID	Well Name	Well Number	Quarter	Location	Dakota Silt Top TVD	KD Top TVD	Kcm Top TVD	Kbb Top TVD	Jm Top TVD
43019306530000	Cherry Cyn St	16-1	NWNE	16-16E-22S	9440	9526	9695		9724
43019306540000	St	24-10A	NWSE	24-16E-22S	8986	9075	9213		9249
43019306560000	Nicor Fed	1	NWNE	28-16E-25S	5824	5909	6024		6121
43019306570000	Grynberg Fed	1	SESW	28-16E-25S	5519	5587	5751		5807
43019306690000	St	16-9	SENE	16-16E-21S	9506	9600	9732		9813
43019306700000	Texas Texas	2	SWSW	36-16S-25E	3664	3739	3833		3912
43019306820000	St	17-3	NENW	17-17E-21S	9505	9615	9737		9765
43019306860000	Fed	12-2	NENW	12-16E-25S	6130	6215	6341		6412
43019306970000	Reinauer	1-5	SWNW	1-17E-24S	5488	5566	5740		5803
43019306980000	Moxa Fed	1	NWSW	9-16E-26S	4677	4778	4914		4965
43019307010000	Hogle	11-12	NWSW	11-17S-24E	5614	5614	5754		5815
43019307020000	Edwards USA	2-12	NWNE	12-17E-24S	4185	4264	4433		4470
43019307030000	Wilson	33-2	NWNE	33-16E-24S	6392	6471	6608		
43019307040000	Calvinco	31-12	NWSW	31-16E-25S	5098	5175	5309		5381
43019307060000	Peterson Sprngs	1	NWSE	14-17E-21S	9252	9353			9516
43019307080000	Bailey Fed	1	SWSE	9-17E-23S	5202	5301	5451		5488
43019307190000	Fed Harris	1	NWNE	21-20E-24S	696	773			
43019307210000	Fed	23-1	NESW	1-16S-24E		7300	7427		7500
43019307260000	Tenneco USA	37931	SENW	11-17E-24S	5589	5674	5824		5879
43019307310000	Tenneco USA	20-11	NESW	20-18E-24S	3448	3530	3672		3719
43019307320000	Tenneco USA	11-1	NENE	11-19E-22S	4034	4131	4242		4322
43019307330000	Reinauer	1-14	SESW	1-17E-24S	4446	4531	4678		4728
43019307350000	Long Cyn St	16-4	NWNW	16-19E-23S	3434	3518	3613		3683
43019307480000	USA	9-12	NESE	12-17E-24S	3919	3996	4130		4195
43019307500000	Fed	21-11	NENW	11-16E-24S	7129	7218	7350		7387
43019307550000	Fed	21-7	NENW	7-16E-25S	5845	5926	6074		6126
43019307560000	Gilliland-Fixx	31-1	NENW	31-19E-24S	1954	2040	2142		2189
43019307580000	UT St	1	SESW	32-16E-25S	4657	4729	4884		4923
43019307590000	UT St	2	SWNW	32-16E-25S	4855	4928	5074		5122
43019307620000	Harvey Fed	1	SWSE	5-16E-25S	6309	6383	6508		6604
43019307660000	Barnhill Fed	1	SESE	21-17E-24S	4512	4597	4723		4791
43019307680000	Bowers-Texoma-Fed	1-31	SWSW	31-19E-24S	1840	1929	2029		2093
43019307710000	Brown USA	35-3	NENW	35-16E-24S	5233	5304	5489		5531
43019307720000	Sulpher Cyn USA	1-15	SWSE	1-18E-23S	4580	4667	4809		4871
43019307730000	WInter Camp	7-14	SESW	7-17E-25S	4115	4192	4304		4380

Well ID	Well Name	Well Number	Quarter	Location	Dakota Silt Top TVD	KD Top TVD	Kcm Top TVD	Kbb Top TVD	Jm Top TVD
43019307790000	TOC TXO Pogo USA	15-9	NESE	15-17E-24S	5154	5240	5358		5429
43019307800000	Ptasynski Fed	1	NENW	15-17E-23S	6112	6203			
43019307900000	Arco Fed	1	SESE	35-15.5E-24S	7400	7481	7611		7682
43019307920000	Moxa Fed	A1	NESE	4-16E-26S	5720	5803	5940		6002
43019307940000	Texaco St	1	SESW	32-15.5E-23S	8764	8838			8988
43019307970000	Credo Fed	1	NESE	5-16E-26S	5923	6008	6132		6218
43019307980000	Credo Fed	A1	SENW	5-16E-26S	6147	6226	6349		6428
43019307990000	Hougen Fed A-1 St	1	NESW	14-17E-24S	5017	5104	5256		5305
43019308340000	Hancock Fed	1X	SENW	5-17E-25S	5598	5673	5801		5883
43019308380000	Wall Fed	1	NESW	30-16E-25S	6209				
43019308400000	Dougherty St	16-3	NENW	16-17E-24S	5270	5349	5501		
43019308410000	Baumgartner Fed	2	SWSW	25-16E-24S	5820	5898	6048		6096
43019308490000	Fed	3-34	SESW	34-15.5E-25S	7281	7359	7483		7565
43019308520000	Ww	5	NESW	18-17E-24S	4344	4416	4558		4611
43019308530000	Ww	3	NENW	13-17E-23S	5520	5603	5767		5838
43019308540000	Credo Fed	A2	SENW	6-16E-26S	6161	6245	6347		6440
43019308560000	Arco Fed	2	NESW	35-15.5E-24S	6811	6889	7039		7074
43019308570000	Callister Fed	1	NWSE	24-16E-24S	5745	5810	5976		6027
43019308590000	Lauck Fed	1	SWNE	29-16E-25S	5617	5694	5812		
43019308670000	Fed	22-1	SWNE	22-19E-24S	2145	2232			
43019308680000	Fed	33-1	SESE	33-19E-24S	1173	1261	1416		1451
43019308910000	Fed	D1	SESE	11-17E-23S	6017	6112	6273		6288
43019308920000	Ww Fed	B1	NWSW	17-17E-24S	5241	5331	5470		5510
43019308930000	Bennion Fed	1	NENW	30-16E-25S	6279	6346	6497		6559
43019308940000	Prospector Capansky	18-2	SESW	18-20E-24S	992	1079	1169		1236
43019308950000	Fed	C1	NENW	12-17E-23S	4773	4861	5009		5072
43019308990000	Patsantaras Pete	2	SWNW	3-20E-24S	1002	1086	1204		1297
43019309170000	Teton Fed	1	NESE	31-15.5E-26S	6409	6486	6592		6685
43019309230000	Mid Cyn	13-13	NWNW	13-16E-24S	6091	6183	6330		6368
43019309250000	Fed	11-30	SENW	30-16E-24S	5486	5562	5703		5754
43019309310000	Fed Lansdale	9-1A	SESE	9-20E-24S	757	835	976		1026
43019309350000	Genie	1	SWNE	4-20E-24S	1151	1241	1349		1416
43019309360000	St	16-1	SWSE	16-19E-24S	2392	2481			
43019309550000	Fed	24-1	NWNE	24-16E-24S	5694	5770	5919		5986
43019309600000	Bryson Cyn Fed	15	NENE	15-17E-24S	5222	5303	5435		5492

Well ID	Well Name	Well Number	Quarter	Location	Dakota Silt Top TVD	KD Top TVD	Kcm Top TVD	Kbb Top TVD	Jm Top TVD
43019309620000	Fed	33-16	SESE	33-16E-25S	5105	5176	5350		5416
43019309630000	Fed	33-8	SENE	33-16E-25S	5389	5477	5625		5682
43019309660000	Bryson Cyn	13	SWNE	8-17E-24S	5735	5817	5935		6009
43019309900000	Lauck Fed	A1	SESE	29-16E-25S	4789	4857	5024		5077
43019309910000	Fed	43-7	NWSE	7-16E-25S	5734	5817	5950		6016
43019309950000	BNT Fed	1	NWNW	27-17E-24S	5300	5390	5515		5569
43019310020000	Arco Fed	H1	NWSW	12-16E-25S	5554	5636	5748		5839
43019310050000	Bryson Wash Fed	1	NENE	23-17E-24S	4397	4490	4621		
43019310090000	Valentine Fed	3	SESW	35-16E-25S	4022	4103	4239		4307
43019310110000	Hancock Gov	11	NWNW	4-17E-25S	4281	4357	4518		4577
43019310120000	Hancock Fed	4-11	NESW	4-17E-25S	4217	4290	4438		4513
43019310130000	Hancock Fed	8-3	NENW	8-17E-25S	4162	4234	4366		4426
43019310140000	Hancock Fed	27-9	NESE	27-17E-25S	2444	2521	2655		2725
43019310170000	BMG Fed	1	NENW	8-16E-26S	5709	5792	5890		5988
43019310190000	Hancock Fed	3-8	SENE	3-17E-25S	3523	3604	3738		3791
43019310200000	Nicor Fed	2	SESE	28-16E-25S	5727	5816	5980		6041
43019310210000	Hancock Fed	20-1	NENE	20-17E-25S	3454	3537	3685		3764
43019310300000	Fed	31-1	SESE	1-16E-24S	6045	6122	6248		6323
43019310310000	BMG Fed	A1	SWSW	9-16E-26S	4267	4343	4466		4525
43019310340000	TXO USA	A1	SWSW	20-16E-25S	5934	5998	6150		6225
43019310350000	Fed	42-8	SWSE	8-16E-25S	6102	6178	6296		6410
43019310390000	Fed Cisco	5	SENW	29-20E-24S	249	335	427		498
43019310460000	Fed	34-31	SWSW	31-15.5E-25S	7277	7347	7486		7580
43019310610000	Cisco Sprgs	1	NESE	4-20E-23S	1793	1878	2011		2057
43019310640000	Cisco Sprgs	C 1	NESE	6-20E-23S	2961	3053			
43019310660000	Bryson Cyn Fed	14	SWNW	9-17E-24S	5741	5830	5972		6028
43019310690000	Harley Dome	19-1	SESW	19-18E-25S	861	939	1101		1145
43019310710000	Harley Dome	17-1	NESE	17-18E-25S	2056	2138	2243		2312
43019310720000	Harley Dome	21-1	SWSW	21-18E-25S	863	943	1052		1131
43019310750000	L Berry St	1	SWSW	2-16E-23S	8025	8098	8263		8263
43019310770000	Fed	1-34	NESE	34-16E-24S	5670	5749	5899		5979
43019310780000	Fed	2-34	SESW	34-16E-24S	5815	5901	6026		6072
43019310920000	Bryson Cyn Fed	17	NWNE	17-17S-24E	5399	5479	5641		5671
43019310930000	Bryson Cyn Fed	16	SENE	10-17E-24S	5200	5274	5462		5504
43019310990000	Fed	17-8	SENE	8-16E-25S	6981	7055	7185		7309

Well ID	Well Name	Well Number	Quarter	Location	Dakota Silt Top TVD	KD Top TVD	Kcm Top TVD	Kbb Top TVD	Jm Top TVD
43019311020000	Fed Buttes	1-6	SWSW	6-20S-25E			198		264
43019311080000	BMG Fed	2	SWSW	8-16E-26S	5060	5139	5249		5326
43019311090000	Lauck	2	NWSW	29-16E-25S	5955	6026	6166		6211
43019311130000	Keas Fed	8	SESE	5-20E-24S	1287	1375	1483		1553
43019311140000	BMG Fed	3	NENE	18-16E-26S	5011	5100	5199		5278
43019311300000	BMG Fed	4	NWNW	17-16E-26S	5326	5409	5543		5587
43019311310000	BMG Fed	5	NESE	7-16E-26S	5130	5213	5325		5428
43019311350000	Fed	14-02	SESW	14-20E-23S	1171	1256	1344		1407
43019311400000	N Bar X Fed	1	NENW	1-17E-25S	3455	3540	3630		3702
43019311480000	HP	2	SWNW	11-16E-23S	7950	8029	8167		
43019311510000	L Berry St	C1	NWNW	2-16E-23S	7370	7455			
43019311530000	Mid Cyn	13-3	NWNW	13-16E-23S	7811	7882	8002		8060
43019311600000	L Berry St	B1	NWSE	3-16E-23S	7960	8049	8176		8243
43019311620000	Arco St	36-7	SWSE	36-15.5E-24S	7238	7313	7458		7540
43019311670000	SAGE Fed	31-31	NWNE	31-16E-25S	5874	5947	6095		6148
43019311690000	Bryson Cyn	18	NENE	9-17E-24S	5603	5692	5822		5879
43019311700000	North Bar X Fed	2	SENW	6-17E-26S	3340	3410	3535		3597
43019311710000	N Credo Fed	1	SWSW	33-15.5E-26S	6444	6531	6659		6739
43019311760000	St	2-7	NENW	2-20E-23S	2043	2129	2237		2268
43019311810000	BMG Fed	6	SESW	7-16E-26S	5273	5366	5458		5530
43019311830000	BMG Fed	7	NWSE	17-16E-26S	4775	4860	4989		5065
43019311920000	Arco St	36-8	SWSW	36-15.5E-24S	6743	6822	6955		7042
43019311930000	N Bar X Fed	3	NWSE	1-17E-25S	3273	3364	3463		3519
43019311940000	N Bar X Fed	4	NWSE	6-17E-26S	3208	3298	3413		3491
43019311950000	Fed	3-4	NWNW	3-17E-25S	3688	3764	3903		3966
43019311960000	Fed Quinoco	18-4	NWNW	18-17E-25S	3820	3904	4031		4105
43019312020000	WInter Camp St	2-8	SENE	2-17E-25S	3429	3511	3606		3681
43019312040000	BMG Fed	8	SWNW	7-16E-26S	5470	5557	5657		5745
43019312240000	st	32-3	NENW	32-16E-26S	3650	3735	3820		3897
43019312250000	Fed	14-2	NWNE	14-17E-24S	4277	4365	4481		4537
43019312260000	Fed	6-16	SESE	6-17E-25S	5051	5129	5237		5320
43019312290000	Hancock Fed	17-1	NENE	17-17E-25S	3590	3671	3805		3857
43019312300000	Hancock St	2-16	SESE	2-17E-25S	3175	3259	3364		3422
43019312310000	Hancock Fed	8-10	NWSE	8-17E-25S	3875	3944	4100		4161
43019312350000	Hancock Fed	15-3	NENW	15-17E-25S	3368	3456	3596		3650

Well ID	Well Name	Well Number	Quarter	Location	Dakota Silt Top TVD	KD Top TVD	Kcm Top TVD	Kbb Top TVD	Jm Top TVD
43019312360000	Hancock Fed	17-3	NENW	17-17E-25S	3795	3866	3981		4079
43019312370000	Hancock St	16-3	NENW	16-17E-25S	3553	3632	3777		3836
43019312400000	Fed	3-11	NENW	11-17E-24S	5591	5665	5839		5881
43019312410000	Fed	10-11	SWSE	11-17E-24S	4492	4569	4695		4766
43019312420000	Fed	7-8	SENE	7-17E-25S	4723	4803	4904		4997
43019312430000	Quinoco St	16-12	SWSW	16-16E-26S	4767	4858	4962		5043
43019312440000	Fed	1	SWSW	5-17E-26S	3137	3234	3321		3400
43019312460000	Credo-Samedan Fed	13-1	NWNE	13-17E-24S	4117	4195	4326		4413
43019312500000	SA	40	NWNE	27-16E-25S	5257	5334	5456		5545
43019312510000	SA	36A	SESE	19-16E-26S	4240	4328	4436		4507
43019312520000	SA	37	SWNE	20-16E-26S	4340	4435	4552		4603
43019312530000	SA	38	SWNE	16-16E-25S	5906	5981	6106		6218
43019312630000	Fed	10-4	NWNW	10-17E-25S	3712	3789	3950		3972
43019312640000	Fed	1-11	NENE	11-17E-24S	5597	5678	5829		5868
43019312660000	St	16-1	NENE	16-17E-25S	3486	3560	3700		3767
43019312820000	Quinoco St	32-9	NESE	32-16E-26S	3520	3607	3715		3814
43019312890000	SA	41	NENE	36-16E-25S	4353	4434	4554		4608
43019312900000	SA	42	NESE	30-16E-26S	4243	4333	4444		4495
43019312910000	SA	43	NESE	29-16E-26S	3829	3913	4022		4093
43019312990000	SA	45	NWSE	20-16E-26S	4213	4306	4421		4485
43019313000000	SA	46	NWNW	28-16E-26S	4580	4672	4777		4843
43019313010000	SA	44	SENE	30-16E-26S	4455	4540	4655		4701
43019313040000	Fed	3-14	SESW	3-17E-25S	3505	3584	3709		3775
43019313060000	Fed	17	NWSW	11-17S-25E	2992	3077	3200		3257
43019313160000	SA	49	NENW	29-16E-26S	4354	4439	4545		4606
43019313170000	Fed	48	SENW	30-16E-26S	4243	4328	4429		4520
43019313180000	1897	47	NWNE	31-16E-26S	3473	3553	3638		3703
43019313200000	Fed	20R	NWSW	10-17E-25S	3586	3666	3828		3896
43019313230000	Fed	2-31	SWSE	31-16E-26S	3541	3629	3754		3825
43019313270000	Fed	10-2	NWNE	10-17E-25S	3043	3119	3231		3316
43019313330000	Fed	3-10	NWSE	9-17S-25E	3641	3718	3827		3925
43019313370000	Fed N	20	SENE	12-17E-25S	2907	2991	3091		3187
43019313470000	Bar-X Fed	23	SESE	1-17E-25S	3078	3162	3273		3327
43019313510000	Fed	9	NENE	17-16E-26S	4879	4965	5100		5160
43019313520000	Fed	21	NENW	12-17E-25S	3044	3128	3232		3317

Well ID	Well Name	Well Number	Quarter	Location	Dakota Silt Top TVD	KD Top TVD	Kcm Top TVD	Kbb Top TVD	Jm Top TVD
43019313530000	Fed	19	SWSW	11-17E-25S	3004	3087	3206		3284
43019313590000	Valentine Fed	4	SESW	34-16E-25S	4465	4537	4692		4761
43019313600000	UT St	3	NENE	32-16E-25S	5224	5302	5461		5513
43019313680000	Jo Reva No	1	NWSW	16-17E-25S	3429	3513	3656		3695
43019313690000	Bar-X Fed	22	NENW	13-17E-25S	2768	2845	2942		
43019313710000	Bar X	25	NWSE	12-17E-25S	2735	2810	2908		3041
43019313780000	Fed	42-24	SENE	24-16E-23S	5997	6082			6246
43019313830000	Bar X	24	SESW	6-17E-26S	3121	3206	3309		3368
43019313840000	Credo Fed	3	NESW	5-16E-26S	5843	5920	6040		6158
43019313850000	BMG Fed	11	NWSW	17-16E-26S	4945	5027	5166		5213
43019313870000	Moon Rdg Fed	31-21X	NWNE	21-16E-21S	9721	9820	9951		
43019313900000	St	21-10	NENW	10-16E-23S	8081	8154	8306		8334
43019313910000	Fed BMG	12	NENW	8-16E-26S	6033	6123	6269		6320
43019313930000	BMG Fed	10	NWSW	17-16E-26S	4744	4835	4943		5017
43019313970000	HP	1-34	NWSE	34-15.5E-23S	7431	7517			7663
43019313980000	Moon Cyn	1	NWSW	32-16E-21S	9797	9903	10023		10055
43019314050000	Moon Cyn	2	NESE	9-16E-21S	9705	9803	9942		10023
43019314150000	Cedar Camp	1-1	NENE	1-16E-22S	8832	8921	9047		9065
43019314160000	Cedar Camp	1-6	NENE	6-16E-23S	8771	8848	8994		9005
43019314480000	Cedar Camp	3-5	NENW	5-16E-23S	8672	8749			8901
43047100180000	Winter Rdg	1	NESW	22-15E-21S	9426	9511	9650		9717
43047105770000	DRO	32-5A	NESE	32-14S-20E	10429	10524	10701	10750	
43047106920000	Ohio 2 Waters	1	NESW	8-14E-25S	6926	7014	7152		7215
43047107640000	Main Cyn	1	NESE	28-15E-23S	8145	8235	8365		8386
43047109600000	Gov	1	NWNW	17-13E-25S	8413	8508	8632		8706
43047111400000	Neilson-Sweet Crk	2	SWNE	14-14E-22S	9140	9216			
43047161970000	Fence Cyn	1	NESE	36-15E-22S	8345	8427			8588
43047161980000	Fence Cyn	2	NESE	26-15E-22S	8026	8111	8285		8316
43047300970000	Fed	31-13	SWSW	31-15E-24S	7522	7613	7720		7764
43047301150000	Texaco Skylline	B-Nct-1	SENW	23-13E-22S	10108	10178	10312		10401
43047301210000	SE Flank Uinta	5-1	NENE	5-15E-23S	8447	8532	8674		8738
43047301260000	SE Flank Uintah	28-1	SWSW	28-15E-22S	9024	9105	9239		9302
43047301350000	Chorney	C-2	SENE	3-14E-22S	9499	9569	9712		9795
43047301430000	Gov AF	1	SESW	27-13E-21S	9591	9680	9834	9910	9973
43047301650000	Chorney Nct	1	SENW	11-13E-22S	10683	10765	10894	10974	11026

Well ID	Well Name	Well Number	Quarter	Location	Dakota Silt Top TVD	KD Top TVD	Kcm Top TVD	Kbb Top TVD	Jm Top TVD
43047301660000	Unit	3	se nw	22-13E-22S	9824	9893	10038	11338	10120
43047301680000	Seep Ridge	4	SENW	24-13E-22S	10100	10182	10305	12694	10382
43047301700000	Texaco Skylline	1	NWNW	20-13E-21S	10988	11080	11270	11338	11422
43047302260000	Gray Knoll Fed	1	SWNE	22-12E-21S	12367	12451	12619	12694	12757
43047302470000	Blk Horse Cyn	1	SESE	17-15E-24S	8207	8276	8439		8505
43047302480000	Blk Horse	2	SESE	29-15E-24S	7545	7630	7790		7833
43047302710000	Crooked Cyn	1	NWNE	20-14E-23S	8885	8967	9110		9164
43047302760000	Seep Ridge	5	SENW	26-13E-22S	9755	9822	9967		10056
43047302840000	Pine Spr	1	NESW	15-14E-22S	9051	9126	9295		9366
43047303230000	Seep Ridge	8	NWSE	14-13E-22S	10441	10515	10660		10744
43047303550000	Wolf Point	1	SESE	2-15E-21S	9661	9747	9893		9968
43047303570000	Buck Camp	1	NENE	22-12E-22S	11379	11462	11610	11677	11740
43047303860000	Crooked Cyn	2	E/2 NWN	34-13E-23S	9498	9570	9700		9772
43047303940000	Main Cyn	14-16	NENW	16-15E-23S	8327	8415			
43047304480000	Blk Horse Cyn	6	NESW	9-15E-24S	8297	8360	8533		8584
43047305710000	Main Cyn	3-16	SESW	16-15E-23S	8267	8365	8495		8497
43047306160000	Main Cyn	11-19	SENW	9-15E-23S	8198	8277	8434		
43047306180000	Main Cyn	13-15	NWNW	15-15E-23S	8017	8105	8216		
43047306220000	Wolf	3-11	SESW	11-15E-21S	9615	9695	9846		9916
43047306390000	Main Cyn	11-10	SENW	10-15E-23S	8099	8177	8300		
43047306440000	Winter Rdg St	11-32	NWNW	32-15E-22S	9091	9185	9324		9376
43047306740000	Main Cyn	15-8	NWNE	8-15E-23S	8339	8420	8592		8606
43047307350000	Main Cyn	2-8	SWSE	8-15E-23S	8340	8418			8602
43047307360000	Main Cyn	7-17	NWSE	17-15E-23S	8285	8367	8541		8552
43047307650000	Blk Horse Cyn Fed	31-1	NWSW	31-15E-24S	7527	7622	7728		7755
43047307730000	Crooked Cyn	3	SENW	32-13E-24S	9006	9100	9264		9315
43047307910000	Trapp Sprs	6-35	NESW	35-14E-23S	8583	8673	8852		8883
43047309440000	Trapp Sprs	8-36	NESE	36-14E-23S	8239	8323	8514		8542
43047309600000	Pine Sprs St	15-6	NWNE	16-14E-22S	8781	8870	9033		9082
43047309630000	Duncan Fed	1	SENW	29-15E-23S	8346	8433			8602
43047309750000	Trapp Sprs	25-1	SESE	25-14E-23S	8368	8453	8636		8661
43047309760000	Sweet Cyn	42-23	SENE	23-14E-24S	8200	8297			
43047309770000	Main Cyn	8-7	NESE	7-15E-23S	8457	8540	8695		8751
43047309780000	Trapp Sprs	13-25	NWNW	25-14E-23S	8647	8733	8886		8937
43047310050000	Squier	1	SENW	31-15E-23S	7590	7674	7826		7884

Well ID	Well Name	Well Number	Quarter	Location	Dakota Silt Top TVD	KD Top TVD	Kcm Top TVD	Kbb Top TVD	Jm Top TVD
43047310270000	Fed	6-14	NESW	14-15E-21S	9539	9627	9771		9864
43047310400000	Sweet	13-6	NESW	13-14E-24S	8164	8262	8401		8450
43047310410000	Trapp Sprs	16-25	NENE	25-14E-23S	8765	8854	9013		9054
43047310430000	Main Cyn	4-4	SWSW	4-15E-23S	8246	8330	8496		8542
43047310450000	Blk Horse	14-5	NENW	15-15E-24S	7504	7571	7729		7801
43047310630000	Pine Sprs	8-20	NESE	20-14E-22S	8095	8188	8337		8391
43047310640000	Blk Horse	14-2	NENW	2-15E-23S	8434	8520	8680		8721
43047310700000	Main Cyn	9-3	SENE	3-15E-23S	8301	8387	8529		8559
43047310710000	Fed	7-15	NWSE	15-15E-21S	9552	9640	9753		9841
43047310720000	Main Cyn	6-3	NESW	3-15E-23S	8284	8368	8492		8546
43047310940000	Meadow Crk	1	SWNE	31-15E-22S	9137	9233	9367		9434
43047311040000	Blk Horse	12-8	SWNW	8-15E-24S	8292	8376	8531		8596
43047311110000	Main Cyn	16-4	NENE	4-15E-23S	8387	8471	8596		8647
43047311340000	Fed Eni	7-1	NENE	7-13E-26S	6643	6728	6881		6955
43047311370000	Fed	5-13	NWSW	13-15E-21S	9401	9488	9624		9695
43047312310000	Eni-Hatch	15-6	NENW	15-13E-25S	8134	8220	8360		8439
43047312430000	St	11-32	SENW	32-15E-23S	7565	7644	7822		7861
43047312470000	Fed	7-30	NWSE	30-15E-23S	8203	8294	8418		8442
43047314960000	Fed	25-16	SESE	25-15E-22S	8368	8453	8610		8643
43047315100000	Agency Draw	16-3	SESE	3-13E-20S	11722	11817	11993	12071	12170
43047315110000	Fed	36-5D	SWNW	36-15E-22S	8821	8908	9060		9070
43047318940000	Bitter	1-25-14-25	SWSW	25-14E-25S	7401	7494	7632		7686
43047333330000	DRO	32-2A	NWNW	32-14E-20S	10432	10528	10679	10747	
43047333370000	DRO	32-6A	SWNE	32-14E-20S	10457	10552	10723	10777	
43047334450000	Chimney Rock	32-11	NESW	32-13E-21S	10633	10715	10883	10943	11011
43047334470000	Chimney Rock	32-13	SWSW	32-13E-21S	10609	10693	10860	10924	10978
43047334480000	Chimney Rock	32-14	SESW	32-13E-21S	10534	10612	10776	10849	10912
43047335300000	FC Delambert	30-2	SESW	30-15E-23S	7677	7763	7899		7946
43047335570000	DRO	32-8A	NENE	32-14E-20S	10486	10581	10758	10809	
43047335580000	DRO	32-12A	NWSW	32-14E-20S	10356	10453	10630	10706	
43047335950000	DRO	28-1A	NWSW	28-14E-20S	10607	10699	10863	10932	10984
43047335960000	DRO	30-6A	SESE	30-14E-20S	10478	10574	10730	10789	10856
43047336160000	DRO	29-4A	SWSE	29-14E-20S	10480	10577	10733	10798	10864
43047336170000	DRO	29-5A	SESE	29-14E-20S	10526	10623	10777	10845	10898
43047336180000	DRO	32-7A	NWNE	32-14E-20S	10468	10568	10697	10772	10843

Well ID	Well Name	Well Number	Quarter	Location	Dakota Silt Top TVD	KD Top TVD	Kcm Top TVD	Kbb Top TVD	Jm Top TVD
43047336190000	DRO	32-9A	SENE	32-14E-20S	10471	10564	10744	10809	
43047336200000	DRO	32-10A	NWSE	32-14E-20S	10411	10509	10676	10727	
43047336210000	DRO	32-11A	NESW	32-14E-20S	10388	10486	10654	10708	10778
43047340980000	DRO	32-16A	SESE	32-14E-20S	10386	10482	10649	10744	10795
43047341020000	DRO	29-6A	NESW	29-14E-20S	10464	10556	10717	10770	10832
43047341030000	DRO	29-7A	SWNW	29-14E-20S	10486	10581	10738	10799	10872
43047341660000	Fence Cyn St	32-2	NWNW	32-15E-23S	8386	8468	8626		8668
43047347420000	NHC	1-9	NENE	9-15E-20S	10209	10306	10467		10516
43047348300000	NHC	10-10	NWSE	10-15E-20S	10240	10336	10481		10541
43047349220000	NHC	4-1	NWNW	1-15E-20S	10145	10236	10389		10455
43047349530000	NHC	14-11	SESW	11-15E-20S	10005	10105	10236		10309
43047349540000	NHC	8-13	SENE	13-15E-20S	9783	9878	10007		10077
43047350540000	NHC	4-13	NWNW	13-15E-20S	9893	9990	10156		10222
43047351400000	NHC	1-6	NWNW	5-15E-20S	10230	10331	10496	10548	
43047352830000	NHC	2-12	NWNE	12-15E-20S	10363	10452	10573		10644
43047354420000					10366	10465	10643	10690	10763
43047355670000	Lindisfarn	1-26	SWSW	26-15E-23S	7619	7713	7833		7867
43047356250000	Ute Tribal	10-2	NWSE	2-15E-20S	10080	10175	10314		10378
43047356850000	HP St	43-32	NESE	32-15E-23S	8080	8161	8302	10591	8316
43047358800000	Fr	9P-36-14-19	NWSW	31-14E-20S	10265	10370	10522		10654

Well Name	API #	Well Depth	Perm (mD)	Por. %	Grain Size
Praire Canyon 2-29	05045060370000	-5325	0.36	5.7	f
		-5348	0.54	8.4	f
		-5349	29	14.2	f
		-5350	35	13	f
		-5351	0.04	0.3	g
		-5352	1.8	6.4	g
		-5353	0.77	11.6	m
		-5354	1.3	7.5	m-c
		-5355	0.78	6.6	m-c
		-5356	1.5	7.2	m-c
		-5357	5.8	13.9	f
		-5358	0.72	10	vf-f
		-5359	0.38	12.8	vf-f
		-5360	5	7.6	vf-f
		-5371	19	19	f
		-5372	30	16.4	m
		-5373	39	19	m
		-5374	23	20.9	f
		-5375	17	20.8	f
		-5376	15	18	f
		-5377	12	19.3	f
		-5378	105	21.4	f
		-5379	28	18	f
		-5380	12	19.6	f
		-5381	38	17.9	f
		-5382	11	15.5	m
		-5383	45	22.1	m
		-5384	12	17.7	m
		-5385	25	20.7	m
		-5386	32	19.3	m
		-5387	75	17.3	f-m
		-5388	10	19.6	f-m
		-5389	5.3	15.9	f-m
		-5390	10	15.3	f-m
		-5391	3.6	12.2	f-m
		-5392	0.6	11	f
		-5393	0.19	5.8	f
		-5394	0.14	7.2	m
		-5395	0.11	12.3	f
		-5397	0.29	3.4	f
		-5398	0.14	8.2	f
		-5399	0.23	9.7	f
		-5400	0.14	8	f
		-5401	0.52	7.8	f-m
		-5420	0.03	6.2	f-c
		-5421	0.34	8.9	f-m
		-5422	0.08	7.4	f
		-5423	1.3	11.4	f
		-5424	4.3	10.8	f
		-5425	1.5	8.6	f
		-5426	0.07	18.3	f
		-5427	0.06	8.1	f
		-5428	1.1	6.2	f
		-5429	14	14.6	f
		-5430	0.24	11.9	f

Well Name	API #	Well Depth	Perm (mD)	Por. %	Grain Size
		-5431	1.5	10.2	f
		-5432	17	12	m
		-5433	4.5	12	g
		-5434	0.83	10.4	m-c
		-5435	2.1	10.8	m-c
		-5436	6.4	9.3	f-c
		-5437	0.18	7.8	f-c
		-5438	0.15	8.4	g
		-5476	0.05	6.5	f
		-5477	0.06	8	vf
		-5478	0.07	10.7	vf
		-5479	0.06	9.4	vf
		-5480	0.05	9.6	f
		-5481	0.09	9.1	f
		-5482	0.1	8.3	f-m
		-5483	0.22	11.6	f-c
		-5484	0.15	15.1	f-c
		-5485	0.19	11.4	f-c
		-5486	0.11	15.7	f
		-5487	0.12	5.6	c
		-5488	0.07	5.6	vf
		-5490	0.08	2.1	vf
		-5491	0.07	5.3	f-c
		-5492	0.04	2.3	f
Mesa Gar Fed 6-3	05045062620000	-7893	0.07	3.1	vf
		-7894	0.009	4.3	vf
		-7895	0.01	3.9	vf
		-7906	0.53	4.3	vf
		-7907	0.11	4.2	vf
		-7908	0.78	5.5	vf
		-7909	0.01	3.9	vf
		-7910	0.009	2.8	vf
		-7911	0.06	4.9	vf
		-7912	1.2	4	vf
		-7918	0.01	4.4	vf
		-7919	0.01	3.3	vf
		-7920	0.09	5.3	vf
		-7921	0.009	3	vf
		-7922	1.2	4.8	vf
		-7923	0.009	2.9	vf
		-7937	0.009	7.5	vf
		-7938	0.03	8.3	vf
		-7939	0.009	6.4	vf
		-7940	0.009	2.9	vf
		-7941		8.3	vf
		-7944	0.04	5.8	vf
		-7945	0.009	2.8	vf
		-7946	0.009	3.4	vf
		-7947	0.009	3.6	vf
		-7948	0.01	3.4	vf
		-7949	0.009	5.4	vf
		-8003	0.009	2.7	vf
		-8004	0.009	2.7	vf
		-8005	0.009	6	vf

Well Name	API #	Well Depth	Perm (mD)	Por. %	Grain Size
		-8006	0.01	4	vf
		-8007	0.2	8.6	vf
		-8008		9.8	vf
		-8009		7.8	vf
		-8024	0.01	2.9	vf
		-8025	0.01	3.3	f
		-8026	3.7	6.2	m
		-8027	0.01	14.8	m
		-8028	0.05	6.4	m
		-8029		17.2	m
Fed 8-1	05077080260000	-2212	0.09	4.8	vf
		-2329	0.09	2	vf
		-2330	0.09	5.6	vf
		-2331	0.09	6.2	vf
		-2336	0.1	14.4	f
		-2337	0.1	12.1	f
		-2338	0.3	15.1	f
		-2339	0.2	13.5	f
		-2340	0.2	10.6	f
		-2341	0.2	12	f
		-2342	0.3	11.8	f
		-2355	0.09	6.9	vf
		-2357	0.09	5.8	vf
		-2358	0.1	4.8	vf
		-2360	0.09	6.3	vf
		-2361	0.09	2.8	f
		-2374	0.8	5.5	vf
		-2375	0.3	6.7	f
		-2376	0.3	8.5	vf
		-2377	0.4	8.4	vf
		-2378	0.2	13	f
		-2379	0.3	8.2	f-m
		-2380	0.2	13	f-m
		-2383	0.5	3.2	vf
		-2384	0.3	4.1	vf
		-2394	0.09	2.9	vf
		-2395	0.09	3.3	vf
		-2398	0.09	3.5	vf
		-2399	0.09	4.2	vf
		-2407	0.09	7	vf
		-2408	0.1	3.3	f
		-2409	0.5	10.5	m
		-2410	0.1	7.3	vf
		-2411	0.1	6.9	vf
		-2412	0.1	10.5	f-m
		-2413	0.2	7.9	f-m
		-2414	0.8	12.2	f-m
		-2415	2.5	13.2	f-m
		-2416	2.8	14.2	f-m
		-2417	4.9	10.7	f-m
		-2418	39	18.8	f-m
		-2419	6.5	15.7	f-m
		-2420	103	17.3	f-m
		-2421	2.3	13.4	f-m

Well Name	API #	Well Depth	Perm (mD)	Por. %	Grain Size
		-2422	13	14.7	f-m
		-2423	35	17.7	f-m
		-2424	37	18.5	f-m
		-2425	30	16.5	f-m
		-2426	4.4	14.9	f-m
		-2427	66	24.6	f-m
		-2428	1.1	16.7	f-m
		-2429	3.2	17.3	f-m
		-2430	6.3	17.7	f-m
		-2431	0.8	15.8	f-m
		-2432	0.4	13.1	f-m
		-2433	0.6	18.5	f
		-2438	0.1	5.4	f
		-2439	0.09	4.3	f
		-2461	0.09	4.1	vf
		-2462	0.09	4	vf
		-2466	0.09	2.8	vf
		-2467	0.2	1.4	vf
		-2468	0.09	5.7	vf
		-2469	0.09	0.9	vf
		-2470	0.1	4.5	vf
		-2471	0.2	4.2	vf
		-2472	0.3	9.4	f
		-2473	0.5	12.4	f
		-2474	0.2	12.6	f
		-2475	1	7	f
		-2476	14	7.9	f
		-2477	10	12	f
		-2478	48	10.2	m-c
		-2479	0.4	13	m-c
		-2480	6	10.5	m-c
		-2481	34	10.7	m-c
		-2482	0.5	14.6	m-c
		-2483	2	7	m-c
		-2484	3.6	10.1	m-c
		-2485	0.3	11.3	m-c
		-2486	1.2	9	m-c
		-2487	0.6	12.1	m-c
		-2488	5.7	7.5	m-c
		-2489	0.7	12.1	m-c
		-2490	2.2	8.2	m-c
		-2491	0.4	10.6	m-c
		-2492	0.4	8.8	m-c
		-2493	0.3	5.4	m-c
Fed 258-1A	43019304690000	-3898	0.05	9.7	vf
		-3899	0.1	11.4	vf
		-3900	0.03	9	vf
		-3901	0.03	7.7	vf
		-3902	0.03	3.2	vf
		-3903	0.11	11.7	vf
		-3904	0.21	11	vf
		-3905	0.14	10.4	vf
		-3906	0.04	3.9	vf
		-3907	0.13	12.3	vf

Well Name	API #	Well Depth	Perm (mD)	Por. %	Grain Size
		-3908	0.08	3.6	vf
		-3909	0.04	2.4	vf
Fed 258-5	43019303640000	-3735	2.3	13.1	m
		-3736	0.69	13.7	f
		-3737	5.7	13.8	f
		-3738	0.52	16.1	f
		-3739	0.65	15.9	f
		-3740	3.1	20.8	m
		-3741	5.4	14.4	c
		-3742	1.1	13.6	m
		-3743	12	11.3	f
		-3744	9.1	10.5	f
		-3745	0.18	7.4	vf
		-3746	0.07	12.7	vf
		-3747	0.11	9.5	f
Fed 1-23	05103086780000	-6987		5	vf-f
		-7004.7		7	vf-f
		-7029		0	f-vc
		-7037.3		4	f-vc
		-7099		14	vf-m
		-7107.1		8	vf-m
		-7119.8		12	vf-m
Fed 4-1-1S-102	05103087190000	-5570		7	vf-f
		-5571		3	vf-f
		-5573.5		4	vf-f
		-5589		10	vf-f
		-5590		12	vf-m
		-5594		6	vf-m
		-5596		5	
		-5675		3	vf-f
		-5678		2	
		-5678.5		6	vf-m
		-5688		0	f-vc
Cedar Bench 32-20	05045067600000	-7809.2		2	vf-f
		-7814.3		4	vf-m
		-7817		4	vf-m
		-7825		3	vf-m
		-7831.9		5	vf-c
		-7835.5		3	vf-c
		-7837.2		2	vf-m
		-7842.1		2	vf-m
		-7851		0	vf-m
		-7854.3		1	vf-m
		-7861.5		1	vf-f
		-7868		1	vf-m
		-7870.5		1	vf-f
		-7874.4		1	vf-f
		-7879.5		2	vf-f
		-7883.8		1	vf-c
Cedar Bench 32-7	05045067390000	-8989.8		1	vf-f

Well Name	API #	Well Depth	Perm (mD)	Por. %	Grain Size
		-8996.4		1	vf-f
		-8998.8		3	vf-f
		-8999.1		2	vf-f
		-8999.7		4	vf-f
		-9000.1		5	vf-m
		-9001		5	vf-m
		-9002		4	vf-m
		-9003.2		1	vf-m
		-9006.1		1	vf-m
		-9009		1	vf-f
		-9010.9		1	vf-f
		-9011		1	vf
		-9015.3		0	vf
		-9016.4		0	vf
		-9076.5		1	vf
		-9079.9		0	vf
Fed B-1	43019305520000	-6185	0.35	7.6	f-m
		-6185.5	0.59	9.5	m-c
		-6186	0.33	13	m-c
		-6186.5	1.6	14.4	m-c
		-6187		5.9	m
NGC 42-23	43047309760000	-8384	0.9	11.7	f-m
		-8390	2.6	13	f-m
		-8414	8.7	15	f-m
		-8419	2.2	11.7	f-m
		-8433	17	18.4	f-m
		-8450	0.1	20.4	vf
		-8451	0.2	19.4	vf
		-8602	0.2	19.1	vf
		-8612	0.2	8.8	vf-f
Columbine 13-24-4-104	5103087150000	-6348		6.3	silt
		-6349	0.02	2.3	silt
		-6350	0.009	1.6	silt
		-6351	0.009	2.9	silt
		-6352	0.11	2.3	silt
		-6353	0.01	5.1	f-m
		-6354	0.03	10.4	f-m
		-6355	0.04	9.5	f-m
		-6356	0.07	9.4	f-m
		-6357	0.11	8.2	f-m
		-6358	0.03	6.5	f-m
		-6359	0.06	9	f-m
		-6360	0.06	9.3	f-m
		-6361	0.11	9.2	f-m
		-6362	0.33	6.5	f-m
		-6363	0.07	11	f-m
		-6364	0.12	11.1	f-m
		-6365	0.16	11.2	f-m
		-6366	0.18	11	f-m
		-6367	0.18	10.2	f-m
		-6368	0.18	9.5	f-m
		-6369	0.18	10.8	f-m

Well Name	API #	Well Depth	Perm (mD)	Por. %	Grain Size
		-6370	0.15	10	f-m
		-6371	0.1	7.6	f-m
		-6372	0.01	3.9	f-m
		-6373	0.06	8	f-m
		-6374	0.1	14.3	f-m
		-6375	0.09	8.5	f-m
		-6376	0.07	7	f-m
		-6377	0.04	6.4	f-m
		-6378	0.08	6.7	f-m
		-6379	0.09	8.2	f-m
		-6380	0.01	5.3	f-m
		-6381	0.03	7.6	f-m
		-6382	0.04	7	f-m
		-6383	0.05	7.4	f-m
		-6384	0.04	7.5	f-m
		-6385	0.06	8	f-m
		-6386	0.09	7	f-m
		-6387	0.05	8.4	f-m
		-6388	0.09	8.6	f-m
		-6389	0.27	7.7	f-m
		-6390	0.08	7	f-m
		-6391	0.03	6	f-m
		-6392	0.16	8.1	f-m
		-6393	0.13	9	f-m
		-6394	0.03	8.8	f-m
		-6395	0.09	9.8	f-m
		-6396	0.12	10.7	f-m
		-6397	0.07	10.3	f-m
		-6398	0.03	8.3	f-m
		-6399	0.09	8.4	f-m
		-6400	0.19	10.7	f-m
		-6401	0.23	9.8	f-m
		-6402	0.16	9.1	f-m
		-6403	0.21	9.4	f-m
		-6404	0.21	9	f-m
		-6405	0.14	8.2	f-m
		-6406	0.08	8.7	f-m
		-6407	0.03	7.9	f-m
		-6408	0.009	1.2	f
		-6409	0.009	1.3	f
		-6411	0.009	3.5	f
		-6412	0.009	1.8	f
		-6413	0.009	1.7	f
		-6414	0.009	3.3	f
		-6415	0.009	2.2	f
		-6417	0.009	2.3	f
		-6418	0.07	3.9	f
		-6419	0.009	2	f
		-6422	0.02	3.7	f
		-6423	0.04	3.4	f
		-6424		2.7	f
		-6425	0.35	3.4	f
		-6432	0.02	2.1	f-m
		-6433	0.02	1.2	f-m
		-6434	0.01	3.6	f

Well Name	API #	Well Depth	Perm (mD)	Por. %	Grain Size
		-6435	0.01	5.7	f
		-6436	0.009	7.7	f
		-6437	0.07	12.4	f
		-6438	0.009	3.8	f
		-6439	0.09	8.8	f
		-6440	0.09	10.7	f
		-6441	0.52	10	f
		-6442	0.16	11.4	f
		-6443	0.07	9	f
		-6444	0.1	10.4	f
		-6445	0.04	7.5	f
		-6451	0.009	3.3	f-c
		-6452	0.06	5.2	f-c
		-6453		21.9	f-c
		-6460	39	16.8	f-c
		-6461	39	20.6	f-c
		-6462	80	22.1	f-c
		-6463	0.24	14.3	f
		-6464	1.3	20.3	f
		-6465	0.28	16.3	f
		-6466	0.47	12.6	f
		-6467	1.5	18.4	f
		-6468	0.76	7.4	f-vc
		-6469	0.69	10.6	f-m
		-6470	1.6	13.8	f-m
		-6471	0.62	17.2	f-m
		-6472	0.34	10.8	f
		-6473	0.92	19.8	f
		-6474	0.67	17.8	f
		-6475	0.13	8.9	f
		-6476	0.64	11.3	f
		-6477	1.8	11	f
		-6478	0.55	15.5	f
		-6479	1.4	13.9	f
		-6480	3	13.6	f
		-6481	1.1	17.7	f-m
		-6482	2.3	18.8	f-m
		-6483	3.3	13.5	f-m
		-6484	0.84	13.8	f-c
		-6485	0.56	13.9	f-c
		-6509	0.07	3	f-m
		-6510	1.3	15.8	f
		-6511	51	19.5	f
		-6512	25	19.8	f
		-6513	26	21	f
		-6514	4.2	12.2	f
		-6515	0.54	12.6	f-m
		-6516	0.31	8.6	f-m
		-6517	0.3	5.4	f-m
San Arroyo 5	43019158880000	-4050	0.1	8.64	
		-4051	0.1	4.25	
		-4052	0.2	12.15	
		-4053	0.1	9.04	
		-4054	0.4	11.57	

Well Name	API #	Well Depth	Perm (mD)	Por. %	Grain Size
		-4055	0.1	12.59	
		-4056	0.7	12.88	
		-4057	0.3	9.08	
		-4057.5	0.7	13.91	
		-4058	0.2	10.1	
		-4059	0.1	5.71	
		-4060	0.4	11.57	
		-4061	0.4	10.98	
		-4062	0.3	10.25	
		-4063	0.5	13.97	
		-4064	0.4	12.94	
		-4077	0.2	8.75	
		-4078	0.2	8.49	
		-4106.5	0.1	4.71	
		-4107.5	0.3	6.59	
		-4113.5	0.1	6.48	
		-4116	0.2	16.85	
		-4117	12.7	19.2	
		-4118	17	16.76	
		-4121	30	19.62	
		-4122	15.7	19.03	
		-4123	11	18.22	
		-4124	0.5	18.73	
		-4127	0.8	19.19	
		-4128	0.8	17.73	
		-4129	10	18.99	
		-4130	20	17.58	
		-4131	14	19.58	
		-4132	9.5	18.71	
		-4133	0.8	17.2	
		-4134	1.4	10.9	
		-4135	2.5	21.4	
		-4136	4.6	25.6	
		-4137	4	14.2	
		-4138		10.6	
		-4139		17.8	
		-4140	0.6	9.4	
		-4141	0.1	10.3	
		-4142.5	0.1	10.3	
Bar X-2	05077050020000	-3005	0	11.2	
		-3006	0.3	3.4	
		-3007	0	1.6	
		-3013	0	7.4	
		-3015	0	6.9	
		-3026	0	2.9	
Trapp Springs 13-25-14-23	43047309780000	-8849	0.1	1.43	
		-8879	0.1	2.27	
		-8882	0.1	9.67	
		-8886	0.1	3.1	
		-8889	0.1	6.55	
Yellow Cat Outcrop	43019004	0	182.963	24.4137	
West Water Outcrop	43019001	0	58.7	20.4804	

Westwater West Point Mosaic

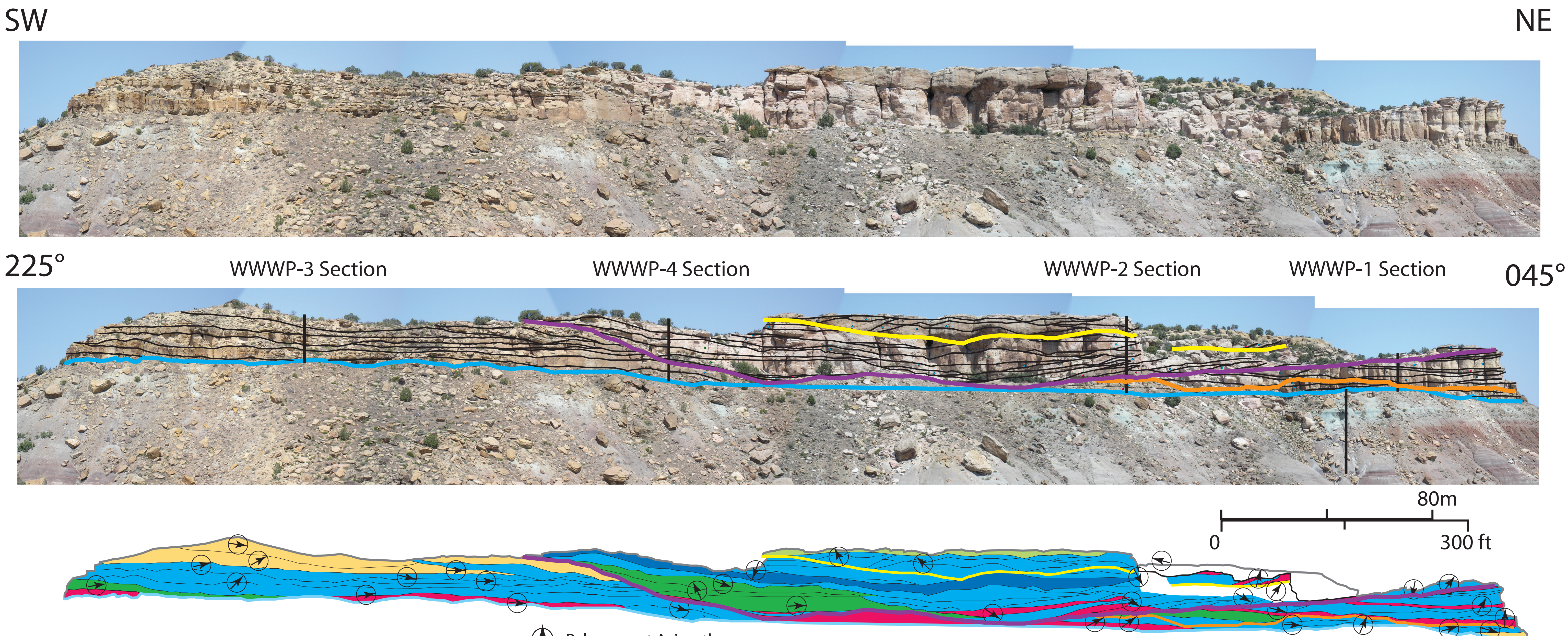

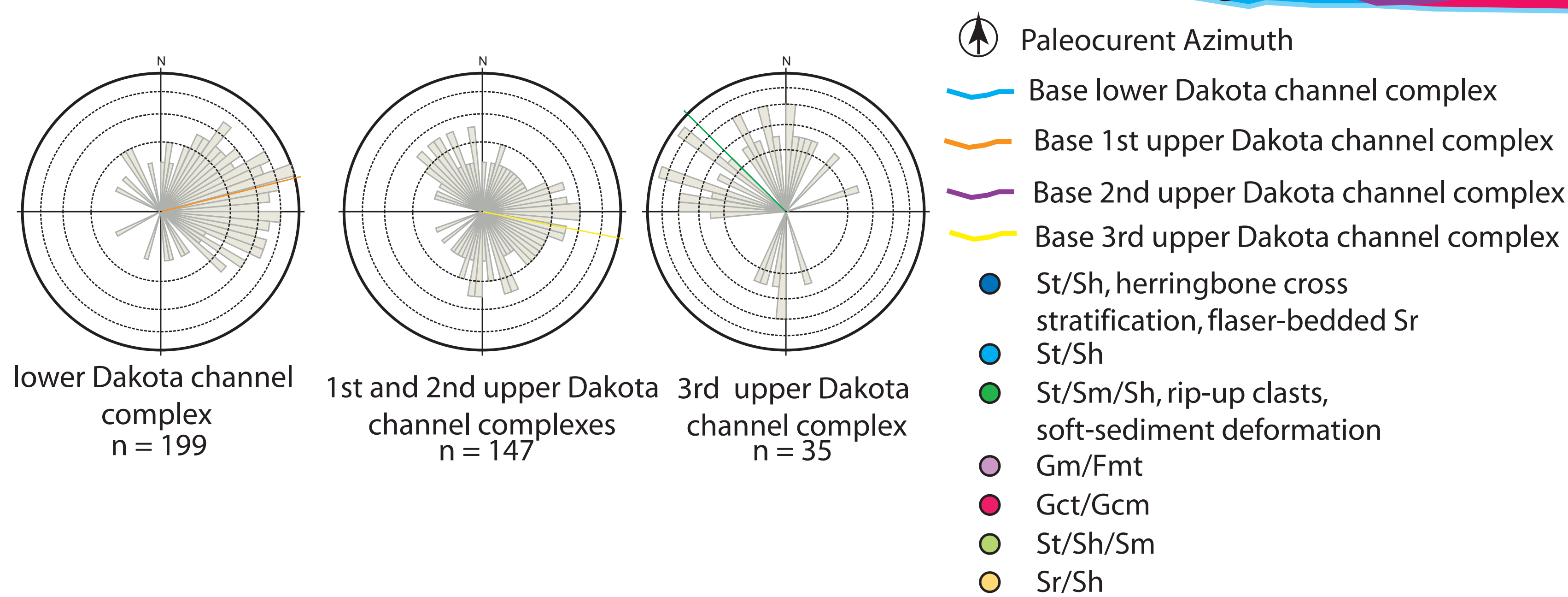

Plate 1. Photo mosaic diagram of Dakota Formation fluvial channel architecture, Westwater West Point outcrop locality. Diagram includes mapped variations in lithofacies and internal bounding surfaces, as well as single and average paleocurrent orientations from each channel complex.

Westwater West Point Sections

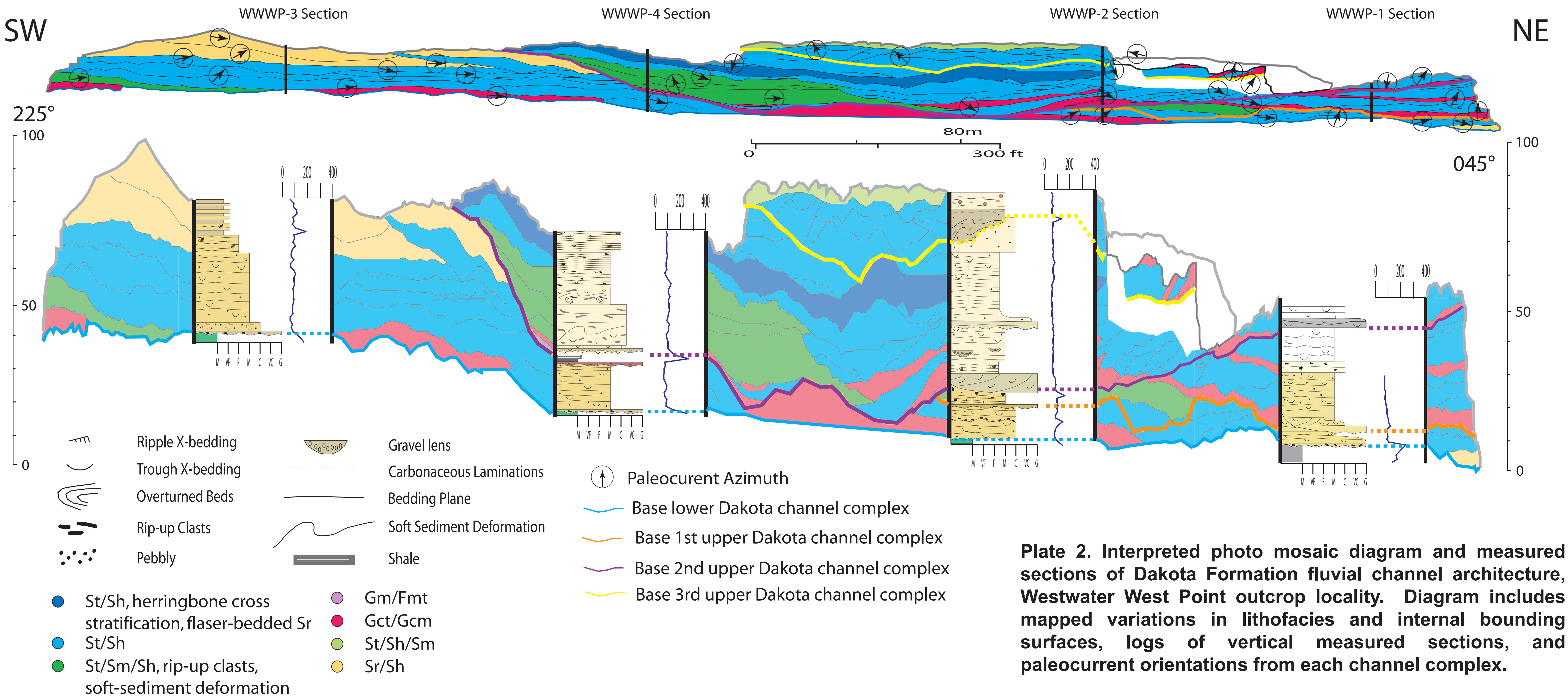

Plate 2. Interpreted photo mosaic diagram and measured sections of Dakota Formation fluvial channel architecture, Westwater West Point outcrop locality. Diagram includes mapped variations in lithofacies and internal bounding surfaces, logs of vertical measured sections, and paleocurrent orientations from each channel complex.

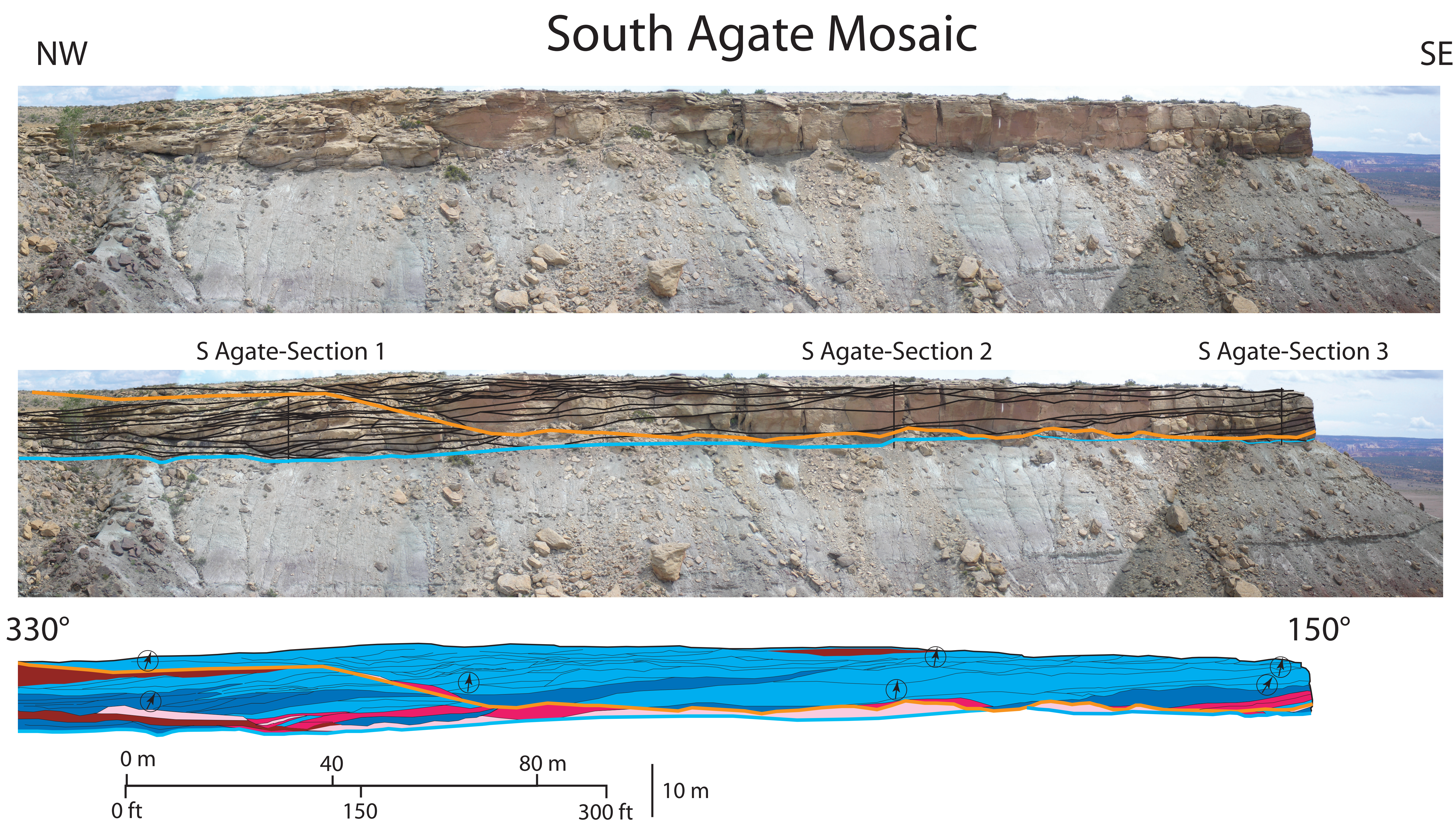

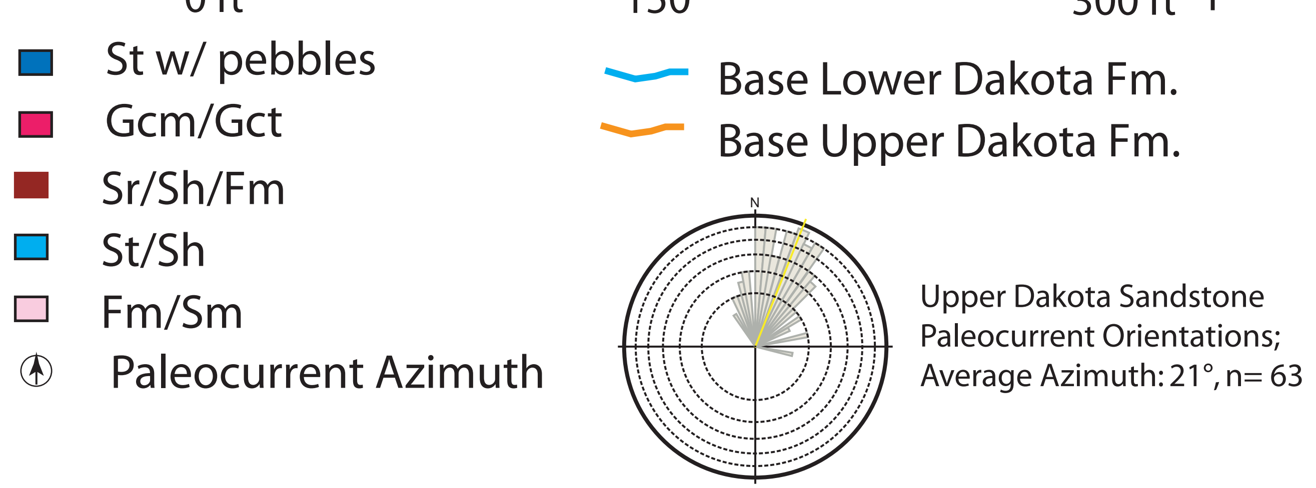

Plate 3. Photo mosaic diagram of Dakota Formation fluvial channel architecture, South Agate outcrop locality. Diagram includes mapped variations in lithofacies and internal bounding surfaces, as well as single and average paleocurrent orientations from each channel complex.

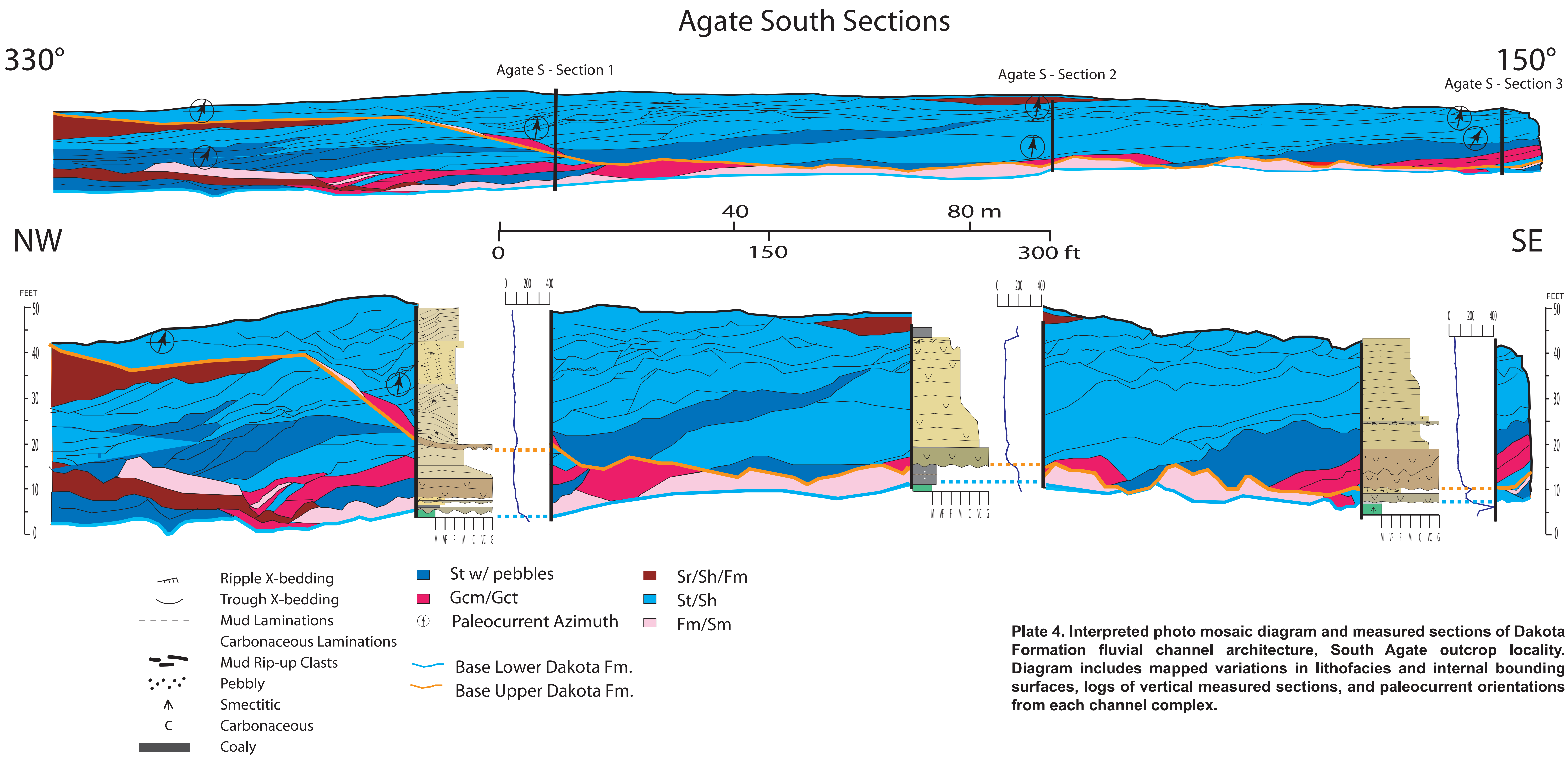

Plate 4. Interpreted photo mosaic diagram and measured sections of Dakota Formation fluvial channel architecture, South Agate outcrop locality. Diagram includes mapped variations in lithofacies and internal bounding surfaces, logs of vertical measured sections, and paleocurrent orientations from each channel complex.